

# Uncertainty Modelling in Aircraft Trajectory Predictions

Thesis

R. Graas

Delft University of Technology  
Faculty of Aerospace Engineering  
Delft, July 2021





# Uncertainty Modelling in Aircraft Trajectory Predictions

## Thesis

by

R. Graas

to obtain the degree of Master of Science  
at the Delft University of Technology

Student number: 4951751  
Project duration: September, 2020 – July, 2021  
Thesis committee: Dr. J. Sun, TU Delft, supervisor  
Prof. Dr. Ir. J.M. Hoekstra, TU Delft, supervisor  
Dr. A. Bombelli, TU Delft

An electronic version of this thesis is available at <http://repository.tudelft.nl/>.



# Preface

During the Summer of 2020, I was hoping to find a thesis opportunity in the field of Air Traffic Management, a research area I find particularly interesting. Fortunately, I found such a study concerning the predictions of aircraft trajectories, which has resulted in this thesis. This thesis was written in partial fulfilment of the requirements for the degree of Master of Science in Aerospace Engineering at the Delft University of Technology.

I would like to express my gratitude to my supervisor Junzi Sun. Even though meeting online, discussing highly technical details related to my study, might not always be convenient, I thoroughly enjoyed our collaboration and I appreciated the assistance and feedback throughout this study. Also, I would like to thank Jacco Hoekstra for the provision of his valuable feedback on my intermediate results.

This thesis concludes my time as a student at the Delft University of Technology. A time I fully enjoyed thanks to my fellow students with whom I spent lots of moments I will pleasantly look back on. Also, my sincere gratitude goes out to my family for their continuous support during my studies. Last, but definitely not least, I would like to express my great appreciation to my girlfriend Celine. Both working on the final phases of our studies kept me motivated and definitely made working from home more pleasant.

*R. Graas  
Delft, July 2021*



# Contents

<b>List of Figures</b>	<b>vii</b>
<b>List of Tables</b>	<b>ix</b>
<b>List of Abbreviations</b>	<b>xi</b>
<b>I Scientific Paper</b>	<b>1</b>
<b>II Scientific Paper Appendices</b>	<b>19</b>
<b>A Data exploration</b>	<b>21</b>
A.1 Data exploration on the complete trajectory set . . . . .	21
A.2 Data exploration on the clusters of trajectories . . . . .	22
<b>B Trajectory clustering with DBSCAN</b>	<b>23</b>
<b>C Prediction results</b>	<b>25</b>
C.1 Comparison between GPR and the PF model . . . . .	25
C.2 Complete overview of predictive results . . . . .	27
<b>III Preliminary Report [previously graded]</b>	<b>29</b>
<b>1 Introduction</b>	<b>31</b>
1.1 Context . . . . .	31
1.2 Research objective. . . . .	32
1.3 Report outline . . . . .	32
<b>2 Trajectory prediction methodologies</b>	<b>33</b>
2.1 Model-based Trajectory Prediction. . . . .	33
2.1.1 Aircraft intent . . . . .	34
2.1.2 Aircraft performance model . . . . .	35
2.1.3 Environmental model . . . . .	36
2.2 Data-driven Trajectory Prediction . . . . .	36
2.2.1 Sources of data . . . . .	37
2.2.2 Clustering aircraft trajectories . . . . .	38
2.2.3 Application of data-driven prediction models . . . . .	39
2.3 Measurement of predictive accuracy. . . . .	40
2.4 Review of the state-of-the-art in trajectory predictions. . . . .	40
<b>3 Modelling uncertainty</b>	<b>43</b>
3.1 Uncertainty identification . . . . .	43
3.1.1 Input uncertainty . . . . .	43
3.1.2 Structural uncertainty . . . . .	43
3.1.3 Sources of uncertainty in aircraft trajectory predictions . . . . .	44
3.2 Uncertainty characterisation. . . . .	45
3.3 Uncertainty propagation. . . . .	46
3.4 Uncertainty management . . . . .	46
3.4.1 Local sensitivity analysis. . . . .	46
3.4.2 Global sensitivity analysis . . . . .	47

<b>4</b>	<b>Probabilistic approach to trajectory predictions</b>	<b>49</b>
4.1	Bayesian statistics . . . . .	49
4.2	Monte Carlo methods . . . . .	51
4.3	Polynomial Chaos Expansion . . . . .	51
4.4	Sequential Monte Carlo methods . . . . .	52
4.4.1	Recursive Bayesian estimation. . . . .	52
4.4.2	Particle filtering methods . . . . .	53
4.4.3	Applications of particle filtering . . . . .	54
4.5	Gaussian Process Regression . . . . .	55
4.5.1	Gaussian Process background . . . . .	55
4.5.2	Model selection . . . . .	56
4.5.3	Predictions based on Gaussian Process Regression . . . . .	57
4.5.4	Applications of Gaussian Process Regression . . . . .	57
4.6	Review of probabilistic prediction techniques . . . . .	58
<b>5</b>	<b>Research approach</b>	<b>61</b>
5.1	Research questions and project breakdown . . . . .	61
5.2	Research scope . . . . .	62
<b>6</b>	<b>Data collection and preparation</b>	<b>65</b>
6.1	Available datasets . . . . .	65
6.1.1	Trajectory data from ADS-B . . . . .	65
6.1.2	Aircraft intent data from filed flight plans . . . . .	66
6.1.3	Meteorological data from ERA5 . . . . .	67
6.2	Coupling data sources . . . . .	68
6.2.1	Merging the flight plan data with the ADS-B data. . . . .	68
6.2.2	Merging the meteorological data with the ADS-B data . . . . .	69
6.3	Preparation of the dataset . . . . .	69
6.3.1	Filtering the dataset . . . . .	69
6.3.2	Flight phase computation . . . . .	70
6.3.3	Adding features to the dataset . . . . .	70
6.4	Overview of final dataset. . . . .	71
6.5	Clustering trajectories . . . . .	75
6.5.1	Application of DBSCAN to an initial subset of the data . . . . .	75
6.5.2	Application of DBSCAN to final dataset. . . . .	78
<b>7</b>	<b>Model development and analysis</b>	<b>81</b>
7.1	Development of predictive models. . . . .	81
7.2	Model experiments . . . . .	82
7.3	Analysis of results . . . . .	82
<b>8</b>	<b>Planning</b>	<b>83</b>
	<b>Bibliography</b>	<b>85</b>

# List of Figures

A.1	The distribution of the airline market segment (left) and the aircraft types (right) of the flights in the complete trajectory set. . . . .	21
A.2	Top five departure airports (left) and aircraft types (right) in each cluster of trajectories. . . . .	22
B.1	Distance to closest trajectory in ascending order. . . . .	23
B.2	DBSCAN clustering results for a range of parameter combinations. . . . .	24
B.3	Outliers identified by DBSCAN. . . . .	24
C.1	Comparison between GPR-C and the PF model showing the median values of the spatial errors over increasing look-ahead times. . . . .	25
C.2	Comparison between GPR-C and the PF model showing the median values of the standard deviations in the predictions of $x$ , $y$ , and the altitude over increasing look-ahead times. . . . .	26
2.1	Schematic overview of the TP process [1] . . . . .	34
2.2	Visualisation of horizontal track errors [2] . . . . .	40
4.1	Illustration of Bayesian statistics showing the prior distribution (dashed), the likelihood function (dotted), and the posterior distribution (solid) [3] . . . . .	50
5.1	Breakdown of the project into three phases . . . . .	62
6.1	Data coverage of a sample of hundred trajectories flown on 01-06-2018 . . . . .	66
6.2	Overview of datasets from Eurocontrol . . . . .	66
6.3	Process flow of the construction of the final dataset . . . . .	71
6.4	Ten most frequent occurrences of departure- (left) and arrival (right) airports . . . . .	73
6.5	Ten most frequent occurrences of airlines (left) and aircraft types (right) . . . . .	73
6.6	Flight phase segmentation of trajectories . . . . .	74
6.7	Average distance of Nearest Neighbours to determine optimal value for epsilon . . . . .	76
6.8	Evaluation of DBSCAN clustering performance for various parameter configurations . . . . .	77
6.9	Visualisation of clustered trajectories obtained from DBSCAN application to flights operating from and to Amsterdam, London Heathrow, and Paris . . . . .	77
6.10	Evaluation of DBSCAN clustering performance for various parameter configurations on one week of flight data . . . . .	78
6.11	Visualisation of clustered trajectories obtained from DBSCAN application . . . . .	79
8.1	Project planning . . . . .	83



# List of Tables

C.1	Predictive results showing the mean ( $\mu$ ), median, and standard deviation ( $\sigma$ ) of the predictive accuracy expressed by the spatial errors of the predictions. . . . .	27
C.2	Predictive results showing the mean ( $\mu$ ), median, and standard deviation ( $\sigma$ ) of the predictive uncertainty expressed by the standard deviations of the predictions. . . . .	28
6.1	Features of the ADS-B dataset . . . . .	65
6.2	Features of the flight points dataset . . . . .	67
6.3	Features of the ERA5 dataset . . . . .	67
6.4	Sample observation from ADS-B dataset . . . . .	68
6.5	Sample of a filed flight plan . . . . .	69
6.6	Categorising aircraft types by their Wake Turbulence Category (WTC) . . . . .	70
6.7	Features of the final dataset . . . . .	72
7.1	Overview of experiments with varying sets of training data to develop GPR models . . .	82



# List of Abbreviations

ADS-B	Automatic Dependent Surveillance-Broadcast
AIDL	Aircraft Intent Description Language
ANN	Artificial Neural Network
ANSP	Air Navigation Service Provider
APM	Aircraft Performance Model
ATC	Air Traffic Control
ATE	Along Track Error
ATFCM	Air Traffic Flow Capacity Management
ATM	Air Traffic Management
BADA	Base of Aircraft Data
CAS	Calibrated Airspeed
CDO	Continuous Descent Operations
CTE	Cross Track Error
DBSCAN	Density-Based Spatial Clustering of Applications with Noise
DST	Decision Support Tool
ECMWF	European Centre for Medium-Range Weather Forecasts
EM	Environmental Model
FF	Fuel Flow
FIR	Flight Information Region
FL	Flight Level
FMS	Flight Management System
FP	Flight Plan
GFS	Global Forecast System
GLM	Generalised Linear Model
GP	Gaussian Process
GPR	Gaussian Process Regression
HTE	Horizontal Track Error
ICAO	International Civil Aviation Organisation
IFR	Instrument Flight Rules
IGI	Intent Generation Infrastructure

---

ISA	International Standard Atmosphere
k-NN	k-Nearest Neighbour
MC	Monte Carlo
MCNN	Multi Cells Neural Network
METAR	Meteorological Aerodrome Report
MLE	Maximum Likelihood Estimate
MLW	Maximum Landing Weight
MTOW	Maximum Take-Off Weight
NM	Network Manager
NN	Neural Network
NOAA	National Oceanic and Atmospheric Administration
ODE	Ordinary Differential Equation
OEW	Operating Empty Weight
PCA	Principal Component Analysis
PCE	Polynomial Chaos Expansion
PDF	Probability Density Function
PF	Particle Filter
PMM	Point Mass Model
RAP	Rapid Refresh
RBF	Radial Basis Function
RDP	Ramer-Douglas-Peucker
RMSE	Root Mean Squared Error
SA	Sensitivity Analysis
SESAR	Single European Sky ATM Research
SMC	Sequential Monte Carlo
TAS	True Airspeed
TBO	Trajectory-Based Operations
TCI	Trajectory Computation Infrastructure
TE	Trajectory Engine
TEM	Total Energy Model
TMA	Terminal Manoeuvring Area
TP	Trajectory Predictor
UQ	Uncertainty Quantification
WTC	Wake Turbulence Category



# Scientific Paper



# Uncertainty Modelling in Aircraft Trajectory Predictions

R. Graas

Under supervision of Dr. J. Sun and Prof. Dr. Ir. J.M. Hoekstra

*Control and Operations, Faculty of Aerospace Engineering  
Delft University of Technology, Delft, The Netherlands*

**Abstract**—Several initiatives are being developed to shift the current paradigm in Air Traffic Management (ATM) from the tactical-based approach to more strategic-based coordination of flights. This transformation of the ATM system relies on the improvement of predictive models that predict the 4D-trajectory of an aircraft. Previous studies primarily applied deterministic models that compute a single predicted trajectory. These models were assessed on their predictive accuracy. However, the accuracy of the predictions is highly impacted by uncertainties that affect the progression of a flight. These uncertainties are commonly related to the lack of detailed information concerning the flight intent, or the inaccuracy of positional and weather-related data. This study applied two probabilistic techniques: the model-based particle filtering model and the data-driven Gaussian Process Regression. Both approaches model the uncertainties and provide a predictive distribution of trajectories that allows for the evaluation of both the accuracy and the uncertainty of the predictions. These models were applied to predict the descent trajectories of aircraft arriving at Amsterdam Airport Schiphol. The results showed that the uncertainty of the predictions could be reduced by incorporating flight-plan data and meteorological data in the predictive models. Also, the accuracy was improved which demonstrates the importance of these sources of data in the predictions of aircraft trajectories. The proposed models have been able to quantify the uncertainty in trajectory predictions that could be used to further develop and improve the management and prediction of 4D-trajectories.

**Index Terms**—Uncertainty modelling, 4D aircraft trajectories, Gaussian Process Regression, Particle Filtering

## I. INTRODUCTION

Vastly increasing air traffic numbers throughout the last decades has challenged the field of air traffic management (ATM). In order to accommodate more flights and improve the performance of the ATM system under higher traffic demands, measures should be taken to increase airspace capacity, which is mostly limited by the workload of air traffic controllers. Research initiatives like Single European Sky ATM Research (SESAR), and the USA equivalent NextGen, aim to develop new, advanced technologies and procedures to improve the efficiency and effectiveness of the ATM system while sustaining the level of safety and security [1].

One of the innovative procedures that should characterise the future ATM system is named Trajectory Based Operations (TBO), which concerns the separation of aircraft through strategic, long-term 4D-trajectories, rather than the current

approaches that are based on tactical, short-term interventions by controllers for conflict resolutions [2]. The 4D-trajectory represents the flight path from departure to arrival in four dimensions: latitude, longitude, altitude, and time.

The effective implementation of concepts like TBO relies on the accurate prediction of the flight path by a Trajectory Predictor (TP). The quality of these predictions is highly impacted by the uncertainties that are associated with the evolution of a flight trajectory. Traditionally, TPs are modelled using deterministic techniques and models which do not explicitly capture the sources of uncertainty that affect the predictive accuracy [3]. These models provide a single trajectory forecast without expressing the uncertainty of the predictions.

This study proposes two probabilistic approaches that incorporate the modelling of uncertainties to predict aircraft descent trajectories arriving at Schiphol Airport. Both a model-based- and data-driven technique are applied which provide a predictive distribution of trajectories rather than a single estimated trajectory. The predictive distribution allows for the quantification of the uncertainty of the predictions. This study aims to apply these probabilistic techniques to model and quantify the uncertainty of the trajectory predictions.

This paper is structured as follows. Section II describes the related work in which previous studies are explored and the main sources of uncertainties are defined. Also, the predictive techniques and their applications in other studies are described. Then, the research methodology is explained in Section III where the probabilistic approaches are elaborated. The results are presented in Section IV, after which a discussion is provided in Section V. The conclusions of this project and recommendations for future work are presented in Section VI and VII respectively.

## II. RELATED WORK

This section elaborates on the performed literature study that explores previous studies concerning aircraft trajectory predictions. First, applications of both model-based- and data-driven approaches are discussed. Subsequently, approaches used to group trajectories with similar features into clusters are presented. These clustering techniques are applied to train the predictive models more effectively. Lastly, different sources of uncertainties in trajectory predictions are presented, together

with a selection of probabilistic techniques that are used to model those uncertainties in predictive models.

#### A. Model-based trajectory prediction

Classical model-based TPs apply a physics-based Aircraft Performance Model (APM) of the aircraft to simulate and predict aircraft trajectories. The structure of such models is based on kinetic assumptions and the aircraft is usually represented as a point-mass [4]. The model parameters are estimated based upon the performance parameters of the aircraft, the expected atmospheric condition, and the expected operational strategies of the flight operated by the Flight Management System (FMS) or the pilot, also referred to as aircraft intent [5]. One of the most widely applied APM is adopted by the Base of Aircraft Data (BADA), developed by Eurocontrol. This model has been widely adopted in the field of ATM research to simulate and predict aircraft trajectories [6].

The aircraft intent describes the way the aircraft is expected to be operated by the FMS or the pilot. The most detailed form of aircraft intent could be derived from the FMS, which provides more information than found in regular flight plans filed before the flight. Bronsvort et al. [7] extracted FMS trajectory data and used it to derive an extensive description of the aircraft intent. The study showed a significant improvement in the predictive accuracy of the descent trajectory when detailed longitudinal intent is specified.

Apart from the aircraft intent and the APM, an environmental model, that includes forecasts of meteorological properties, is a fundamental building block of a model-based TP. Alligier [8] included temperature and wind fields as atmospheric properties affecting the climb performance of an aircraft. De Leege et al. [9] used surface winds and altitude winds as the meteorological inputs to predict the trajectory of an aircraft flying a Continuous Descent Operation (CDO). The implementation of the wind components in the TP positively affected the predictive accuracy.

Although the use of APMs has positively contributed to the development of more accurate TPs, most models are limited due to the simplifications of the flight dynamics. Besides, assumptions are introduced when aircraft-specific parameters like the aircraft mass or the fuel consumption are not known precisely.

#### B. Data-driven trajectory prediction

The increasing availability of trajectory data has given rise to the popularity of data-driven techniques that apply machine learning models to predict aircraft trajectories. Several studies have extracted trajectory data from radar observations [10]–[12]. However, the improved accuracy obtained from Automatic Dependent Surveillance-Broadcast (ADS-B) technology has made ADS-B the preferred source of trajectory data. ADS-B is a satellite-based surveillance technology that allows aircraft to transmit identification, velocity, and positional information to surrounding aircraft and ground stations. Data-driven approaches often aggregate the trajectory data with meteorological data and data that expresses the aircraft intent.

The meteorological data could be extracted from various databases. De Leege et al. [9] extracted wind fields from the Global Forecast System (GFS), which is a global weather forecast model produced by the National Centers for Environmental Prediction (NCEP). This model has a spatial resolution of 28 kilometres and provides meteorological forecasts up to an altitude of 55 kilometres. Zhang et al. [13] resorted to the database maintained by the European Centre for Medium-Range Weather Forecasts (ECMWF), which has a grid resolution of approximately 80 kilometres. The ERA5 dataset, part of the ECMWF, uses a grid resolution comparable to the GFS model and provides hourly estimates of a large number of atmospheric variables.

Aircraft intent data is commonly derived from ICAO flight plans [14]. These plans typically contain the type of aircraft, cruising speed, cruising level, and waypoints describing the intended route [15].

A data-driven predictive model aims to exploit different sources of data to extract relevant features of the trajectory that could be used to predict the position of the aircraft. A broad variety of machine learning techniques are applied in studies that develop data-driven TPs. Hamed et al. [16] proposed statistical regression models that assumed the aircraft position to be a function of a set of dependent variables. The past aircraft positions, current speed, temperature, and wind conditions were selected as dependent variables. The study concluded that the regression model obtains more accurate predictions compared to the model-based approach that used the BADA APM. De Leege et al. [9] used Generalised Linear Models (GLM) to predict arrival times of descending aircraft. The study identified the aircraft type, initial altitude, and initial ground speed as the input variables with the greatest statistical power to predict the arrival time. Also, Neural Networks have been widely adopted in data-driven trajectory predictions [17], [18]. Wang et al. [5] applied the so-called Multi Cells Neural Network (MCNN) to predict air traffic in the Terminal Manoeuvring Area (TMA). The term 'multi cells' refers to multiple sets of trajectories that were identified from trajectory clustering techniques. A Neural Network (NN) was applied to each of these trajectories.

#### C. Trajectory clustering

To train predictive models more effectively, the developed model is commonly trained on sets of trajectories that share similar features. These sets are found after applying clustering techniques. One of the most frequently applied methods is the Density-Based Spatial Clustering of Applications with Noise (DBSCAN) [19]. DBSCAN groups together trajectories that are in the vicinity of each other based on a specified distance metric. The algorithm uses two parameters:

- *eps* ( $\epsilon$ ) is a distance threshold used to decide whether two trajectories are sufficiently close to be in the same cluster.
- *MinPts* defines the minimum required number of trajectories to form a cluster.

This algorithm has proven to be effective in clustering trajectories while discarding outliers [20], [21].

#### D. Performance evaluation of TPs

The majority of studies evaluated the TP on the predictive accuracy which could either be expressed by the spatial- or the temporal error between the predicted- and actual trajectory [7], [14]. Several sources of uncertainty affect the predictive accuracy. For example, an APM includes simplifications of the flight dynamics and might require estimations of unknown parameters like the mass of the aircraft. Besides, weather forecasts inherently contain an element of uncertainty, and the lack of detailed aircraft intent descriptions also introduces a source of uncertainty. The majority of studies do not consider these uncertainties and produce a single predicted trajectory, without stating the level of certainty of the prediction. The following sections will elaborate on different sources of uncertainty in trajectory predictions and explain probabilistic techniques that model these uncertainties.

#### E. Modelling uncertainty

Modelling uncertainty in predictive analytics involves the process of Uncertainty Quantification (UQ), which aims to describe how the uncertainty in input parameters of a predictive model affects the uncertainty of the predictions of the target variable. The initial step to this process involves the identification of different sources of uncertainty.

A variety of studies have been conducted to identify the main sources of uncertainty in aircraft trajectory predictions [22], [23]. When using an APM to simulate the aircraft trajectory, initial conditions should be specified that describe the initial state of the aircraft in terms of initial speed, position, and aircraft mass. Inherent inaccuracy in ADS-B data introduces uncertainty in position and speed measurement, and the possibly unknown aircraft mass requires the implementation of estimations [3]. Also, measurements and forecasts of meteorological parameters inevitably introduce uncertainty to the model. Besides, the lack of knowledge concerning the operational strategy of the airline is considered a major source of uncertainty, since flight plans generally provide limited information. Besides, the aircraft might deviate from its plan based on crew preferences or ATC interventions [23], [24].

Uncertainty in parameters is commonly expressed mathematically by a Probability Density Function (PDF), where many studies apply the Gaussian distribution to represent a variable, with the nominal value as its mean and the level of uncertainty expressed by the variance of the PDF [24]. Alternatively, Álvaro Rodríguez-Sans et al. [25] modelled the variable as a nominal value plus a precision error, where the precision error was modelled by a PDF.

Subsequently, the input uncertainties are propagated through probabilistic models using computational tools to identify the joint effect of the stochastic factors on the predictions of the target variable. These models apply the Bayesian framework where available prior knowledge is updated with information of observed data, resulting in a posterior distribution that could be used to infer predictions. Unlike a deterministic approach, the predictions are represented by a posterior predictive distribution rather than a single point estimate [26]. This posterior

predictive distribution is used to express the range of possible outputs at some level of confidence. Commonly, a sensitivity analysis is applied to analyse the effects of changes in model inputs on the output of the predictive model [26], [27].

A variety of probabilistic techniques could be used to model the uncertainties in trajectory predictions. The following sections will elaborate on two techniques used in this study: the model-based Particle Filtering method (PF) and the data-driven Gaussian Process Regression (GPR).

#### F. Particle Filtering

The Particle Filter (PF), also referred to as Sequential Monte Carlo method, is a simulation-based technique used for the estimation of nonlinear system states [28]. The posterior distribution of interest is represented by a set of weighted particles. The simulations are performed with a specified state- and observation model incorporated in a state-space model defined below (Eq. 1).

$$\begin{aligned} \mathbf{x}_t &= f(\mathbf{x}_{t-1}) + \omega_{t-1} \\ \mathbf{y}_t &= h(\mathbf{x}_t) + \mathbf{v}_t \end{aligned} \quad (1)$$

where  $x_t$  and  $y_t$  represent the set of system states and observations at time  $t$  respectively. The state transition function and the observation functions are presented by  $f$  and  $h$ . Both models incorporate a noise model defined by  $\omega_t$  and  $v_t$ .

The goal of the PF is to compute the probability of the system state at time  $t$  given all historic observations up till time  $t$ . This posterior distribution is expressed as  $p(\mathbf{x}_t | \mathbf{y}_{1:t})$  and could be computed using Bayes' Rule:

$$p(\mathbf{x}_t | \mathbf{y}_{1:t}) = \frac{p(\mathbf{y}_t | \mathbf{x}_t) p(\mathbf{x}_t | \mathbf{y}_{1:t-1})}{p(\mathbf{y}_t | \mathbf{y}_{1:t-1})} \quad (2)$$

The PF computes the posterior distribution recursively by using incoming measurements from the observation model. Initially, at  $t = 0$ ,  $N$  particles are drawn from the prior initial state distribution. Each particle is weighted equally. Hereafter, the PF algorithm repetitively performs the following three steps [28].

##### 1) Measurement update

The weights of the particles are updated using new measurements from the observation model. These weights are updated according to the likelihood of the observation  $y_t$  being related to the state at time  $t$   $x_t$ . Hence, the weights are proportional to the observation likelihood  $p(x_t | y_t)$ . Finally, the weights are normalised such that all weights sum to 1 again.

##### 2) Resampling

A new set of particles is chosen based on the importance weights assigned to them during the measurement update. After the resampling step, the particles are weighted equally again.

##### 3) State update

The particles are propagated forward in time using simulation of the state model.

The PF has been widely adopted to estimate unknown parameters and infer predictions in systems that show non-linear and possibly non-Gaussian behaviour. Sun et al. [29] applied the PF to estimate the mass of the aircraft and its thrust setting during the initial phase of the climb. Both states were initially drawn from uniform distributions, with the mass limited by the Operating Empty Weight (OEW) and the Maximum Take-Off Weight (MTOW). A performance model and ADS-B observations were used to propagate the particles forward in order to generate the posterior predictive distribution of both states. Results showed that the PF yielded a mean absolute error of approximately 4.3% of the true mass. Lympieropoulos and Lygeros [28] applied the PF to predict aircraft climb trajectories that were subjected to uncertain parameters due to inaccurate weather information and unknown mass of the aircraft. The study showed that, as new measurements arrived, the predicted trajectory converged to the real trajectory. The model was able to capture the non-linear dynamics of the aircraft to accurately predict the position of the aircraft.

### G. Gaussian Process Regression

Gaussian Processes (GP) represent a collection of random variables indexed by time or space, where any finite set of those variables forms a multivariate normal distribution. The random variables express the evaluation of a function  $f(x)$  at a possibly multidimensional input location  $x$ . The goal of GPR is to learn the underlying distribution from a set of specified training data points. The set of training data could be fitted by potentially infinitely many functions, and GPR provides an elegant approach to assign a probability to each of these functions [30]. Hence, the GP defines a probabilistic distribution over functions. The mean of this distribution represents the most probable characterisation of the data.

GPR is a non-parametric regression approach that applies the Bayesian framework, where the prior information is characterised by a GP formed by its mean function  $m(x)$  and covariance function  $k(x_i, x_j)$  (Eq. 3).

$$f(x) \sim GP(m(x), k(x_i, x_j)) \quad (3)$$

For simplicity, the mean function  $m(x)$  is often assumed to be zero. The characteristics of  $f(x)$  are fully specified by the selected covariance function, also called the kernel. The kernel takes two points  $x_i$  and  $x_j$  as inputs and returns a similarity measure. Hence, the kernel is used to specify the correlation between different data points. The kernel is evaluated for each pairwise combination of  $N$  data points to retrieve the covariance matrix  $K(X, X)$ .

$$K(X, X) = \begin{bmatrix} k(x_1, x_1) & \dots & k(x_1, x_N) \\ \vdots & \ddots & \vdots \\ k(x_N, x_1) & \dots & k(x_N, x_N) \end{bmatrix} \quad (4)$$

A variety of kernels are discussed in literature [30], [31], where the most commonly adopted kernel is the Radial Basis Function (RBF) (Eq. 5) which is applied to model smooth functions.

$$k(x_i, x_j) = \sigma_f \exp\left(-\frac{\|x_i, x_j\|}{2\ell}\right) \quad (5)$$

The RBF includes two hyperparameters:  $\sigma_f$  defines the amplitude that specifies the maximum allowable covariance, and  $\ell$  expresses the length scale parameter which specifies the rate of decay of correlation between points farther away from each other. These parameters could be tuned to adapt the shape and smoothness of the function.

When the covariance function is selected, and the hyperparameters are learned, GPR is applied to estimate the value of a function evaluated at any set of new inputs  $X^*$ . The joint distribution of (possibly noisy) observations  $y$  and predicted values  $y^*$  is expressed as a multivariate normal distribution (Eq. 6).

$$\begin{bmatrix} y \\ y^* \end{bmatrix} \sim \mathcal{N}\left(0, \begin{bmatrix} K(X, X) & K(X, X^*) \\ K(X^*, X) & K(X^*, X^*) \end{bmatrix}\right) \quad (6)$$

The predictive distribution  $y^*$ , conditional on the training data  $(X, y)$  and the provided test data  $X^*$ , is then represented as follows:

$$\begin{aligned} y^* | X^*, X, y &\sim \mathcal{N}(\mu, \Sigma) \\ \mu &= K(X^*, X) K(X, X)^{-1} y \\ \Sigma &= K(X^*, X^*) - K(X^*, X) K(X, X)^{-1} K(X, X^*) \end{aligned} \quad (7)$$

An application of GPR to predict a function  $f(x)$  is shown in Figure 1. The 95% prediction interval, depicted by the shaded grey area, increases when moving further away from the observations. When the training data is assumed to be noiseless, the predicted function converges in these data points.

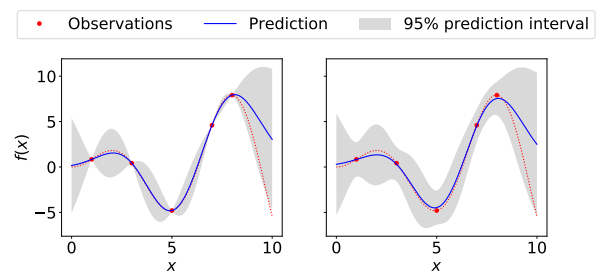


Figure 1. Example of one-dimensional GPR application to predict  $f(x)$  with the RBF kernel. The noiseless case is presented in the left graph, while the graph to the right incorporates noisy observations.

Several applications of GPR were found in the literature. Tran and Firl [32] modelled the speed of a car in  $x$ - and  $y$ -direction as two independent GPs in order to model and predict the traffic near intersections. The same approach was

used by Goli et al. [31] to model traffic in a road transportation network. Rong et al. [33] applied GPR to obtain the distribution of the lateral position of a ship along its trajectory. The predictions were updated when new positional observations arrived. The studies described above all made use of the RBF kernel. Other studies used GPR to estimate aircraft-specific parameters like the aircraft mass and the fuel flow rate [34], [35].

### III. METHODOLOGY

The project was split up into three phases. The initial phase concerned the collection and preparation of the dataset, which also includes the clustering of the trajectories on which the predictive models were trained. The development of those models is part of the second phase. Ultimately, the final phase comprised a predictive analysis that evaluated the accuracy and uncertainty of the predictive models.

#### A. Data collection

The previous section emphasised the importance of aircraft intent and meteorological parameters to improve the accuracy of a TP. For this purpose, different sources of data were exploited to construct a set of data that incorporates these flight features.

1) *ADS-B data*: The ADS-B data acts as the foundation of the final dataset. This data was sourced from the ground station configuration of TU Delft which receives ADS-B messages with a coverage of approximately 400 kilometres. A decoded set of ADS-B data contains velocity and position updates at irregular timestamps [36]. Each data entry is linked to a specific ICAO code, which was used to uniquely identify an aircraft. Eventually, DBSCAN used the timestamp and the ICAO code as main features to cluster ADS-B sequences to extract and identify continuous flights from the dataset [21].

2) *Aircraft data*: An aircraft database was exploited to add aircraft-specific parameters to the dataset. The type of aircraft could be added to each ADS-B observation using the ICAO registration. To indicate the mass of the aircraft, which usually is not publicly accessible, the Wake Turbulence Category (WTC) of the specific aircraft type was included in the dataset. Wake turbulence is the disturbance of the air behind an aircraft, and the strength of the turbulence is primarily dependent on the aircraft's weight. ICAO specifies the WTC based on the Maximum Take-Off Weight (MTOW) of the aircraft.

3) *Flight Plan data*: The aircraft intent was expressed using information extracted from flight plans that were released by Eurocontrol. Eurocontrol provided a selection of individual months of flight plan data. The most recent month, June 2018, was chosen for this study. A variety of datasets were provided (Table I).

Table I  
FLIGHT PLAN DATA OBTAINED FROM EUROCONTROL.

Dataset	Description
Flights	Flight-specific information like: flight identification (ECTRL ID), departure- and arrival airport, market segment of airline
Filed flight points	Sequence of three-dimensional waypoints over time describing the intended route of the flight
Actual flight points	Updated flight route based on radar measurements

Each ADS-B observation was aggregated with its corresponding ECTRL ID using the ICAO registration and rounded timestamps of the actual flight points. The aircraft intent was expressed by adding the upcoming three waypoints from the actual flight points to the ADS-B dataset. In order to identify the next three waypoints for each ADS-B record, the distance from departure airport was computed to establish a variable that describes the progress of the flight. Based on this variable, the next three waypoints were selected from the filed flight points. Each waypoint comprises the latitude, longitude, and altitude of the aircraft together with a time component. This time component ( $t_{wp}$ ) expresses the difference in total flight time up till the specific waypoint ( $T_{planned}$ ) and the actual flight time since take-off as observed from the ADS-B record ( $T_{actual}$ ) (Eq. 8).

$$t_{wp} = T_{planned} - T_{actual} \quad (8)$$

4) *Meteorological data*: Meteorological forecasts were extracted from the ERA5 database. This database provides estimates of a large variety of meteorological parameters on an hourly basis. The data is formatted in a grid with a spatial resolution of 30 kilometres and divides the atmosphere into 137 different pressure levels up to a height of 80 kilometres. For this study, the wind speeds in three dimensions and the temperature were extracted from the database. Since the available ADS-B data covers a sub-region of Europe, the extraction of meteorological data is limited to this region with longitudes ranging from -10 to 30 degrees and latitudes ranging from 30 to 70 degrees. These boundaries ensure that all flights could be aggregated with the selected meteorological parameters. A linear interpolation model was developed to express the parameters as a function of the four dimensions (latitude, longitude, altitude, and time). This function was evaluated at the given ADS-B records, such that each observation would be aggregated with the meteorological forecasts.

#### B. Data preparation

As observed from Figure 2, a variety of preparation steps were executed to construct the final dataset. These steps are described below.

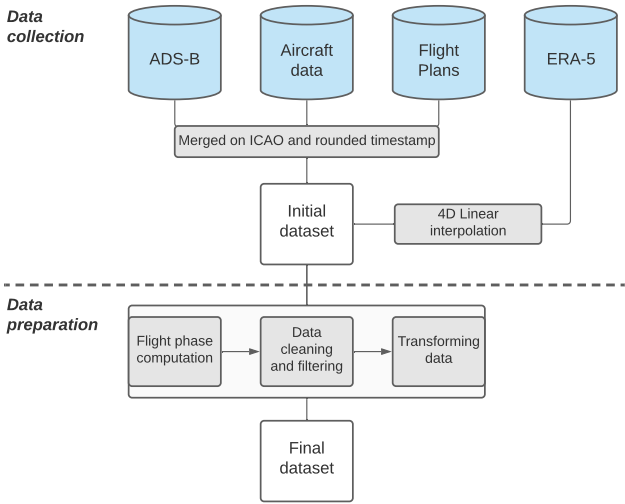


Figure 2. Process overview of the collection and preparation of data.

a) *Flight phase computation*: This study aimed to predict aircraft trajectories during the descent phase of the flight, which required the identification of the flight phase. A Python library, developed by Sun et al. [36], was used to segment the trajectories into different flight phases, being climb, cruise, level, and descent. The phases were identified using fuzzy logic operators that considered the ground speed, rate of climb, and altitude in order to establish the most probable flight phase.

b) *Data cleaning and filtering*: To establish a complete set of data and ensure that the quality of the data was sufficient for the predictive analysis, certain cleaning and filtering steps were performed. These steps include, among others, the consistent formatting of variables and the linear interpolation of missing numerical values. Besides, flights that contained less than 30 records were removed from the dataset. To obtain regular intervals between the data records, the dataset was resampled into five-second intervals. The final dataset comprised partial trajectories of descending aircraft arriving at Schiphol Airport. Ultimately, a consistent dataset was established that included partial descent trajectories whose initial data point was found above 25,000 feet (FL250), while the final data point was located at the arrival airport.

c) *Data transformation*: The final step performed to obtain the final dataset was the transformation of certain features. The position of the aircraft, originally expressed in latitude and longitude, was converted to a Cartesian reference frame with a fixed, random origin to derive  $x$ - and  $y$ -coordinates. This was required for the particle filter, discussed in the later section, which uses a Cartesian reference frame to model the speed- and position updates of the aircraft. The categorical features were converted to numeric variables using one-hot encoding, which splits the categories into

separate columns and assigns binary variables to indicate the appropriate category. The WTC categorises Heavy ( $MTOW \geq 136,000$  kg), Medium ( $7,000 \text{ kg} < MTOW \leq 136,000$  kg), and Light ( $MTOW \leq 7,000$  kg) aircraft. Furthermore, five different market segments were defined that described the airlines' operations: cargo, business aviation, unscheduled (e.g. charter), low-cost, or traditional scheduled.

An overview of the features that were used as predictors to the predictive models is found in Table II.

Table II  
FEATURES USED IN TRAJECTORY PREDICTION MODELS.

ADS-B	FP <sup>1</sup>	ERA5	Other
rate of climb [ft/min]	$x_i$ [m]	wind x [m/s]	WTC [-]
ground speed [kts]	$y_i$ [m]	wind y [m/s]	Market [-]
track [deg]	$alt_i$ [ft]	wind z [Pa/s]	
	$t_i$ [s]	temp. [K]	

<sup>1</sup> The upcoming three waypoints are included ( $i \in \{1,2,3\}$ )

### C. Clustering trajectories

DBSCAN was used to cluster trajectories into groups of flight tracks that show similar spatial patterns. The algorithm used the  $x$ - and  $y$ -coordinates of the flight trajectories to specify the spatial pattern. After resampling, each flight track was represented by 30 data points. Subsequently, the features of the dataset were scaled such that each feature ranged between zero and one. The algorithm requires the specification of two parameters:  $\epsilon$  and MinPts. Initially, the MinPts was specified, after which the optimal value for  $\epsilon$  was found using the  $k$ -Nearest Neighbour ( $k$ -NN) algorithm [37]. This method relies on computing the minimum distance of each trajectory to its  $k$  nearest trajectories, where  $k$  was set to MinPts. Then, the computed distances were plotted in ascending order, and the optimal value for  $\epsilon$  was found at the point of greatest curvature. To compute distances between trajectories, the widely adopted Euclidean distance metric was used [19].

The performance of the clustering algorithm was evaluated with a visual inspection together with the evaluation of the Silhouette coefficient. This metric, ranging between -1 and 1, specifies the similarity of the trajectory to its own cluster, and the dissimilarity to other clusters. The higher the coefficient, the better the clustering results.

### D. Development of Particle Filter model

The implementation of the PF is based upon the study of Sun et al. [29] that applied the PF to estimate the aircraft mass ( $m$ ) and thrust setting ( $\delta_T$ ) during a 30-second segment right after take-off. The OpenAP APM was used to simulate the aircraft trajectories by propagating the particles, that represent the observable states, forward in time [38]. The weights of the particles are updated using incoming observations. The observable states comprise the aircraft position and ground speed in

a Cartesian reference frame with its origin placed at the first position. Besides, the wind speed ( $\vec{v}_w$ ) and temperature ( $\tau$ ) are part of the observable states. The state- and measurement vector at time  $t$  are:

$$\begin{aligned} \mathbf{x}_t &= [m_t, \delta_{T,t}, x_t, y_t, z_t, \vec{v}_{a,t}, v_{z,t}, \vec{v}_{w,t}, \tau_t] \\ \mathbf{y}_t &= [\tilde{x}_t, \tilde{y}_t, \tilde{z}_t, \tilde{v}_{g,t}, \tilde{v}_{z,t}, \tilde{v}_{w,t}, \tilde{\tau}_t] \end{aligned} \quad (9)$$

The true airspeed ( $\vec{v}_{a,t}$ ) in the observed states is computed by subtracting the wind speed vector ( $\vec{v}_{w,t}$ ) from the measured ground speed ( $\vec{v}_{g,t}$ ). The observations are subjected to noise caused by sensor errors. An observation noise model is incorporated to account for these uncertainties. The observation noise was assumed to be uncorrelated additive Gaussian noise, such that the noise model  $\mathbf{v}$  in Eq. 1 could be modelled as a multivariate Gaussian distribution. ADS-B transponders need to comply with regulations that specify the minimum accuracy of sensors. Uncertainty indicators of the velocity- and position updates are transmitted through ADS-B. These indicators were used to select the standard deviation of the measurements to construct the observation noise model [29].

Sun et al. [29] applied the PF to a 30-seconds segment and assumed the aircraft mass to be constant. This study, however, analyses the entire descent trajectory. Therefore, the aircraft mass was updated at each time step by incorporating the fuel flow (FF), according to Eq. 10.

$$m_{t_1} = m_{t_0} - FF \quad (10)$$

Initially, a set of 50,000 particles were drawn from the initial distribution  $p(\mathbf{x}_0)$ . The majority of the observable states were drawn from normal distributions, with the mean equal to the initial measurement, and the standard deviation obtained from the noise model. The aircraft mass was drawn from a uniform distribution with the Operating Empty Weight (OEW) as the lower limit, and the Maximum Landing Weight (MLW) as the upper limit. The thrust setting, drawn from a uniform distribution, was limited by 0.01 and 0.30. When new measurements arrive, the weights of the particles were properly adjusted based on the likelihood of the state to be corresponding to the new measurement. Starting from the initial observation of the flight, these measurements arrive at a five-second interval until FL250 is reached. A resampling step is incorporated every time step to prevent the impoverishment of the particles. This step redistributes the particles by replacing low-weighted particles with high-weighted particles. Also, certain restrictions were included to remove particles with unlikely states by assigning zero weight to these particles. Then the redistributed particles were propagated forward in time according to the simulation of the model.

### E. Development of GPR model

The GPR model was developed using the multivariate GPR implementation from the scikit-learn library in Python, which implemented the algorithm as described by Rasmussen and Williams [30]. To effectively exploit the historical traffic patterns, each cluster of flights was used to train a GPR

model. The features of each dataset, corresponding to a cluster, were standardised by removing the mean and scaling to unit variance. This made sure that the output function would have zero mean, which is a common assumption in GPR modelling. Besides, many covariance functions include scale parameters that are trained more effectively on standardised datasets. The flights in the standardised dataset were split into two subsets used for training and testing, where 25% of the flights were assigned to the training set. To predict the progression of an individual testing flight, both the data of the historical, training flights as well as past data of its own flight are used to develop the model. Therefore, the implementation of GPR is split into two stages.

Three main building blocks are required to train a GPR model. First of all, a training dataset was constructed that contained both the target variables (x, y, and altitude) as well as the predictor variables. Three different GPR models, trained on different sets of predictors, were developed on each cluster of trajectories (Table II). Secondly, a covariance function (kernel) was selected. This function highly influences the shape of the predicted trajectory. Three different kernels were selected that model relatively smooth functions: RBF, Rational Quadratic, and the Matérn kernel. These kernels have been combined with a sum-kernel including a linear kernel. This linear kernel accounts for modelling relatively straight segments. Thirdly, the alpha parameter is specified to prevent numerical issues during fitting and could be interpreted as the additional variance on the training data.

Table III  
THREE DIFFERENT GPR MODELS TRAINED ON DIFFERENT SETS OF PREDICTOR VARIABLES.

GPR Model	Predictor variables
GPR-A	ADS-B data only
GPR-B	ADS-B and Flight Plan data
GPR-C	ADS-B, Flight Plan, and ERA5 data

The first stage aimed to develop a GPR model (GPR-1) based on the training data from historical trajectories in each cluster. To limit the processing time, the number of data points that form each trajectory was reduced with the Ramer-Douglas-Peucker (RDP) algorithm. This algorithm tries to simplify a curve connected by points, by representing that curve with fewer points. This required the specification of a maximum distance that the simplified 3D-trajectory is allowed to deviate from its original trajectory. This distance was set to 100 meters, which was established by visually inspecting whether the simplified trajectories were still able to capture the turns performed by the aircraft.

The best-fitted kernel and its corresponding hyperparameters were found after applying k-fold cross-validation. This technique shuffles the training set and splits it up into k groups. Then, the model is fitted on k-1 groups and tested on the remaining group. This is repeated until all groups have been

assigned as the test group. The predictive accuracy is estimated for each round, and the results were averaged to determine the best-fitted model.

To predict the trajectories of the testing flights, each flight was fitted to a second model (GPR-2) that was trained on a dataset specifically constructed for each flight. This dataset comprises not only past historical observations of the particular flight, but also predicted positions generated by GPR-1. The start of the prediction horizon, at time  $T_0$ , is specified at the point where the trajectory reached FL250. The predicted positions were obtained by sampling from GPR-1 on unseen data points of the flight below FL250. To sample from GPR-1, a dataset containing the predictor variables of the actual flight below FL250 should be constructed. This required the estimation of the ADS-B predictors (ground speed, rate of climb, and track angle) beyond  $T_0$ . These variables were predicted using a separate GPR model with an RBF kernel, which was trained using past trajectory data and training data from the set of training flights. The FP data and the ERA5 variables were not predicted as the FP data is available prior to the flight and the meteorological dataset contains forecasts that cover the predictive horizon. GPR-1 exploited the set of predictor variables to sample 1000 data points at each timestamp beyond  $T_0$  until the final waypoint of the FP was reached. The means of the samples were selected to construct the training dataset for GPR-2. Figure 3 provides an example of the construction of training data, which shows both the historical observations ( $< T_0$ ) as well as the GPR-1 samples ( $> T_0$ ). The finalised training dataset was used to develop GPR-2 using the same procedure that was used to train GPR-1. In this case, the variance of the samples beyond  $T_0$  from GPR-1 was used to specify the alpha parameter on the training data.

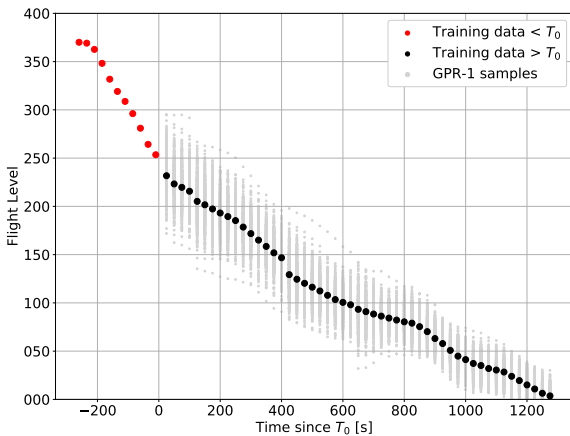


Figure 3. Construction of training data for GPR-2.

#### F. Analysis of the predictions

The developed predictive models were applied to model and predict the descent trajectories from a specified altitude (FL250) to the arrival at Schiphol Airport. While this study focused on the quantification of the uncertainty of the predictions, the accuracy was also measured. As the models provide

a predictive distribution, both the uncertainty and accuracy of the predictions could be considered. The mean of the predictive distribution was considered as the most probable prediction and thus used to compute the accuracy metrics. The accuracy of the predictions is related to the spatial and temporal errors between the actual- and predicted trajectory. The horizontal- and vertical errors were computed, where the Horizontal Track Error (HTE) was further specified in the Along-Track Error (ATE) and the Cross-Track Error (CTE). The ATE is the longitudinal distance, parallel to the predicted trajectory, between the predicted- and actual position of the aircraft. The CTE is the spatial error perpendicular to the predicted flight track. The computations of the horizontal errors rely on the flat earth approximation which is justified by the relatively small distances that are covered. The vertical error is the difference in altitude between the predicted- and actual trajectory, with a negative error indicating that the predicted position is lower than the actual aircraft position. The temporal error is measured at FL100 and indicates the difference in time when the predicted- and actual trajectory have reached this altitude.

The uncertainty was quantified by computing the standard deviation ( $\sigma$ ) of the sampled predictions of the 3D-position, indicating the spread of the predicted position of the aircraft. Both accuracy- and uncertainty measures were evaluated at every 1000 feet starting from the start of the prediction horizon at  $T_0$ . Besides, different look-ahead times were evaluated to analyse the progression of the predictive metrics over time.

## IV. RESULTS

### A. Constructed dataset

A final dataset was constructed which forms the foundation on which both the PF as well as the GPR models were developed. This dataset comprises 9363 partial trajectories of flights arriving at Schiphol Airport. The majority of flights are operated by traditional airlines performing scheduled flights. Most flights are operated by short-haul aircraft like the B737 and the A320. While both the PF and the GPR models are constructed using this dataset, the PF model only exploits the ADS-B data and the meteorological data. The flight plan data is only consulted to train the GPR models. More information concerning the final dataset is found in Appendix A.

### B. Clustering trajectories

Initially, DBSCAN was applied to cluster the flights arriving at Schiphol Airport. The minimum number of trajectories required to form a cluster (MinPts) was set to 100. The k-NN distance plot showed the greatest point of curvature at an  $\epsilon$  of approximately 0.50. This value does not express any physical distance because all features were standardised. To find the optimal combination of MinPts and  $\epsilon$ , MinPts was evaluated over a range between 40 and 800 in steps of 40, while  $\epsilon$  was varied between 0.40 and 0.70 in steps of 0.02. An extensive analysis of the results for different parameter combinations is found in Appendix B. The optimum clustering results were obtained when MinPts was set to 80, with  $\epsilon$  equal

to 0.60. This resulted in a Silhouette score of 0.39. Eventually, four clusters were identified, and only 6.5% of the flights were labelled as an outlier. The results showed that the majority of outliers were flights that were put in a holding pattern awaiting clearance from ATC to proceed with the landing. As these irregular flying patterns could disrupt the predictive algorithms, these flights were removed from the dataset. A visual representation of the identified clusters is presented in Figure 4.

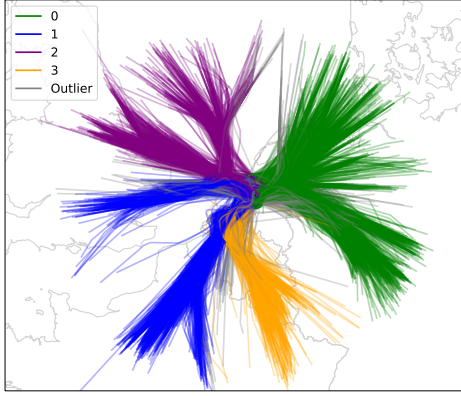


Figure 4. Clusters of trajectories identified by DBSCAN algorithm.

The results showed that DBSCAN has not effectively identified all groups of similar trajectories. As shown in Figure 4 above, a large set of flights arriving from the East have been grouped into one cluster. Besides, aircraft arriving from the Southwest and the Northwest clearly show distinct sets of trajectories which have not been identified by DBSCAN with the tuned parameters. To improve the clustering results, a second clustering step was performed by applying the K-means algorithm to clusters 0, 1, and 2. This algorithm requires the specification of the number of clusters. For this purpose, the number of clusters to be found in the initial clusters 0, 1, and 2, was set to 2. The resulting clusters, obtained after the second clustering step, are depicted in Figure 5. The legend contains the number of flights found in each cluster.

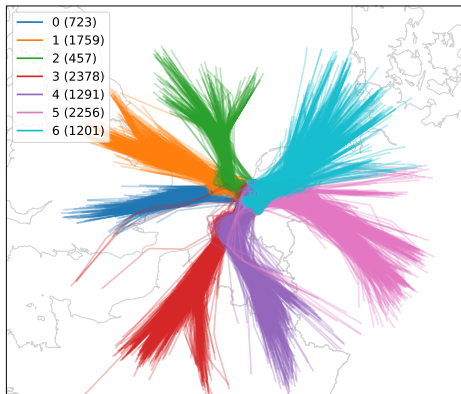


Figure 5. Refined clusters of trajectories after K-means application.

### C. Predicting trajectories

The predictive models were applied to predict the descent trajectories for each cluster found by the clustering algorithms. This section discusses the results of a variety of experiments that have been conducted. These experiments evaluate the predictive metrics obtained from different models.

1) *GPR predictions on clusters*: Figure 8 summarises the accuracy- and uncertainty metrics for all seven clusters. The results visualise the distribution of the median value for each metric evaluated over each individual predicted trajectory from a cluster. Three different GPR models were evaluated. The mean vertical error is found to be centred around zero for all clusters and models. However, GPR-A consistently shows the largest spread of vertical errors. Especially in clusters 0 till 4, GPR-A provides the largest ATE, while GPR-B and GPR-C show comparable results. The distribution of CTE shows smaller order of magnitudes compared to the ATE, with negligible differences among the three models.

The predictive uncertainty is visualised in the bottom row, which expresses the standard deviation ( $\sigma$ ) of the predictive distribution of  $x$ ,  $y$ , and the altitude. The results show that the predictive distributions obtained from GPR-A show the largest spread. Besides, GPR-B generally obtains slightly lower standard deviations compared to GPR-C. Considering the standard deviation of the horizontal position ( $x$  and  $y$ ), it is observed that clusters 0, 1, and 5 show considerable larger deviations in the predicted  $x$ -position compared to the  $y$ -position. While the opposite result is particularly found in clusters 2, 3, and 4 where  $\sigma_x$  is smaller than  $\sigma_y$ . This result is also visualised in Figure 6, in which the standard deviations are plotted in a contour plot for each cluster trained with GPR-A.

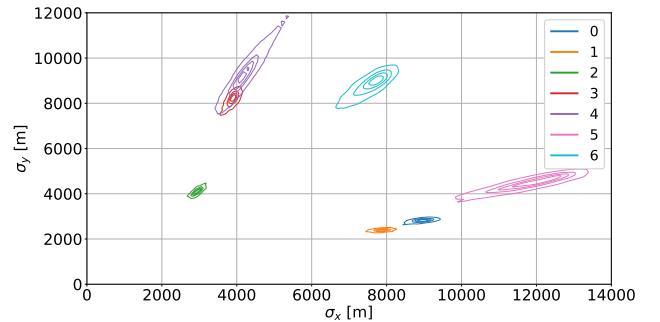


Figure 6. Contour plot showing the average standard deviations of the prediction of the horizontal position for each cluster obtained from model GPR-A.

2) *Comparison between GPR models*: The previous section evaluated the predictive capability obtained from three GPR models trained on each cluster. This section elaborates on the accuracy and uncertainty of the predictions of the cluster with the most flights: cluster 3. The predictive metrics are evaluated at different flight levels to analyse the progression of the predictive capability over the descent profile (Figure 9).

Until FL070, the distribution of vertical errors is centred around zero with GPR-C showing the smallest variance in predictive errors. During the final stage of the descent, below FL070, all models tend to overestimate the altitude of the aircraft. Initially, at FL240, the ATE does not deviate among the three models. Hereafter, GPR-B and GPR-C produce significantly smaller errors. Below FL070, the three models produce comparable results in terms of the ATE. While GPR-B and GPR-C improve the spatial accuracy along the flight track in the initial stage of the prediction horizon, the CTE does not differ among the different models. The CTE remains constant in the initial stage of the descent but rapidly increases once the altitude drops below FL070. Eventually, the errors decrease again once the aircraft gets closer to its final destination.

The spread of the predictive distributions, expressed by the standard deviation, is higher for GPR-A compared to GPR-B and GPR-C. This means that the sampled predictions from a GPR model become more concentrated if the model is trained on ADS-B data enriched with FP-data and meteorological data. The uncertainty of the predictions quickly rises until it reaches the maximum at FL200. Hereafter, the standard deviation of the predictive distributions in  $x$ ,  $y$ , and altitude all decrease until FL100 is reached. The results show that the relative difference in  $\sigma$  between the three models is comparable in each position.

3) *Effect of aircraft- and airline type:* The effect of the aircraft- and airline type was evaluated by extending model GPR-C with training data that incorporated predictor variables describing the WTC category and the airline market segment. Half of the flights in cluster 0 are operated with WTC M aircraft, while the other half is operated by WTC H aircraft. The vast majority of airlines operate in the traditional scheduled market segment. The indices of the predictive metrics, relative to model GPR-C, are presented in Table IV to show the relative difference between the models. A comparison of both models shows that the standard deviation of the predicted 3D-position increases by 33%, while the horizontal and vertical errors of the predictions are comparable (Table IV).

Table IV  
COMPARISON BETWEEN MODEL GPR-C, INDEXED AT 100, AND AN EXTENDED MODEL INCLUDING AIRCRAFT- AND AIRLINE DATA. (CLUSTER 0)

Model	HTE	VE	$\sigma_x$	$\sigma_y$	$\sigma_{alt}$
GPR-C	100	100	100	100	100
GPR-C (extended)	104	98	133	133	133

4) *Comparison between GPR and PF:* Just like the GPR models, the PF model generates a predictive distribution of the position of the aircraft. This section compares the results obtained from the model-based PF and the data-driven GPR models.

The time error defines the temporal difference when the predicted- and actual trajectory have reached FL100. As presented in Figure 7, the distribution of time errors from the GPR models generally centres around zero seconds with no remarkable differences among the different clusters. On the contrary, the PF is more likely to overestimate the change in altitude resulting in negative temporal errors at FL100.

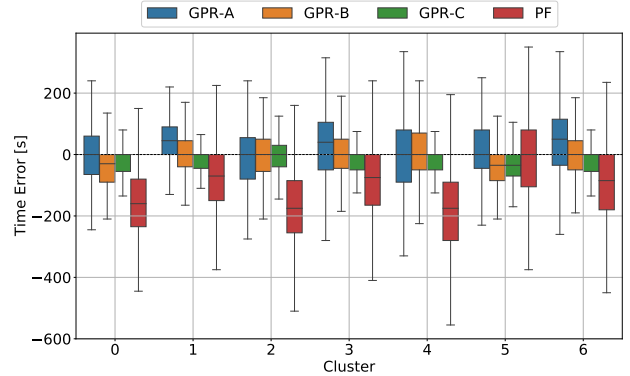


Figure 7. Temporal error measured at FL100 for different models and different clusters. A negative value indicates that the predicted trajectory reached FL100 before the actual trajectory.

Figures 10 and 11 present the accuracy- and uncertainty metrics for all models evaluated at different look-ahead times for flights from cluster 3. Again, the GPR models generate distributions of vertical errors centred around zero meters, with GPR-C providing the most consistent results. The PF model is more likely to overestimate the change in altitude, with average vertical errors of -415 m at a look-ahead time of 10 minutes. In comparison, GPR-A, GPR-B, and GPR-C provide average vertical errors of 120 m, 60 m, and -54 m respectively. The PF model generates the smallest ATE for look-ahead times up to five minutes. Also, the CTE is smaller or comparable to the GPR models for these look-ahead times. This effect was observed in all clusters. An overview of the predictive results for all clusters is found in Appendix C. When the look-ahead time further increases, both spatial errors gradually increase while this effect is less visible for the GPR models. At a look-ahead time of 15 minutes, the spatial errors of the PF become significantly higher compared to the results obtained from GPR-C.

The top row of Figure 11 shows how the standard deviations of the predictions from the PF model evolve over increasing look-ahead times. The standard deviation of the predicted altitude ( $\sigma_{alt}$ ) increases drastically until it reaches a maximum and starts decreasing again. The standard deviation in the predicted horizontal positions ( $\sigma_x$  and  $\sigma_y$ ) gradually increase over time with larger deviations in the predicted  $x$ -position, compared to the  $y$ -position. Generally, the uncertainty of the predictions from the PF model is considerably higher compared to the GPR models. However, at a look-ahead time of only one minute, the standard deviation of the predicted  $x$ - and  $y$ -position are comparable or slightly smaller than the results of the GPR models.

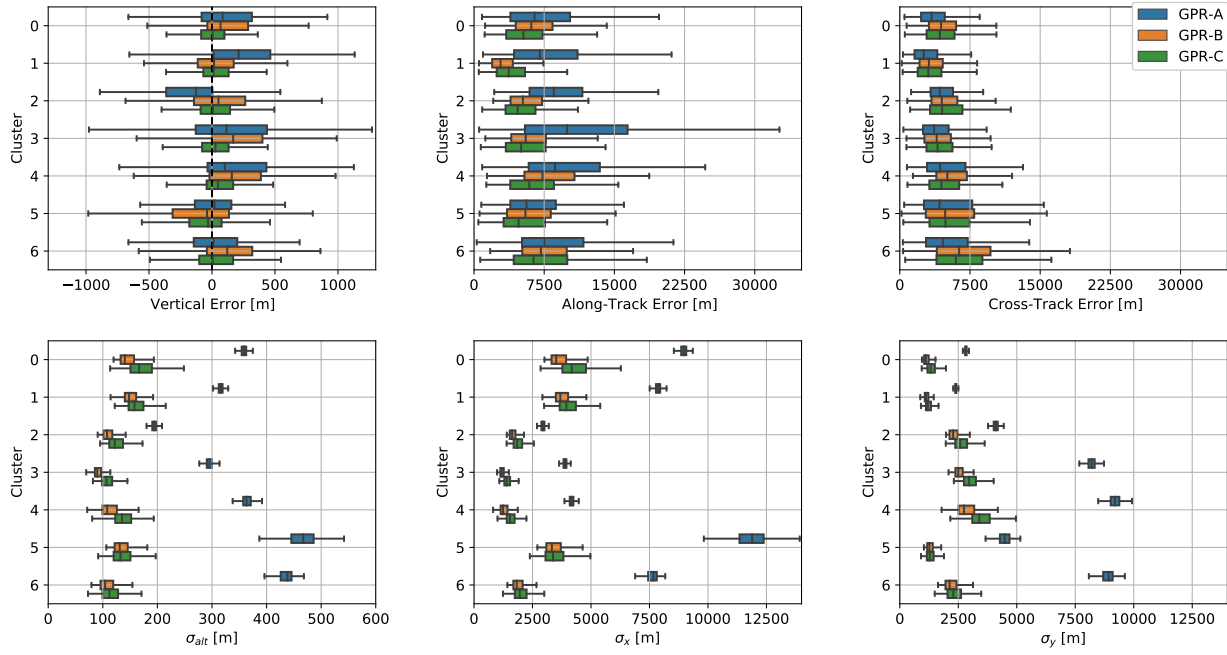


Figure 8. Predictive metrics of all clusters showing the predictive errors (top row) and the standard deviation of the predictive distributions (bottom row).

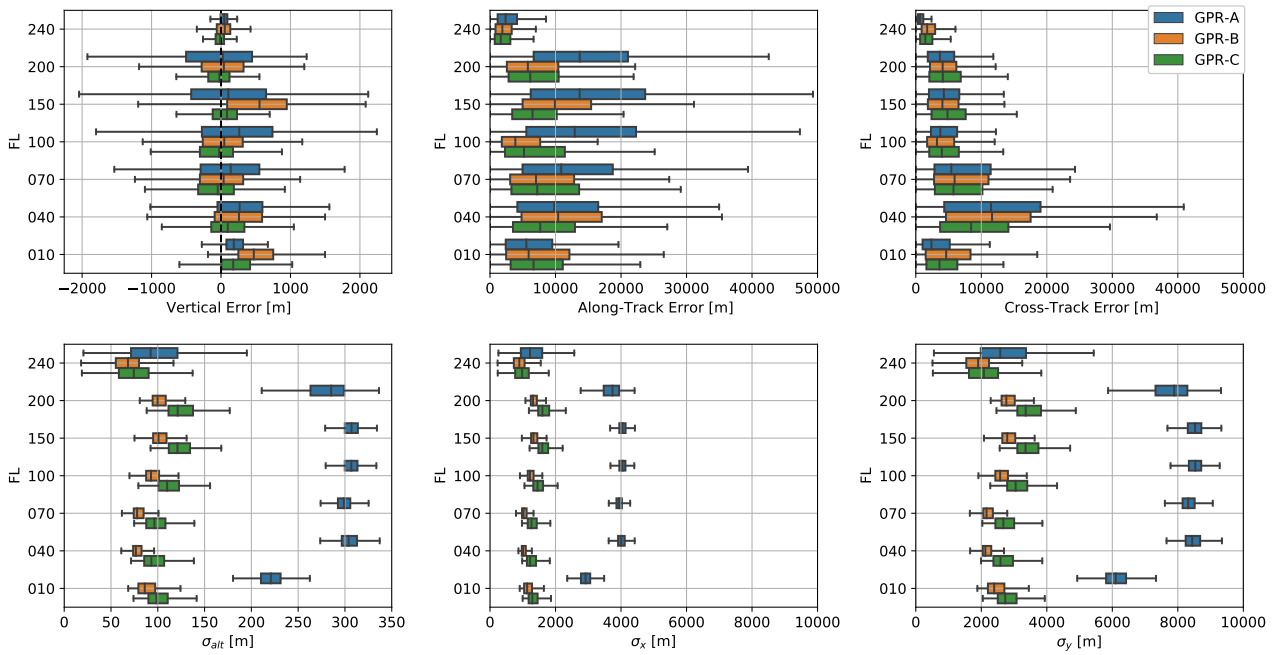


Figure 9. Predictive metrics of cluster 3 showing the predictive errors (top row) and the standard deviation of the predictive distributions (bottom row) for a variety of flight levels.

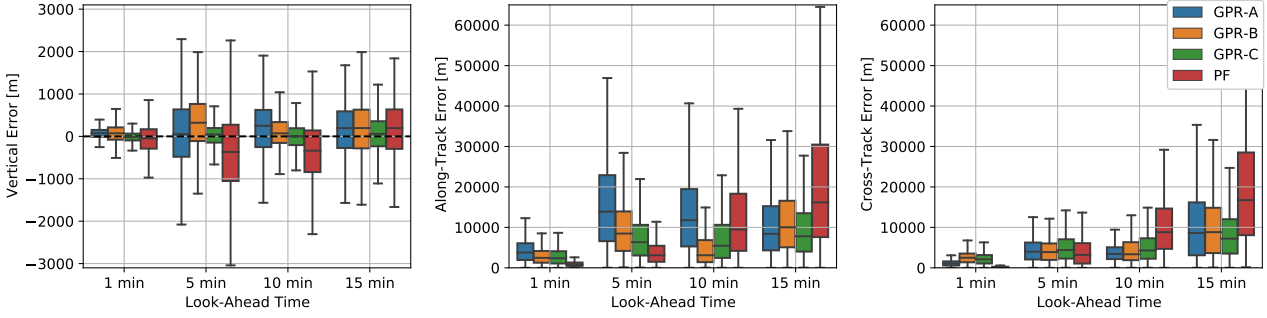


Figure 10. Comparison of predictive accuracy between the PF model and the GPR models for increasing look-ahead times in cluster 3.

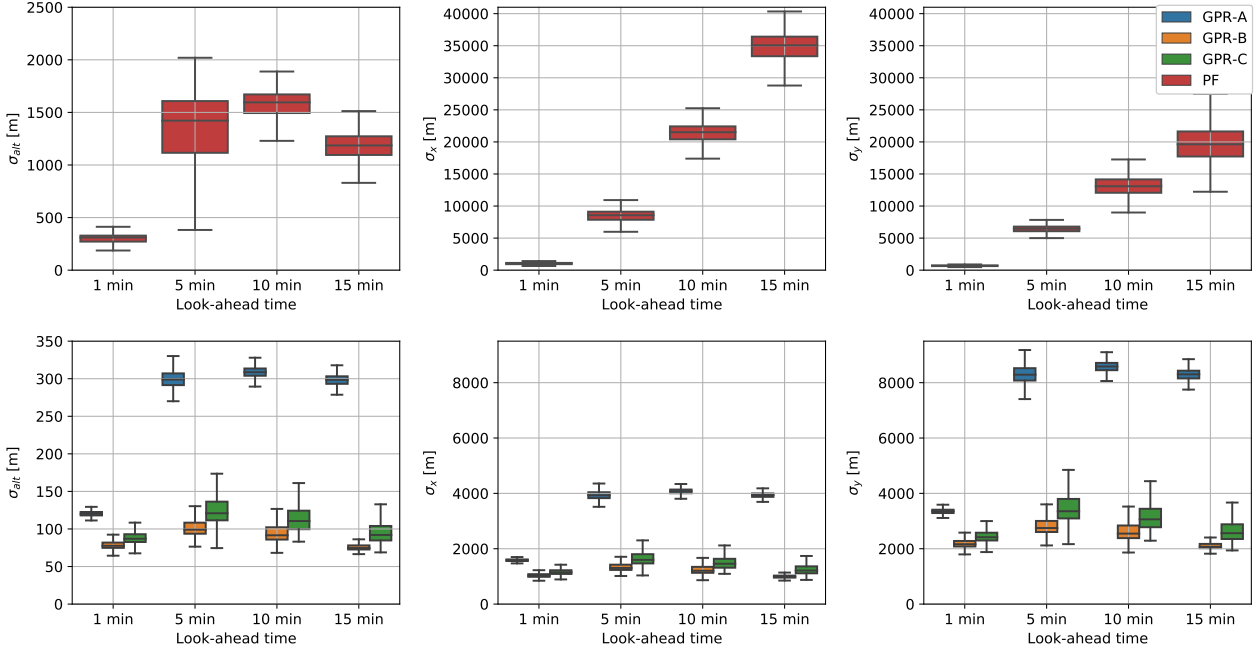


Figure 11. Comparison of the predictive uncertainty, expressed by the standard deviation of the predictions, between the PF model and the GPR models for increasing look-ahead times in cluster 3.

## V. DISCUSSION

### A. Clustering trajectories

DBSCAN used the standardised  $x$ - and  $y$ -coordinates of resampled trajectories as features to distinguish different sets of trajectories using a density-based approach. The results showed, that this approach was ineffective in capturing all clusters of trajectories. Only four clusters were identified. Tuning the parameters showed that if more clusters were identified, this was accompanied by a significant increase in the share of outliers that would exceed 25% of the total flights. The selected DBSCAN model identified roughly 6% of the flights as outliers, and these flights were removed as they showed irregular flight tracks. The effective identification of

these outliers is one of the advantages of DBSCAN. A second clustering step, using K-means on the starting positions of the trajectories, turned out to be an effective follow-up step to identify all clusters.

### B. Gaussian Process Regression

Three different GPR models with varying sets of predictor variables were trained on the identified clusters of trajectories. The results showed that the predictive accuracy could be improved when incorporating flight plan data and meteorological data when training the GPR models. Generally, the distribution of the results obtained from GPR-C shows smaller variances, which indicates that this model obtains more consistent results compared to GPR-A. The major improvements were observed

in clusters 0 up till 4, which showed significant reductions in the ATE. The differences in spatial accuracy between the models in clusters 5 and 6 were less distinct. These clusters are less distinctive as both show a larger spread in trajectory shapes. The effect of including more predictor variables diminishes when the model is trained on less distinct clusters. This proves the importance of the effective clustering of trajectories before training the data-driven models.

The results also showed that the predictive uncertainty, expressed by the standard deviation of the predictions, of GPR-A is considerably higher compared to GPR-B and GPR-C. Together with the improvement in accuracy, this proves the impact of introducing aircraft intent to train predictive models. Further extending the model with meteorological data did not result in a reduction of the standard deviation of the predictions. The standard deviation of the predicted x- and y-position is largely dependent on the direction of the flight track. Trajectories oriented in either a Northerly or Southerly direction (Cluster 2, 3, 4) showed larger deviations in the prediction y-coordinate, while the opposite effect was found for trajectories flying in either an Easterly or Westerly direction (Cluster 0, 1).

The predictive metrics were evaluated for different flight levels to investigate the progression of the predictive capability of the models along the descent profile. Above FL100, the effect of including aircraft intent and meteorological data results in the reduction of the ATE compared to model GPR-A. However, the results showed the difficulty of predicting the final stage of the descent trajectory below FL040, where both the vertical error and the CTE increase significantly for all models. During this final stage, the flights are subjected to ATC commands that guide the aircraft to the appointed runway. This causes the flight tracks, within a single cluster, to diverge in this final stage of the flight as aircraft are assigned to different approach tracks. This complicates the training of the models and results in larger predictive errors, with large increases in the CTE. Also, the number of waypoints in a filed FP below FL100 is sparse. Generally, only two or three waypoints describe the aircraft intent in this final stage. This causes the effect of FP data to diminish in this final stage. The initial stage of the descent, between the top of descent and FL100, is usually represented by more waypoints. The uncertainty of the predictions, quantified by the GPR models, initially increases right after the start of the prediction horizon. Hereafter, the standard deviation gradually decreases until FL100 is reached. The Initial Approach Fix (IAF) is located at this flight level. The aircraft proceeds from the en-route segment to the IAF to start the initial segment of the instrument approach. Therefore, many routes will converge to the IAF, which is captured by the GPR models as shown by the decreasing uncertainty until FL100 is reached. Even though, particularly the CTE increased around FL040, the standard deviations do not increase during this stage. This is caused by the fact that the position of the arrival destination, as found in the flight plan, was added as a training data point. Therefore, the uncertainty decreases until this location is reached.

An extended GPR model trained with categorical data, containing the aircraft WTC category and the airline market segment, did not provide any improvements. The accuracy was not affected, while the uncertainty of the predictions increased. It was found that the relative change of the standard deviation of each predicted spatial dimension ( $\sigma_x$ ,  $\sigma_y$ , and  $\sigma_{alt}$ ) was nearly identical among the different models. This trend was observed in all experiments that compared the GPR models. This suggests that the multivariate GPR implementation in scikit-learn ineffectively considers the correlation among the output variables: x, y, and altitude. Most GPR implementations, found in the literature study, treated the multidimensional case by modelling each response variable individually without considering the correlation between the variables [31]. The key challenge in modelling multivariate response variables in GPR is the specification of a covariance function that both incorporates the correlation between data points as well as the correlation between the target variables [39].

### C. Particle Filtering

While GPR is trained on historical data obtained from other flights in combination with past observation of the flight to be predicted, the PF model only makes use of past observations from the particular trajectory. The PF model uses the observations starting from the top of descent until FL250 is reached, after which the predictions are generated using the performance model of the aircraft. The short-term predictions of the PF model, with look-ahead times shorter than five minutes, showed more accurate results with smaller ATE and CTE compared to the GPR models. However, the PF model generally overestimates the change in altitude of the aircraft resulting in negative vertical errors. On average, the predicted trajectory reached FL100 approximately 90 seconds before the actual flight did. These errors are likely to be caused by inaccurate estimation of aircraft mass and thrust rating which both affect the performance of the aircraft. The uncertainty metrics at short look-ahead times of the PF model were comparable to the GPR results. However, when predicting further in time, the PF model is outperformed by all GPR models. This was expected since the PF model, in contrast with the GPR models, does not exploit any other training data of other flights. The PF model only exploits historical observations of the trajectory to be predicted. The uncertainty increases over time as no new observations are used by the PF model. However,  $\sigma_{alt}$  eventually decreases since the lower limit of the altitude is specified at zero ft. Therefore, each particle is removed from the set once it has reached negative altitudes. This decreases the prediction interval of the predictions, thus the standard deviation. Overall, the PF model would be more accurate in predicting the initial stage of the descent from FL250, which is mostly linear. However, in the long term, the accuracy- and uncertainty of the predictions deteriorate due to model simplifications, assumptions related to the aircraft mass and thrust setting, and the lack of data used in the final stage of the descent.

## VI. CONCLUSION

While the majority of studies concerning trajectory prediction focused on the measurement of the predictive accuracy, this thesis aimed to also quantify the uncertainty of predicted descent trajectories. The model-based Particle Filtering technique and the data-driven Gaussian Process Regression were applied and both provide a predictive distribution that allows for the quantification of accuracy- and uncertainty metrics. Before the application of GPR, the trajectories of flights arriving at Schiphol Airport were clustered using the density-based technique DBSCAN. Even though the DBSCAN did not effectively capture all clusters, it was used to identify and remove outliers. Eventually, the application of K-means on the starting positions of the partial trajectories was efficient to cluster all sets of similarly shaped trajectories. The clustering of trajectories contributed to the improvement of the predictive accuracy of the data-driven models.

The application of the GPR models showed that the uncertainty of the descent trajectory predictions could be reduced by incorporating flight plan data when training the models. Adding meteorological data to the set of predictor variables did not result in a reduction of the uncertainty, but did show an improvement in predictive accuracy. The main improvements were observed throughout the initial stage of the descent. The uncertainty of the GPR predictions decreased until FL100 is reached, which is the effect of the IAF that represents the position where the aircraft trajectories are merged to initiate the approach segment. In the final stage of the descent, the predictive errors are likely to increase. Besides, the additional value of the FP data diminishes because of the sparsity of this dataset, which generally only includes a limited number of waypoints in this final stage. Also, training a GPR model in this stage is more complicated because the evolution of trajectories is dependent on the arrival procedure of the airport and ATC commands that guide the aircraft to the appointed runway.

The Particle Filter model showed to be more accurate in predicting the horizontal spatial coordinates of the trajectory for look-ahead times shorter than five minutes. However, the PF model tended to overestimate change in altitude, resulting in larger vertical errors compared to the GPR models. While the uncertainty of the predictions was comparable to the GPR models for short look-ahead times, the uncertainty of the PF model increases rapidly for longer look-ahead times. This was expected as the PF model solely relies on past historical observations until the start of the prediction horizon.

Both models have been able to model and quantify the uncertainty in trajectory predictions. An advantage of GPR is the fact that the characterisation of the sources of uncertainty is not required. Also, the effect of different predictor variables on the predictive uncertainty could be evaluated by training several GPR models. The quantification of the predictive uncertainty could contribute to the improvement of the prediction and management of 4D-trajectories. As expected, the uncertainty in the predictions obtained from the GPR models

was considerably lower compared to the PF model, since the GPR models also exploit training data from historical flights. Especially, the introduction of flight plan data contributed to the reduction in uncertainty of the predictions. It should be noted that a reduction in the spread of the predictions does not necessarily mean that the predictive model can be more certain about the correctness of the predictions. Especially in the final stage of the descent, both models have proven the difficulty of accurately estimating the aircraft position.

## VII. RECOMMENDATIONS

To further investigate the application of the proposed models, and potentially improve the predictive accuracy, several recommendations could be provided. The results of the GPR models showed that the expression of the aircraft intent, using FP data, could contribute to the reduction in uncertainty of the trajectory predictions. However, the FP data generally encompasses only a few waypoints that describe the final stage of the descent. It is recommended to explore methods or data sources that could extend the description of the intended trajectory of the aircraft. It is expected that the GPR models could be further improved when more extensive data is taken into account. Also, the clustering of trajectories has proven to contribute to better predictive results using the data-driven GPR. The predictive results are likely to be further improved when the clusters of trajectories are even more refined.

This study evaluated the predictive models on the descent segment of the flight. Additional research could be performed to apply the probabilistic predictive models to different phases of the flight, like the climb- or cruise phase. Also, this study focused on the prediction of single trajectories without considering the interactions with other aircraft. A collaborative trajectory predictor that fuses the predicted trajectories of multiple aircraft has the potential to further improve the predictive accuracy.

The multivariate GPR implementation from the scikit-learn library was applied to predict the 3D-position of the aircraft. However, the predictive results suggested that the model did not effectively take into account the correlation between the predicted spatial dimensions. Further research is required to incorporate the correlation between the three spatial dimensions when applying GPR in the multivariate case.

Finally, it is expected that the PF model could be improved when more accurate estimations of the mass and thrust setting are included in the model. These parameters highly influence the performance of the aircraft, thus impact the progression of the flight predictions.

## REFERENCES

- [1] E. C. Fernández, J. M. Cordero, G. Vouros, N. Pelekis, T. Kravaris, H. Georgiou, G. Fuchs, N. Andrienko, G. Andrienko, E. Casado, D. Scarlatti, P. Costas, and S. Ayhan, "DART: A machine-learning approach to trajectory prediction and demand-capacity balancing," *SESAR Innovation Days*, no. November, 2017.
- [2] A. Rodríguez-Sanz, F. Gómez Comendador, R. M. Arnaldo Valdés, J. A. Pérez-Castán, P. González García, and M. N. G. Najar Godoy, "Air Traffic Management based on 4D Trajectories: A Reliability Analysis using Multi-State Systems Theory," *Transportation Research*

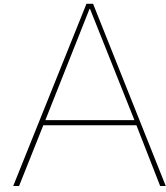
- Procedia*, vol. 33, pp. 355–362, 2018. [Online]. Available: <https://doi.org/10.1016/j.trpro.2018.11.001>
- [3] E. Casado, C. Goodchild, and M. Vilaplana, "Identification and Initial Characterization of Sources of Uncertainty Affecting the Performance of Future Trajectory Management Automation Systems," *Proceedings of the 2nd International Conference on Application and Theory of Automation in Command and Control Systems*, no. May, pp. 170–175, 2012.
  - [4] I. Lymeropoulos, J. Lygeros, and A. Lecchini, "Model based aircraft trajectory prediction during takeoff," *Collection of Technical Papers - AIAA Guidance, Navigation, and Control Conference 2006*, vol. 2, no. August, pp. 843–854, 2006.
  - [5] Z. Wang, M. Liang, and D. Delahaye, "Short-term 4D trajectory prediction using machine learning methods," *SESAR Innovation Days*, no. November, 2017.
  - [6] E. Gallo, F. A. Navarro, A. Nuic, and M. Iagaru, "Advanced aircraft performance modeling for ATM: BADA 4.0 results," *AIAA/IEEE Digital Avionics Systems Conference - Proceedings*, pp. 1–12, 2006.
  - [7] J. Bronsvoort, G. McDonald, M. Paglione, C. Garcia-Avello, I. Bayraktutar, and C. M. Young, "Impact of missing longitudinal aircraft intent on descent trajectory prediction," *AIAA/IEEE Digital Avionics Systems Conference - Proceedings*, pp. 1–14, 2011.
  - [8] R. Alligier, "Predictive distribution of mass and speed profile to improve aircraft climb prediction," *Journal of Air Transportation*, vol. 28, no. 3, p. 114, 2020.
  - [9] A. M. de Leege, M. M. van Paassen, and M. Mulder, "A machine learning approach to trajectory prediction," *AIAA Guidance, Navigation, and Control (GNC) Conference*, pp. 1–14, 2013.
  - [10] R. Alligier, D. Gianazza, and N. Durand, "Learning the aircraft mass and thrust to improve the ground-based trajectory prediction of climbing flights," *Transportation Research Part C: Emerging Technologies*, vol. 36, pp. 45–60, 2013. [Online]. Available: <http://dx.doi.org/10.1016/j.trc.2013.08.006>
  - [11] I. Lymeropoulos and J. Lygeros, "Improved multi-aircraft ground trajectory prediction for air traffic control," *Journal of Guidance, Control, and Dynamics*, vol. 33, no. 2, pp. 347–362, 2010.
  - [12] W. Kun and P. Wei, "A 4-D trajectory prediction model based on radar data," *Proceedings of the 27th Chinese Control Conference, CCC*, pp. 591–594, 2008.
  - [13] J. Zhang, J. Liu, R. Hu, and H. Zhu, "Online four dimensional trajectory prediction method based on aircraft intent updating," *Aerospace Science and Technology*, vol. 77, pp. 774–787, 2018. [Online]. Available: <https://doi.org/10.1016/j.ast.2018.03.037>
  - [14] M. A. Konyak, "Improving Ground-Based Trajectory Prediction through," no. August, pp. 1–25, 2009.
  - [15] R. A. Coppenbarger, "En route climb trajectory prediction enhancement using airline flight-planning information," *1999 Guidance, Navigation, and Control Conference and Exhibit*, pp. 1077–1087, 1999.
  - [16] M. G. Hamed, D. Gianazza, M. Serrurier, and N. Durand, "Statistical prediction of aircraft trajectory: regression methods vs point-mass model," *10th USA/Europe ATM R&D Seminar*, vol. 2013, no. June, p. pp. 2013. [Online]. Available: <https://hal-enac.archives-ouvertes.fr/hal-00911709>
  - [17] Y. Pang, N. Xu, and Y. Liu, "Aircraft trajectory prediction using lstm neural network with embedded convolutional layer," *Proceedings of the Annual Conference of the Prognostics and Health Management Society, PHM*, vol. 11, no. 1, 2019.
  - [18] K. Yang, M. Bi, Y. Liu, and Y. Zhang, "LSTM-based deep learning model for civil aircraft position and attitude prediction approach," *Chinese Control Conference, CCC*, vol. 2019-July, pp. 8689–8694, 2019.
  - [19] J. Bian, D. Tian, Y. Tang, and D. Tao, "A survey on trajectory clustering analysis," 2018. [Online]. Available: <http://arxiv.org/abs/1802.06971>
  - [20] M. Gariel, A. N. Srivastava, and E. Feron, "Trajectory clustering and an application to airspace monitoring," *IEEE Transactions on Intelligent Transportation Systems*, vol. 12, no. 4, pp. 1511–1524, 2011.
  - [21] J. Sun, J. Ellerbroek, and J. Hoekstra, "Flight extraction and phase identification for large automatic dependent surveillance-broadcast datasets," *Journal of Aerospace Information Systems*, vol. 14, no. 10, pp. 566–571, 2017.
  - [22] P. Weitz, "Determination and visualization of uncertainties in 4D-trajectory prediction," *Integrated Communications, Navigation and Surveillance Conference, ICNS*, pp. 1–9, 2013.
  - [23] K. T. Mueller, J. A. Sorensen, and G. J. Couluris, "Strategic aircraft trajectory prediction uncertainty and statistical sector traffic load modeling," *AIAA Guidance, Navigation, and Control Conference and Exhibit*, no. August, pp. 1–11, 2002.
  - [24] E. Casado, M. L. Civita, M. Vilaplana, and E. W. McGookin, "Quantification of aircraft trajectory prediction uncertainty using polynomial chaos expansions," *AIAA/IEEE Digital Avionics Systems Conference - Proceedings*, vol. 2017-Septe, no. 699274, 2017.
  - [25] A. Rodríguez-Sanz, F. Gómez Comendador, R. M. Arnaldo Valdés, J. A. Pérez-Castán, P. González García, and M. N. G. Najar Godoy, "4D-trajectory time windows: definition and uncertainty management," *Aircraft Engineering and Aerospace Technology*, vol. 91, no. 5, pp. 761–782, 2019.
  - [26] S. Sankararaman and M. Daigle, "Uncertainty quantification in trajectory prediction for aircraft operations," *AIAA Guidance, Navigation, and Control Conference, 2017*, pp. 1–11, 2017.
  - [27] J. Rudnyk, J. Ellerbroek, and J. M. Hoekstra, "Trajectory prediction sensitivity analysis using monte carlo simulations," *2018 Aviation Technology, Integration, and Operations Conference*, pp. 1–20, 2018.
  - [28] I. Lymeropoulos and J. Lygeros, "Adaptive aircraft trajectory prediction using particle filters," *AIAA Guidance, Navigation and Control Conference and Exhibit*, no. August, pp. 1–16, 2008.
  - [29] J. Sun, H. A. P. Blom, J. Ellerbroek, and J. M. Hoekstra, "Particle filter for aircraft mass estimation and uncertainty modeling," *Transportation Research Part C: Emerging Technologies*, vol. 105, no. June, pp. 145–162, 2019.
  - [30] C. E. Rasmussen and C. K. I. Williams, *Gaussian Processes for Machine Learning*. Massachusetts Institute of Technology, 2006. [Online]. Available: [www.GaussianProcess.org/gpml](http://www.GaussianProcess.org/gpml)
  - [31] S. A. Goli, B. H. Far, and A. O. Fapojuwo, "Vehicle Trajectory Prediction with Gaussian Process Regression in Connected Vehicle Environment," *IEEE Intelligent Vehicles Symposium, Proceedings*, vol. 2018-June, no. Iv, pp. 550–555, 2018.
  - [32] Q. Tran and J. Firl, "Modelling of traffic situations at urban intersections with probabilistic non-parametric regression," *IEEE Intelligent Vehicles Symposium, Proceedings*, no. Iv, pp. 334–339, 2013.
  - [33] H. Rong, A. P. Teixeira, and C. Guedes Soares, "Ship trajectory uncertainty prediction based on a Gaussian Process model," *Ocean Engineering*, vol. 182, no. August 2018, pp. 499–511, 2019. [Online]. Available: <https://doi.org/10.1016/j.oceaneng.2019.04.024>
  - [34] Y. S. Chati and H. Balakrishnan, "A Gaussian Process Regression approach to model aircraft engine fuel flow rate," *Proceedings - 2017 ACM/IEEE 8th International Conference on Cyber-Physical Systems, ICCPS 2017 (part of CPS Week)*, pp. 131–140, 2017.
  - [35] Y. Chati and H. Balakrishnan, "Statistical modeling of aircraft takeoff weight," *12th USA/Europe Air Traffic Management R and D Seminar*, no. Atm, 2017.
  - [36] J. Sun, "Large-Scale Flight Phase identification from ADS-B Data Using Machine Learning Methods PhD student, ATM Control and Simulation, Aerospace Engineering Large-Scale Flight Phase identification from ADS-B Data Using Machine Learning Methods," 2016. [Online]. Available: [http://www.icrat.org/icrat/seminarContent/2016/presentations/38/ICRAT\\_2016\\_Presentation\\_file\\_38.pdf](http://www.icrat.org/icrat/seminarContent/2016/presentations/38/ICRAT_2016_Presentation_file_38.pdf)
  - [37] N. Rahmah and I. S. Sitanggang, "Determination of Optimal Epsilon (Eps) Value on DBSCAN Algorithm to Clustering Data on Peatland Hotspots in Sumatra," *IOP Conference Series: Earth and Environmental Science*, vol. 31, no. 1, 2016.
  - [38] J. Sun, J. M. Hoekstra, and J. Ellerbroek, "OpenAP: An open-source aircraft performance model for air transportation studies and simulations," *Aerospace*, vol. 7, no. 8, 2020.
  - [39] B. Wang and T. Chen, "Gaussian process regression with multiple response variables," *Chemometrics and Intelligent Laboratory Systems*, vol. 142, pp. 159–165, 2015. [Online]. Available: <http://dx.doi.org/10.1016/j.chemolab.2015.01.016>





# Scientific Paper Appendices





# Data exploration

## A.1. Data exploration on the complete trajectory set

The dataset that was used to develop and analyse the predictive models contained 9363 partial trajectories of flights arriving at Schiphol Airport in June 2018. Figure A.1 shows the distribution of the market segments of the airlines together with the ten most frequently found aircraft types in the complete dataset. The vast majority of flights (65%) are operated by traditional airlines executing scheduled operations. Also, 30% of the flights are operated by low-cost airlines that generally operate short-haul flights with narrow-body aircraft. As observed in the right graph, narrow-body aircraft like the B738, B737, and the A320 were the most frequently found aircraft in the dataset.

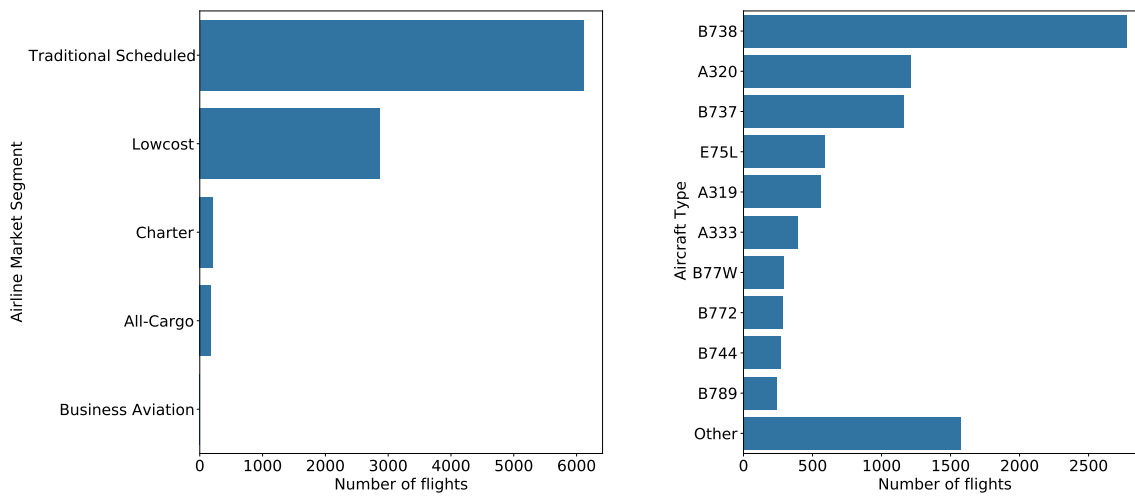


Figure A.1: The distribution of the airline market segment (left) and the aircraft types (right) of the flights in the complete trajectory set.

## A.2. Data exploration on the clusters of trajectories

A total of seven clusters of trajectories with similar spatial patterns were identified. Figure A.2 below depicts the top five departure airports and aircraft types found in each cluster. The majority of flights originated from European airports. However, a significant share of intercontinental flights is found in clusters 0 and 1, with flights arriving from the USA and the Caribbean.

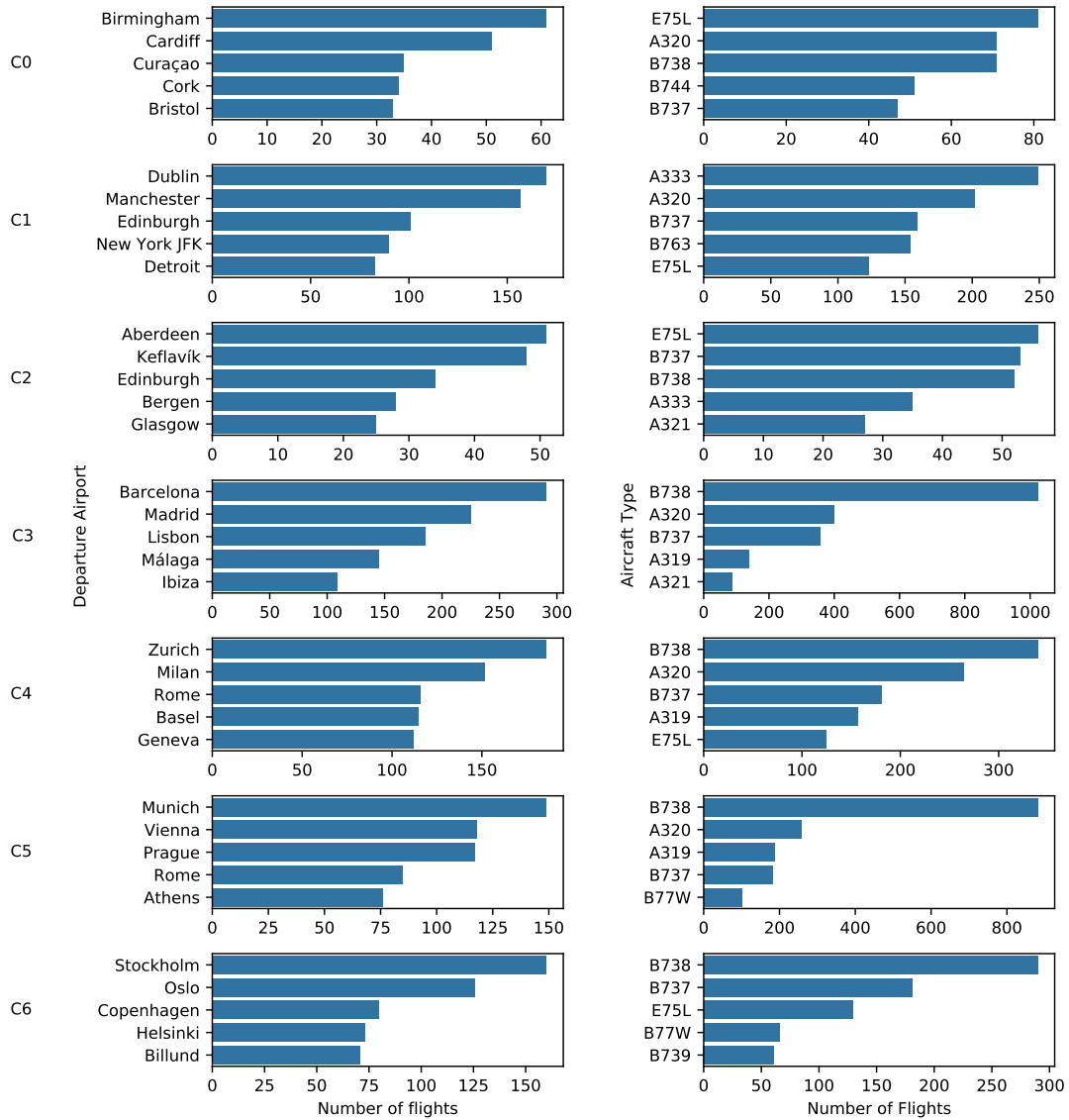


Figure A.2: Top five departure airports (left) and aircraft types (right) in each cluster of trajectories.

# B

## Trajectory clustering with DBSCAN

The DBSCAN algorithm was applied to group trajectories with similar spatial patterns. The algorithm comprises two parameters that have to be tuned:  $\epsilon$  and MinPts.  $\epsilon$  specifies a maximum distance between trajectories. Two trajectories would be grouped into the same cluster when the distance between both trajectories is smaller than  $\epsilon$ . MinPts defines the minimum number of trajectories required to form a cluster. These parameters should be tuned to effectively cluster the trajectories. If  $\epsilon$  is tuned too small, a large set of trajectories would be assigned as outliers. On the contrary, if the selected value of  $\epsilon$  is too high, the majority of trajectories would be assigned to the same cluster. An initial selection of  $\epsilon$  was made by computing the distance to the closest neighbour for each trajectory using the k-NN algorithm. The computed distances were plotted in ascending order, resulting in the following graph (Figure B.1).

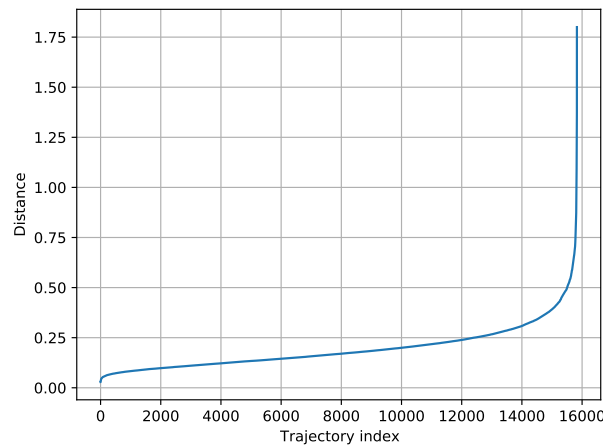


Figure B.1: Distance to closest trajectory in ascending order.

The optimal value of  $\epsilon$  lies at the point of maximum curvature, which is approximately at a distance of 0.50. Eventually,  $\epsilon$  was varied from 0.40 till 0.70 to find the optimum parameter. The clustering algorithm was evaluated by analysing the Silhouette score, the percentage of outliers, and a visual inspection to identify whether a sufficient number of clusters was identified. The clustering results, for a range of parameter combinations, are depicted in Figure B.2. The results show that the Silhouette score increases when  $\epsilon$  gets higher. When the MinPts parameter increases, the Silhouette score decreases while the percentage of outliers increases. The third figure presents the obtained number of clusters (including a cluster of outliers). Ultimately,  $\epsilon$  was set to 0.60, while MinPts was set to 80. This resulted in a Silhouette score of 0.39, while 6.5% of the flights were labelled as an outlier. DBSCAN identified four clusters of trajectories (excluding the outliers) using these parameter settings.

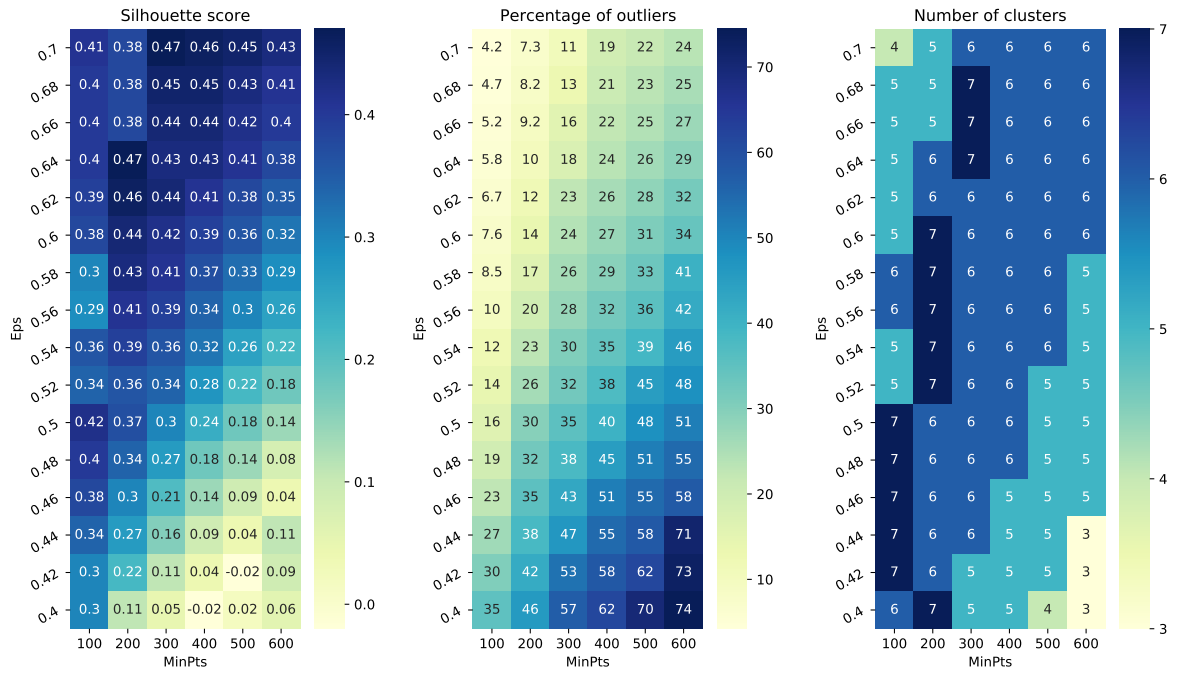
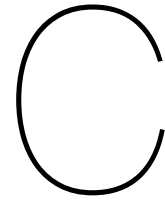


Figure B.2: DBSCAN clustering results for a range of parameter combinations.

Figure B.3 depicts the flights that have been labelled as an outlier. As shown, the majority of these flights were put in a holding pattern by Air Traffic Control.



Figure B.3: Outliers identified by DBSCAN.



# Prediction results

## C.1. Comparison between GPR and the PF model

The GPR model that was trained on ADS-B data, flight-plan data, and meteorological data (GPR-C) was the best performing GPR model. The predictive results of this model are compared to the Particle Filtering model as shown in Figure C.1. The PF model was found to obtain negative vertical errors, while the GPR-C obtained more accurate position predictions in the vertical plane. A consistent trend among all clusters was found in the other spatial errors (ATE and CTE) in which the PF model obtains more accurate results for look-ahead times shorter than ten minutes.

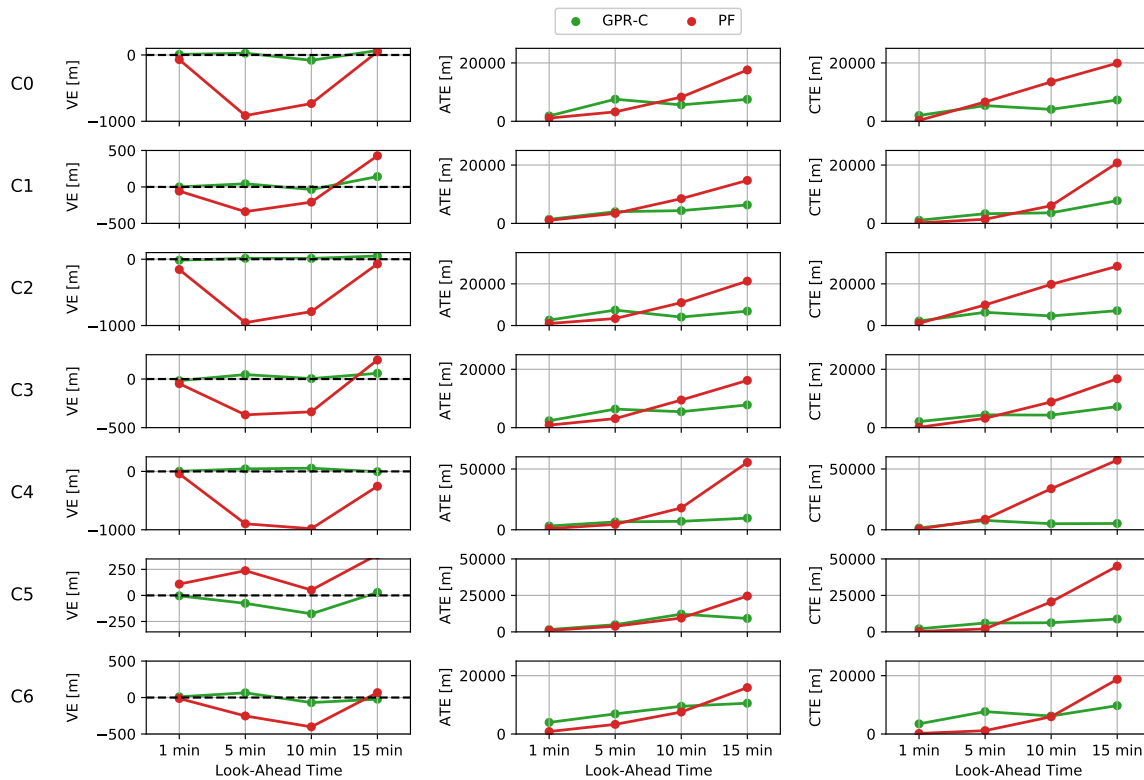


Figure C.1: Comparison between GPR-C and the PF model showing the median values of the spatial errors over increasing look-ahead times.

Figure C.2 below depicts the uncertainty of the predictions of the position of the aircraft over varying look-ahead times. The uncertainty in the predictions obtained from the PF model is strictly higher compared to the GPR-C results. Also, the uncertainty increases when the look-ahead time gets longer.

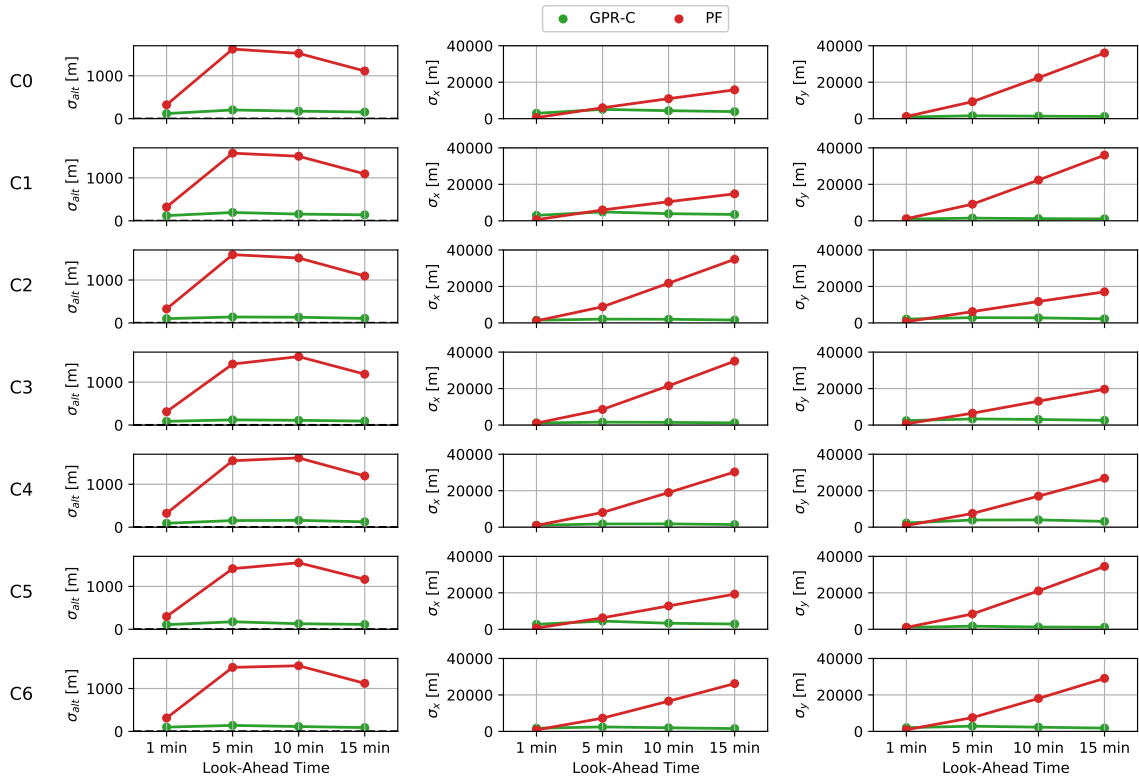


Figure C.2: Comparison between GPR-C and the PF model showing the median values of the standard deviations in the predictions of  $x$ ,  $y$ , and the altitude over increasing look-ahead times.

## C.2. Complete overview of predictive results

A complete overview of the accuracy metrics, expressed by the spatial errors, obtained on all clusters with different models is shown in Table C.1.

Table C.1: Predictive results showing the mean ( $\mu$ ), median, and standard deviation ( $\sigma$ ) of the predictive accuracy expressed by the spatial errors of the predictions.

Cluster	Model	VE [m]			ATE [m]			CTE [m]		
		$\mu$	Median	$\sigma$	$\mu$	Median	$\sigma$	$\mu$	Median	$\sigma$
0	GPR-A	79	62	512	8383	6331	7951	5596	3346	6298
	GPR-B	119	89	588	8149	6104	7660	6217	4360	6356
	GPR-C	4	6	303	6729	5135	6449	5746	4127	5788
	PF	-280	-188	883	15767	6348	21896	17114	9702	21763
1	GPR-A	199	127	539	8586	6728	7720	4743	2558	6221
	GPR-B	15	22	453	4662	2895	5300	5193	3108	6071
	GPR-C	30	18	284	5069	3618	5193	4669	2913	5344
	PF	29	88	803	11758	4802	18139	13918	3925	22753
2	GPR-A	-214	-100	553	10483	8347	8564	6686	4375	7810
	GPR-B	47	34	509	7288	5460	6801	6607	4497	7166
	GPR-C	29	7	294	6350	4666	6014	6422	4481	6717
	PF	-335	-229	943	21005	7676	30843	21728	13361	25518
3	GPR-A	112	91	613	11577	8196	11124	5475	3498	6716
	GPR-B	186	161	535	7780	5535	7596	5669	3841	6286
	GPR-C	10	17	331	6922	5063	6549	5329	3922	5461
	PF	-31	35	888	15906	6092	23738	12387	6135	16831
4	GPR-A	164	106	637	11163	8239	10684	8059	4340	10002
	GPR-B	165	137	590	9613	7348	8644	7462	5131	7534
	GPR-C	59	36	339	7916	5825	7518	6727	4438	7193
	PF	-324	-213	958	34316	15039	43246	44535	29230	49083
5	GPR-A	4	4	477	8975	5904	10467	7773	4174	9310
	GPR-B	-68	-5	596	8420	5407	10365	7973	4784	9146
	GPR-C	-43	-5	344	7626	4787	9622	6970	4655	7718
	PF	285	336	788	19234	5831	30453	24164	8048	33964
6	GPR-A	16	3	519	10386	7322	10389	7840	4505	8888
	GPR-B	137	110	598	9609	7077	8716	9425	6241	9478
	GPR-C	33	17	334	8715	6370	8243	8171	5798	8077
	PF	-9	43	821	15277	5483	23437	12740	3865	19270

A complete overview of the uncertainty metrics, expressed by the standard deviation of the predictions, obtained on all clusters with different models is shown in Table C.2.

Table C.2: Predictive results showing the mean ( $\mu$ ), median, and standard deviation ( $\sigma$ ) of the predictive uncertainty expressed by the standard deviations of the predictions.

Cluster	Model	$\sigma_{\text{alt}}$ [m]			$\sigma_x$ [m]			$\sigma_y$ [m]		
		$\mu$	Median	$\sigma$	$\mu$	Median	$\sigma$	$\mu$	Median	$\sigma$
0	GPR-A	294	358	118	7357	8953	2953	2316	2820	931
	GPR-B	138	142	58	3459	3567	1434	1090	1124	452
	GPR-C	162	168	70	4058	4196	1753	1278	1318	553
	PF	1096	1138	506	11689	9993	8959	24361	19849	19915
1	GPR-A	262	316	99	6541	7861	2469	1990	2391	752
	GPR-B	149	151	64	3720	3758	1604	1132	1144	487
	GPR-C	157	160	67	3917	3998	1665	1192	1215	506
	PF	1067	1097	501	10056	8767	7876	21549	16252	18981
2	GPR-A	174	194	58	2632	2942	883	3666	4101	1228
	GPR-B	105	108	38	1589	1629	580	2213	2276	804
	GPR-C	119	122	47	1806	1849	718	2514	2574	998
	PF	1081	1111	490	23094	18858	18827	13254	10692	10807
3	GPR-A	247	295	94	3258	3887	1240	6862	8189	2614
	GPR-B	87	90	36	1152	1192	468	2428	2511	988
	GPR-C	103	106	40	1363	1395	528	2874	2940	1112
	PF	1093	1127	503	23007	18433	19035	13680	11591	10552
4	GPR-A	316	365	142	3612	4180	1620	7971	9221	3582
	GPR-B	118	114	58	1350	1299	665	2982	2872	1467
	GPR-C	133	136	68	1523	1560	774	3365	3444	1724
	PF	1126	1152	502	22676	19018	17913	20010	16552	15894
5	GPR-A	373	470	172	9507	11951	4392	3595	4516	1664
	GPR-B	136	134	83	3466	3413	2130	1312	1291	795
	GPR-C	136	136	83	3474	3455	2112	1316	1309	788
	PF	1015	1027	509	12635	9807	11337	19906	14455	17759
6	GPR-A	350	437	149	6134	7665	2619	7143	8932	3054
	GPR-B	108	105	49	1890	1839	852	2205	2146	995
	GPR-C	114	112	50	1991	1962	873	2323	2290	1018
	PF	1034	1042	500	17522	13310	15326	18439	13666	16313



Preliminary Report [previously graded]



# Introduction

This chapter discusses the context of this project that evolves around the prediction of aircraft trajectories and the main incentive of this research project is clarified (Section 1.1). The research objective of this project is phrased (Section 1.2) and the outline of this preliminary report is provided (Section 1.3)

---

## 1.1. Context

Air Traffic Management (ATM) concerns the dynamic, integrated management of air traffic and airspace by the safe, economic, and efficient provision of air traffic services, airspace management, and air traffic flow management [4]. Until the outbreak of the Coronavirus in 2020, air traffic numbers have increased steadily over the past few years. The air traffic network in the Eurocontrol area has experienced an increase of 1.5 million flights in 2019 compared to 2013 [5]. This increase in the number of flights has had its effect on the congestion of the airspace sectors, which has led to the deterioration of performance measures such as punctuality and flight delays. In order to accommodate more flights and improve the performance of the ATM system under higher traffic demands, measures should be taken in order to increase airspace capacity, which is mostly limited by the workload of air traffic controllers. Even though the positive trend in air traffic numbers has ended abruptly due to the ongoing pandemic and corresponding travel restrictions, the objective to improve the efficiency and the performance of the ATM system still remains in place. Research initiatives like Single European Sky ATM Research (SESAR), and the USA equivalent NextGen, aim to develop and introduce new, advanced technologies and procedures to improve the efficiency and effectiveness of the ATM system while sustaining the level of safety and security.

One of the main pillars of these research programmes is the paradigm shift from a tactical to a strategic ATM system. In the conventional ATM system, airspace users file a flight plan and air traffic controllers provide tactical interventions (clearances) as the flight progresses. To accomplish the aforementioned objectives, the concept of 4D trajectory management is introduced. This new concept, also described as Trajectory-Based Operations (TBO) forms the basis of the future strategic ATM system. When introducing TBO, airspace users, Air Navigation Service Provider (ANSP), and airports agree on a negotiated aircraft trajectory. The objective of TBO is to define a trajectory that is as close as possible to the desired intentions of the airspace user. ANSPs and airports facilitate this trajectory while the airspace users fly along the agreed track with the required accuracy and precision in three spatial dimensions (altitude, longitude, latitude) and time [6]. When implementing the concept of TBO, decisions are made on a strategic basis, which improves the ATM system efficiency while reducing the number of tactical interventions made by air traffic controllers which affects the predictability of the flight. With increased predictability of flights and the reduction of tactical actions, the airspace capacity would be increased as controllers would be capable of managing more flights [7].

The vision of TBO is enabled when the automation of the ATM system progresses, where the human actors in the system increasingly rely on highly sophisticated Decision Support Tools (DST) like aircraft trajectory predictors. In order to ensure the safe separation of all individual flights, all having

their defined trajectory, it is essential to have trajectory predictions in place in order to identify potential conflicting situations among these different flights. Therefore, trajectory prediction capabilities are fundamental building blocks to the implementation of TBO, where the management of air traffic is more strategic-based. A trajectory predictor (TP) estimates the future flight path given an aircraft performance model, flight intent, and meteorological conditions. Given these sources of information, the TP aims to compute the latitude, longitude, and altitude of the aircraft at a particular look-ahead time [8]. TPs are being applied by different stakeholders in the aviation system for different purposes. These purposes comprise demand assessment and capacity planning in Air Traffic Flow Capacity Management (ATFCM), the execution and planning of flights by airspace users, and conflict detection and resolution by Air Traffic Control (ATC). These different objectives by different parties require different TPs with varying look-ahead times [9].

The performance of the TP is assessed on its predictive accuracy, which is measured by computing the difference between the predicted- and actual trajectory of the aircraft through space and time. The accuracy of these TPs is highly impacted by the uncertain nature of the execution of a flight that is subjected to a variety of parameters that are not always precisely known throughout the entire flight. For example, weather forecasts always contain an inherent element of uncertainty and aircraft-specific parameters like the cost index and the take-off weight are not always known as this information is not openly shared. Therefore, the prediction of an aircraft trajectory is a stochastic problem due to the inherent uncertainties of the parameters that influence the evolution of the trajectories. Several studies have investigated the predictions of aircraft trajectories and aimed to obtain correct predictions with high levels of accuracy. However, due to the uncertain nature of the evolution of the trajectories, further research is required to investigate the uncertainty that is associated with the obtained predictions.

## 1.2. Research objective

Traditionally, a deterministic approach is applied when predicting aircraft trajectories. This approach neglects the uncertainties that are associated with the relevant parameters that affect the trajectory. These techniques only produce point estimates, being a single predicted trajectory that is the most likely to be traversed by the aircraft. These predictions are then assessed on their accuracy by measuring the deviation of the predictions from the actual trajectories. Deterministic techniques suffer from degraded accuracy since these methods do not consider uncertainties that are associated with the aircraft trajectory predictions. Naturally, the evolution of a trajectory is subjected to a variety of input parameters that are not always precisely known, which characterises the stochastic nature. Hence, a stochastic, also referred to as probabilistic, technique is desired to compute the predictions. Common uncertainties are associated with aircraft-specific performance parameters, weather conditions, and intended flight operations. Even though some studies have applied a stochastic approach to incorporate the uncertainties in the predictions, further research is required to identify how the uncertainties in particular input parameters affect the overall predictive capability of a TP, which translates into the following research objective:

*The research objective of this thesis is to quantify and model the uncertainties that are associated with the predictions of aircraft trajectories by making use of stochastic prediction techniques.*

## 1.3. Report outline

A literature review is conducted to elaborate on the state-of-the-art in terms of the prediction of aircraft trajectories and to discover existing techniques that could be applied to model the uncertainties in aircraft trajectory predictions. Chapter 2 elaborates on the methodologies related to the prediction of aircraft trajectories, which involves both model-based and data-driven techniques. Chapter 3 elaborates on the principles of uncertainty modelling, which discusses the entire process to incorporate uncertainties in a predictive model. Subsequently, Chapter 4 explores and reviews various applicable probabilistic techniques. Chapter 5 elaborates on the approach of this project, which is broken down into three phases. The first phase, which involves the collection and preparation of data, is described in Chapter 6. Subsequently, Chapter 7 discusses the model development and the experimental setup that is used to evaluate the results. Ultimately, the planning of this project is provided in Chapter 8.

# 2

## Trajectory prediction methodologies

This chapter reviews the state-of-the-art concerning the principle of predicting aircraft trajectories. Commonly, there are two approaches to the prediction of aircraft trajectories: model-based or data-driven. Section 2.1 elaborates on the former approach and discusses the fundamentals of model-based predictive models. Section 2.2 elaborates on the data-driven approach that exploits several sources of data in the predictive models. Usually, these data-driven models are applied to individual clusters of trajectories with similar temporal and spatial features. This requires the application of trajectory clustering techniques to identify these groups of trajectories. The majority of studies evaluate the predictive models by analysing the predictive accuracy. Common measures of predictive accuracy are discussed in Section 2.3. Ultimately, the state-of-the-art in terms of the prediction of aircraft trajectories is evaluated and the main research gap is addressed in Section 2.4

---

### 2.1. Model-based Trajectory Prediction

A Trajectory Predictor (TP) computes the predicted 4D-trajectory that the aircraft is expected to follow. Hence, the output consists of three spatial dimensions (altitude, longitude, latitude) defining the position plus time acting as the fourth dimension to indicate at what point in time the position is reached. Mathematically, the trajectory could be expressed by a set of vectors, ordered in time, containing the aircraft states. Apart from the position and time, the state vectors might also contain other aircraft states like speed, attitude, and weight. Classical TPs are model-based and commonly apply a deterministic approach based on formulations of the aircraft's equations of motion. This approach is widely used and has already shown promising levels of accuracy. It should be noted that these approaches simplify the behaviour of the aircraft to obtain results with reasonable computational costs [10]. The outputs of the TP are computed using the aircraft intent, a meteorological model including historical observations and forecasts, and a model of the aircraft performance that includes the initial state of the aircraft.

Figure 2.1 provides a schematic overview of the TP process. The flight intent describes the goals, preferences and constraints for a particular flight executed by the aircraft operator. The constraints that apply to the flight originate from airport resources, airspace capacity, aircraft characteristics, and safety requirements [1]. The flight intent is ambiguous as multiple trajectories could be flown with the same flight intent. The Intent Generation Infrastructure (IGI) solves this ambiguity by imposing enhanced user preferences, constraints, and operational context. This eventually results in the generation of a unique aircraft intent, which provides the TP with a description of how the flight is being operated to meet the objectives of the operator while complying with the specified constraints [1]. The Trajectory Engine (TE) in the Trajectory Computation Infrastructure (TCI) computes the predicted trajectory by subsequent integration of the equations of motion. The TE makes use of two other models that provide additional information. The Aircraft Performance Model (APM) provides aircraft-specific information concerning the performance of the aircraft. These models mathematically describe the forces and moments that act on the aircraft throughout the flight. This information is used to define the equations of

motion. The Environmental Model (EM) includes meteorological parameters, like wind, temperature, and pressure that affect the performance of the aircraft [7].

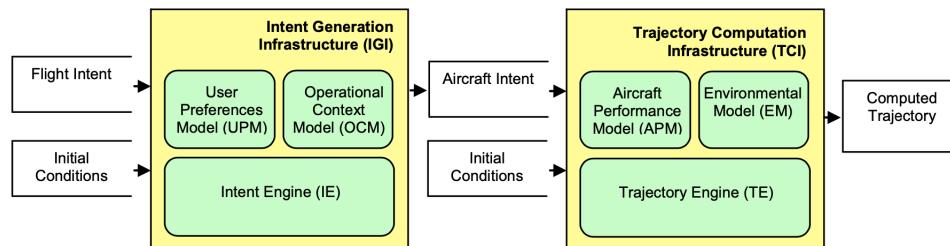


Figure 2.1: Schematic overview of the TP process [1]

### 2.1.1. Aircraft intent

As discussed in the previous section, the aircraft intent describes the way the aircraft is to be commanded manually by the pilot and/or automatically by the Flight Management System (FMS). Therefore, the aircraft intent plays a crucial role in the prediction of the trajectory as it defines how the aircraft is expected to operate throughout the flight. The information contained in the aircraft intent defines the configuration of the aircraft (deployment of landing gear or extension of flaps) but also involves operational procedures (hold a given airspeed or altitude) [7]. The aircraft intent could be derived from FMS, which could provide detailed trajectory information. However, an unambiguous description of the aircraft intent is not always accessible in studies that aim to involve aircraft intent in a TP. Therefore, this requires the introduction of assumptions to define the aircraft intent, which increases the level of uncertainty associated with the outputs of the TP. In order to enhance the used aircraft intent information by the TP, several studies have tried to make accurate inferences concerning the aircraft intent by using aircraft-derived data. Some results of these studies are discussed below.

Konyak et al. [11] tested the hypothesis that the communication of aircraft intent would improve the accuracy of a ground-based TP applied to a single flight following an optimised descent profile. This study identified that TPs that only made use of a flight plan filed before the execution of the flight only had access to limited information about the aircraft intent. This gap of information has risen the desire to generate intent inference algorithms in order to enhance the available information regarding the way the aircraft is being operated throughout the flight. The most accurate description of the intended trajectory could be obtained from the FMS onboard the aircraft. The FMS has full access to aircraft performance capability, airspace constraints, and airline procedures. However, the study had no access to the FMS data, which is why the study resorted to other available data sources. The study used flight plans, ATC clearances, and extensive notes made by the crew. These notes contain, among others, cruise speeds, descend speeds, communications with ATC, wind data, and fuel weights. Using the available data, a detailed description of the aircraft intent was generated, which eventually would be provided to the TP to obtain more accurate predictions. The aircraft intent was described using the Aircraft Intent Description Language (AIDL) developed by Boeing Research Technology Europe.

The AIDL provides a formal standardised language to describe the aircraft intent. The AIDL format is characterised by a set of instructions and a set of rules. The set of instructions are used to model certain commands. The set of rules uses combinations of instructions to conceptualise specific actions resulting in the aircraft intent. The instructions could be subdivided into the following five groups [12]:

- **Set** instructions identify a change of a particular parameter, from an initial value to a target value, that influences the configuration or motion of the aircraft (e.g. throttle, flaps, speed brakes, landing gear)
- **Law** instructions model the advanced modes and guidance laws of controlling the aircraft. These commands control any state of the motion of the aircraft (e.g. speed, altitude, throttle). Usually, these instructions capture dependencies between state variables (e.g. law that describes the dependency between the Mach number and altitude)

- **Hold** instructions model commands that are used when a motion or configuration should be maintained (e.g. hold constant speed)
- **Open loop** instructions model commands of the pilot that directly affect the configuration of the controls (e.g. change in path angle after elevator deflection).
- **Track** instructions model the guidance along a predefined geometry. This could either be a bi-dimensional or tri-dimensional geometric representation of the trajectory.

As mentioned, the set of rules make sure that a sequence of instructions is generated to unambiguously define an aircraft trajectory. This is known as the aircraft intent. The study of Konyak et al. [11] used the available track data to reverse-engineer back to the aircraft intent, which subsequently was formatted using the AIDL language. The results showed that the predictive accuracy improved significantly when incorporating the AIDL format to specify the aircraft intent in the TP. The results also discovered that regular TPs are more susceptible to changes in the aircraft motion from the steady-state. Regular TPs required as long as a minute to recognize the particular deviation before it was able to correct its predicted trajectory. This would require frequent monitoring of the aircraft states to obtain reliable predictions. On the other hand, TPs with AIDL-specified aircraft intent would only change the predicted trajectory once there is a change in aircraft intent [11].

Bronsvort et al. [13] studied the effect of missing longitudinal aircraft intent on the predictions of descent trajectories. Generally, the flight plans that are used to derive the aircraft intent only contain basic information. This might be sufficient for the cruise phase of the flight, which is relatively straightforward compared to the climb and descent phase. The lack of detailed aircraft intent in terms of the climb and descent profiles requires the TP to introduce assumptions and simplifications that impact the predictive accuracy. The study compared the longitudinal accuracy of the predicted trajectories from a ground-based TP to the predicted trajectories obtained from the onboard FMS. This research argued that the lack of the intended speed schedule during the descent is a significant factor that causes large errors in the predictions of the ground-based TP. These regular TPs used a nominal static descend speed to compute the vertical profile of the descent. A significant improvement would be made possible once trajectory data extracted from the FMS was used to further specify a more detailed aircraft intent. The implementation of this data has the potential to reduce the vertical errors from thousands of feet to a few 100ft, while the temporal errors might be reduced from the order of minutes to only a few tens of seconds.

Zhang et al. [14] also identified the aircraft intent as a key factor in the prediction of 4D trajectories. The aircraft intent was inferred from aircraft states like speed, altitude, and thrust. Once the difference between the predicted trajectory and the actual trajectory exceeded a pre-defined threshold, the aircraft intent was updated. The study showed that updating the aircraft intent could contribute to the increase in predictive accuracy.

### 2.1.2. Aircraft performance model

The conventional TP is model-based, which utilises a mathematical model of the aircraft flight dynamics to compute the motion of the aircraft under given flight and weather conditions. The computed aircraft motion forms the foundation of the predicted trajectory. Typically, the aircraft model is a simplified representation using a Point Mass Model (PMM), where all forces like thrust, drag, lift, and weight act through the centre of mass of the aircraft. Usually, there are two common approaches to model the motion of the aircraft [15]:

1. The *kinetic* approach models the forces that are applied to the aircraft, which allows the computations of the motion by making use of Newton's Law.
2. The *kinematic* approach directly models the motion of the aircraft, without modelling the underlying physics.

One of the most common aircraft performance models (APM) is adopted by the Base of Aircraft Data (BADA) developed by Eurocontrol. This APM follows a kinetic, mass-varying approach to model the

aircraft performance, and several studies have adopted this model to predict aircraft-specific parameters and aircraft trajectories [15, 16]. The intended use of BADA is to simulate and predict trajectories for the purpose of strategic planning in the field of ATM and the BADA model has been used in a variety of studies that required information related to the performance of the aircraft [17]. The BADA APM is built up into four different models: actions, motion, operations, and limitations. The action model defines the computations of the forces that are acting on the centre of mass, which results in the aircraft's motion. These actions entail aerodynamic forces (drag  $D$  and lift  $L$ ), propulsive forces (thrust  $T$ ), and gravitational forces (weight  $W$ ). The Total Energy Model (TEM) is central in this model and is used to predict the motion of the aircraft by applying Newton's laws to the predefined forces. The TEM is expressed by Equation 2.1 below.

$$(T - D)v = W \frac{dh}{dt} + mv \frac{dv}{dt} \quad (2.1)$$

where  $v$  represents the True Airspeed (TAS), the time derivative of the altitude ( $h$ ) is the vertical speed, and  $m$  is the mass of the aircraft. The variation of mass is accounted for by specifying a fuel consumption model. The complete mathematical BADA model defines a set of Ordinary Differential Equations (ODE) that define the evolution of the states of the aircraft. Subsequent integration of the system of ODEs, while incorporating initial states of the aircraft, is used to obtain the predicted state of the aircraft through a specified time interval. As discussed, the way the aircraft is being operated (aircraft intent) affects the trajectory. The trajectory of an aircraft flying at a constant Mach number will not be identical to a constant Calibrated Airspeed (CAS) operation. The operations model takes into account how the aircraft is being operated. The limitations model ensures that the model is constrained by its performance and operational limitations [18].

### 2.1.3. Environmental model

The environmental model in a TP accounts for the atmospheric properties (temperature, wind, and pressure) at each point throughout the flight. These atmospheric conditions might vary over time and the position of the aircraft and these variances might have a significant impact on the evolution of the aircraft trajectory [16]. Among the different meteorological parameters, the wind conditions arguably have the largest effect on the performance of the aircraft. Both the wind speed and the direction of the wind should be taken into account in the prediction model [19]. Several studies have already proven the importance of meteorological data as an input to the TP. Alligier [15] included temperature and wind fields as atmospheric properties affecting the climb performance of an aircraft. De Leege et al. [20] used surface winds and altitude winds as the meteorological inputs to predict the trajectory of an aircraft flying a Continuous Descent Operation (CDO). The surface winds were extracted from the meteorological aerodrome report (METAR), while the altitude winds were obtained from the Global Forecast System (GFS). The study examined the effect of the implementation of meteorological data on the predictive accuracy of the TP and showed that the predictive accuracy increased significantly when the wind components were included in the TP.

## 2.2. Data-driven Trajectory Prediction

The previous section discussed the classical model-based approach to aircraft trajectory predictions. However, with the increasing availability of data, several studies aimed to effectively utilise the available data and apply machine learning techniques to apply a data-driven approach to predict trajectories. A data-driven approach is completely different from the model-based TPs since a data-driven approach does not take into account any representation of the dynamics of the aircraft. Instead, it exploits trajectory information extracted from either ground-based surveillance systems or onboard systems. The expected advantage of the data-driven approach is that these techniques allow more accurate predictions by taking into account and learning from all relevant, historic trajectory data, while also considering any other contextual features that affect the evolution of the trajectory [10]. Furthermore, unlike the model-based approach, the data-driven methods do not rely on the parameters of the performance models that might now always be precisely known. The sections below will elaborate on the common sources of data used in these approaches, the preparation of this data, which involves the clustering of trajectories. Eventually, several examples of studies that used a data-driven approach to predict aircraft trajectories are discussed.

### 2.2.1. Sources of data

The data-driven approach to the prediction of aircraft trajectories requires a sufficient amount of accurate data that is extracted from various sources. Subsequently, these various sources of data should be interlinked to obtain a coherent and meaningful set of data that could be used in the process of trajectory prediction. The collection of reliable, meaningful data often is a complicated process in the field of ATM where certain information is not openly shared among different stakeholders. For example, operational information like the cost index or the aircraft take-off weight is considered as competitive information and hence is not openly shared [10]. Positional data from flown trajectories are used to reconstruct flights to train the machine-learning algorithm. Just like the model-based approach, meteorological conditions and aircraft intent information is incorporated in the predictive algorithms. Hence, the trajectory data is commonly enriched with meteorological datasets and flight intent information obtained from flight plans.

#### Trajectory data

While certain studies have used radar track data to reconstruct aircraft trajectories [21–23], the preferred source of trajectory data is the Automatic Dependent Surveillance-Broadcast (ADS-B) data. ADS-B is a satellite-based surveillance technology that allows aircraft to broadcast identification (ICAO address), velocity, and position information to surrounding aircraft and ground stations [24]. An increasing number of aircraft are being equipped with ADS-B which provides more accurate positioning data compared to the use of ground-based radars. This fact in combination with the open accessibility has made it a popular source of trajectory data for studies in the ATM field. For this study, the ADS-B data could be used to reconstruct the trajectories flown by particular aircraft by extracting the position updates (longitude, latitude, and altitude) obtained from the ADS-B transmitter equipped onboard the aircraft. Eventually, the flown trajectory is obtained by sequencing the position updates from ADS-B broadcasts.

#### Meteorological data

Previous studies have proven the significance of the effect of including meteorological conditions (like wind speed, wind direction, and temperature) in the predictions of aircraft trajectories. In order to enrich the trajectory dataset with corresponding meteorological conditions, a meteorological dataset should be used that includes measurements of the relevant parameters over the range of altitudes and geographical positions that the aircraft operates in. The meteorological databases commonly provide the data through the use of GRIB files, which represents the region of interest as a grid with geographical points. The meteorological parameters are defined for each point [25]. The spatial resolution of these grids is important to consider when selecting a source of meteorological data. The National Oceanic and Atmospheric Administration (NOAA) Rapid Refresh (RAP) was used by multiple studies because of its high spatial resolution of thirteen kilometres [26, 27]. RAP, which only covers the continent of North America, not only includes historical measurements but also provides weather forecasts that are updated every hour with forecasts lengths of 18 hours. An alternative model that provides global coverage is the NOAA Global Forecast System (GFS) with a spatial resolution of 28 kilometres. This dataset provides measurements up to an altitude of 55 kilometres [28]. The vertical range is divided into 64 layers. This model has been used by De Leege et al. to obtain altitude winds [20]. This study also used METAR reports for the weather conditions close to the airport. Zhang et al. [14] extracted the wind field (wind speed and direction) from the European Centre for Medium-Range Weather Forecasts (ECMWF), which has a grid resolution of approximately 80 kilometres. The ERA5, also part of ECMWF, uses an even finer grid with a spatial resolution of around 30 kilometres, which is comparable to the GFS model. This dataset includes meteorological parameters up to an altitude of 80 kilometres, divided into 37 pressure levels.

#### Aircraft intent data

Aircraft intent is commonly included in the predictions by making use of ICAO flight plans that are filed before the flight. These flight plans are filed by the crew and submitted to the relevant air traffic service units. The flight plans provide specified information concerning the intended flight. Flight plans typically include the type of aircraft, departure airport, time of departure, cruising speed, cruising level, and the route to be followed [29]. The data included in flight plans is only limited and is not sufficient to unambiguously define the intended trajectory to be flown by the airspace user. As mentioned in

subsection 2.1.1, several studies have tried to compensate for the lack of a detailed description of the aircraft intent. These studies relied on the use of data link communications with onboard equipment like the FMS to infer the aircraft intent from these sources of real-time data [13].

### 2.2.2. Clustering aircraft trajectories

The data-driven approach to trajectory prediction requires certain pre-processing steps that have to be applied to the initial set of raw trajectory data. The preparation of the data involves, among others, aggregating different sources of data, handling missing values, standardising variables, and dividing the final dataset into subsets used for training and testing the applied model. Besides, a key building block in the prediction of aircraft trajectories is the accurate clustering of aircraft trajectories with similar spatial and temporal characteristics [30]. The principle behind the clustering of trajectories is that each cluster will be used to train a predictive data-driven model. Hence, the predictions of a certain trajectory will be based upon the trained model derived from the specific cluster that the trajectory to be predicted belongs to.

Clustering is an unsupervised machine learning technique to group similar entities into clusters according to a defined similarity measure. Many different point-based clustering algorithms are presented in the literature, like K-means, BIRCH, OPTICS, DBSCAN, and HDBSCAN [31]. Applying these algorithms to cluster trajectories requires the specification of a proper distance function to compute the similarity between trajectories. A common distance measure is the Euclidean distance, which requires the trajectories to be of equal length. Other warping-based distance measures, like Dynamic Time Warping (DTW) distance, are specifically used to measure the similarity between different time series. Other measures that specifically focus on the shape of the trajectories are the Hausdorff and the Fréchet distances [31]. The sections below discuss several applications of trajectory clustering algorithms.

#### Density-Based clustering techniques

One of the most commonly applied techniques in clustering trajectories is the Density-Based Spatial Clustering of Applications with Noise (DBSCAN) [32]. A density-based clustering technique groups data into regions of high and low density. For this purpose, DBSCAN requires two input parameters to be specified: *Eps* and *MinPts*.

- **eps** specifies the maximum distance between two data points for one to be considered as in the neighbourhood of the other.
- **MinPts** specifies the minimum number of points that form a cluster.

The parameters above are then used to make a distinction between three types of data points. A point is classified as a core point, border point, or outlier. A core point is a point with at least *MinPts* number of neighbouring points within a distance of *eps*. A border point is a point that is reachable from a core point and has less than *MinPts* number of points within a distance of *eps*. Points that neither are classified as core- or border points are referred to as the outliers. Each cluster is formed by neighbouring core points and their corresponding border points.

This density-based approach has proven to be able to efficiently cluster aircraft trajectories into an unknown number of arbitrary shaped clusters, while effectively discarding outliers [33, 34]. Churchill and Bloem [35] also applied DBSCAN to cluster taxi trajectories on the airport surface. The temporal variation between similarly shaped taxi trajectories might be large as aircraft can stop throughout the execution of the taxi trajectory. Therefore, a two-level hierarchical approach was applied where the trajectories were clustered in space and time using DBSCAN. Song et al. [36] applied DBSCAN to introduce the principle of a typical trajectory. This typical trajectory was implemented in a predictive model as the intended flight path.

Having the ability to handle an unknown number of clusters is advantageous as the number of different types of trajectories is commonly not known in advance. Other algorithms, like K-means, do require the specification of the number of clusters as an input to the algorithm. Besides, the property of effectively dealing with outliers offers a significant benefit in processing ADS-B data, where trajectories of low data quality will be considered as outliers and could be removed from the analysis [34].

DBSCAN might not perform well when the data includes clusters with highly varying densities. Borsora et al. [37] applied a variation of the algorithm called Hierarchical DBSCAN (HDBSCAN). This algorithm only requires the specification of *MinPts* and performs better on data with varying densities.

### Hierarchical clustering techniques

Bombelli et al. [38] applied agglomerative hierarchical clustering techniques to spatially and temporally cluster the trajectories, where the spatial clustering was based on the Fréchet distance. The agglomerative hierarchical clustering is a bottom-up approach where initially all trajectories are classified as individual clusters. Then, at each step, the two most similar clusters are combined until all trajectories are included in one single big cluster. Eventually, the number of clusters is based on the specification of the pruning distance that defines the desired clustering resolution, which should be based on domain knowledge and depends on the field of application. Bombelli et al. [38] spatially grouped trajectories with common origin and destination. However, solely clustering trajectories on their spatial similarities would be insufficient. Grouping trajectories should also account for the similarity in the temporal domain since two spatially similar trajectories might be flown with different speeds. For this reason, the average cruise speed of the trajectories was computed to further divide the spatial trajectory clusters.

### Partitioning the trajectory into segments

Lee et al. [39] observed that clustering a trajectory as a whole might be inefficient since certain portions of trajectories might show similar behaviour, while the trajectory as a whole might not. Therefore, a partition-and-group framework was applied, where each trajectory was partitioned into a set of line segments, after which these line segments were clustered using a density-based approach. This principle could be helpful in the clustering of aircraft trajectories, where a flight could be broken down into a climb, cruise, and descent segment. This requires a technique that exploits historical data to identify the phases of the flight. Sun et al. [34] proposed a method that was based on fuzzy logic which uses three inputs (altitude, rate of climb, and ground speed) in combination with logic operators to determine the phase of the flight.

### 2.2.3. Application of data-driven prediction models

With the increasing and improved collection of data in the ATM field, data-driven approaches have become one of the common methods in the predictions of aircraft trajectories [40]. This approach has the main advantage that it ignores the required parameters to a performance model as it only relies upon real historical data collected from the aircraft or other additional data sources. Up till now, several studies have applied different techniques to exploit the historical trajectory data to compute predictions of aircraft trajectories. This section describes a selection of applications in which aircraft trajectory predictions are data-driven.

Hamed et al. [41] proposed statistical regression models to predict the trajectory during the climb phase with a look-ahead time of 10 minutes. Regression methods assume the aircraft position to be a function of a set of dependent variables. This study selected the past aircraft positions, the current speed, the temperature deviation from the standard atmosphere, and the predicted wind at different altitudes as the regression input variables. The results of the data-driven approach were compared to the outcomes of the model-based approach where the BADA APM was used. Meteorological data and radar track data were used to obtain the set of explanatory variables that were fed to the regression model. In order to reduce the dimensionality of the model, a Principal Component Analysis (PCA) was performed to identify the reduced set of significant components. The study concluded that the regression model performed significantly better than the TP using the point-mass model. This was expected as the regression model learns from historical, actual data, while the point-mass model uses fixed values for certain parameters. De Leege et al. [20] applied the step-wise regression method named Generalised Linear Models (GLM) to predict arrival times of descending aircraft. Step-wise regression methods are used to systematically include or exclude explanatory variables from the GLM based on their statistical significance in explaining the outputs. Sufficient explanatory power of the model was obtained when using the aircraft type, initial altitude, and the initial ground speed as the input variables. Further improvements could be obtained when surface- and altitude winds are included in the model. These regression-based models were compared to the use of Artificial Neural Networks (ANN), and the re-

sults showed that the regression models marginally outperformed the ANN.

Neural Networks have shown to be popular methods in data-driven trajectory predictions and have been successfully applied by many studies [42, 43]. Wang et al. [44] applied the so-called Multi Cells Neural Network (MCNN) to address the short-term prediction of trajectories in the Terminal Manoeuvring Area (TMA). The term 'multi cells' refers to multiple sets of trajectories that were identified from the results of clustering techniques. The neural network was applied to each of these trajectories, and the results proved that these methods provided robust and accurate short-term predictions.

### 2.3. Measurement of predictive accuracy

The studies described in previous sections all aim to contribute to a more accurate prediction of aircraft trajectories. When following a deterministic approach, a single, most likely trajectory is computed as a result of the predictive model. Subsequently, this predicted trajectory is compared to the actual trajectory that is reconstructed from the observed data. The comparison aims to express the predictive accuracy by defining the error between the predicted and actual trajectory and different metrics could be used to define this prediction error. Usually, the prediction errors are either spatial or time errors. The visualisation in Figure 2.2 provides an overview of the definitions of the horizontal spatial prediction errors. As could be observed, the horizontal error simply measures the distance between the predicted position and the actual position at a specified point in time. This horizontal error is decomposed into a cross-track error and an along-track error.

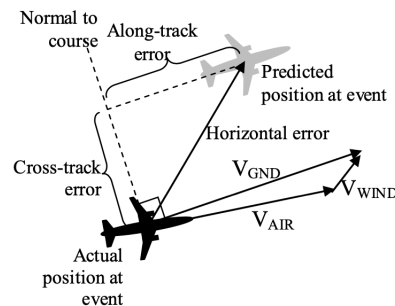


Figure 2.2: Visualisation of horizontal track errors [2]

Another spatial accuracy metric is defined by the vertical error, which simply computes the difference in altitude between the predicted and actual position at a specified point in time.

Besides the spatial errors specified above, a temporal metric defined as the time error could be used to predict the accuracy of the TP. The time error is the computed difference in time of the occurrence of a particular event (e.g. reaching a particular waypoint). The time error could be a helpful metric for TPs that are used to merge and sequence aircraft along the descent track towards the runway [2].

A statistical analysis of the measured errors could be performed in order to obtain a comprehensive view of the capability of the TP to generate accurate results. De Leege et al. [20] converted the results of the time error into probability density functions and showed how the variance of the distribution increased with increasing look-ahead times. Statistical properties of the errors could also be used to compare the predictive accuracy of different TP. Alligier et al. [45] compared two different methods that predicted the climb trajectory of an aircraft by evaluating the Root Mean Squared Errors (RMSE) and the standard deviation of the errors of both approaches.

### 2.4. Review of the state-of-the-art in trajectory predictions

The review of the state-of-the-art concerning the predictions of aircraft trajectories identified that commonly there are two approaches: model-based or data-driven. Traditionally, model-based approaches are applied in which the aircraft is represented by a point-mass model and its motion is characterised by a set of differential equations that describe the evolution of the states of the aircraft. In addition to

the APM, a meteorological model together with an (inferred) aircraft intent are included to compute the predictions. The prediction of the trajectory is based on the subsequent integration of the states over time. With the increasing availability of data, however, more studies have approached the prediction problem using a data-driven approach. The advantage of such an approach is that it potentially allows for more accurate predictions as the predictive model learns from all historical observations while taking into account a variety of factors that influence the evolution of the aircraft trajectory. Furthermore, data-driven approaches do not rely on aircraft performance parameters, such as aircraft mass which is commonly not precisely known.

The data-driven approach applies machine learning techniques like regression, classification, and neural networks to a dataset that includes parameters that affect the evolution of the trajectory. Commonly the trajectory is reconstructed from ADS-B data. To enhance the value of the data, the trajectory data is commonly enriched with meteorological conditions and forecasts. The aircraft intent is usually derived from the filed flight plans.

Even though some effort has been put into the prediction of trajectories in a multi-aircraft environment [23], the majority of studies focus on the prediction of a single trajectory flown by a particular aircraft. Furthermore, it was observed that the studies commonly select one particular phase of the flight, since the prediction error is likely to vary throughout different phases of the flight. Modelling the aircraft performance during climb and descent is more difficult compared to the cruise phase, hence the predictions of these phases are likely to be less accurate [46]. Rodríguez et al. [47] identified the descent phase as the most challenging part of the flight for predictive purposes. The complexity of the descent phase is related to the fact that multiple aircraft are merging and sequencing into a bounded airspace, while aircraft speed and wind may vary substantially during the descent.

All studies discussed previously aimed to identify the accuracy of the established predictive model by measuring the error between the predicted and actual trajectories. The measure of accuracy could be used to select the most appropriate method for the prediction of trajectories. Hamed et al. [41] compared the accuracy of a data-driven to a model-based approach and concluded that the data-driven model significantly outperformed the approach that implemented the Point Mass Model. However, the predictive accuracy is highly impacted by the stochastic nature of the evolution of the trajectories which introduces uncertainties in many parameters. Examples of these uncertainties include unknown aircraft parameters like take-off mass and thrust, wind forecast errors, and other data measurement errors obtained from ADS-B. Furthermore, the aircraft intent derived from flight plans is not likely to remain constant as the actual operated flight could deviate from its flight plan due to ATC interventions and other unforeseen circumstances. As discussed previously, traditionally the prediction outputs are usually the result of solving a deterministic mathematical model that represents the motion of the aircraft. Assumptions and simplification in these models also introduce errors, which is a source of uncertainty. A deterministic approach does not consider these uncertainties, and only computes a single predicted trajectory that does not contain any information regarding the confidence of the predicted trajectory. For these reasons, a probabilistic or stochastic approach is desired to predict aircraft trajectories while taking into account different sources of uncertainty. These approaches allow for a more extensive evaluation of the uncertainty in the predictions, rather than solely assessing the models on their predictive accuracy.

The next sections will elaborate on the importance of modelling uncertainties in the predictions of aircraft trajectories. The main sources of uncertainties will be identified, and appropriate probabilistic techniques will be explored.



# 3

## Modelling uncertainty

Modelling uncertainty in predictive analytics involves the process of Uncertainty Quantification (UQ), which concerns the estimation of the impact of uncertainties in the input variables on the uncertainty of the prediction of the target variable. The main goal is to account for all relevant sources of uncertainty and quantify their contributions to the uncertainty in the predictions. When UQ is applied to predictive analytics, the output is a probabilistic framework of possible outcomes. This is dissimilar to the deterministic approach to predictive modelling, which computes a point estimate that represents the most likely outcome. The probabilistic approach in trajectory predictions allows the user to robustly and efficiently predict the most likely trajectory together with associated confidence and uncertainty of the predicted output [48]. The UQ process commonly involves four steps. First of all, the relevant sources of uncertainty that affect the target variable should be identified (Section 3.1). Subsequently, the input uncertainties should be characterised, which is commonly done by expressing the uncertainty using probability density functions (PDF) to represent the particular input variable (Section 3.2). Then, these uncertainties in input variables are propagated through the model to systematically compute the joint effect of the input uncertainty on the predicted outcomes (Section 3.3). Ultimately, uncertainty management is a general term used to refer to activities that focus on managing or reducing the uncertainty in the final prediction. Hence, this phase focuses on analysing the results and identifying the main contributors to the output uncertainty (Section 3.4).

---

### 3.1. Uncertainty identification

McKay [49] describes that modelling uncertainty relates to the variability in the model predictions due to plausible alternative input values (input uncertainty) or to plausible alternative model structures (structural uncertainty). Hence, commonly two types of sources of uncertainties are distinguished in the modelling and prediction process.

#### 3.1.1. Input uncertainty

The inputs to the model characterise the relevant features that influence the performance of the model. Input uncertainty refers to the effect of not precisely knowing the exact value of certain inputs that are fed to the predictive model. These uncertainties usually come from a lack of knowledge on the deterministic and stochastic properties of the input data [50]. The inherent imprecision of measurements also contributes to the uncertainty related to the input data.

#### 3.1.2. Structural uncertainty

Structural uncertainty refers to the model that is used to compute the predictions, which contains the set of input parameters as well as the relationships among them. The structural uncertainty, also commonly referred to as epistemic uncertainty, arises from the accuracy of the mathematical model that is used to describe a physical process. Any simplification or assumption made in the mathematical description will impact the predictive accuracy and hence introduce structural uncertainty in the predictions. For example, neglecting air friction in a free-fall model is a simplification that would likely

result in a discrepancy between the model and the true physics.

### 3.1.3. Sources of uncertainty in aircraft trajectory predictions

Considerable research has already been performed to identify potential sources of uncertainties that arise when the trajectory of an aircraft is being predicted. This section will elaborate on the most common sources of uncertainties.

#### Initial conditions

In a model-based approach, the initial conditions are required to perform the integration of the differential equations representing the motion of the aircraft. These initial conditions relate to the initial position, speed, and weight of the aircraft. While the initial speed and position of the aircraft could be obtained from surveillance data like ADS-B, the initial aircraft weight usually is not publicly accessible. Obtaining position and velocity inputs from surveillance data also introduces uncertainty due to the inherent inaccuracy of the position and velocity measurements. The uncertain aircraft weight requires estimations and assumptions which introduces considerable discrepancies and especially affects the accuracy of the expected fuel consumption throughout the flight [51].

#### Aircraft intent uncertainties

The evolution of the aircraft trajectory is highly influenced by the aircraft intent that describes how the pilot or the FMS commands the aircraft to operate the flight. The lack of knowledge concerning the operational strategy of the airline is considered to be a major source of uncertainty. Even though some information could be derived from the filed flight plans before the flight, this plan usually lacks a detailed description of the entire trajectory. Besides, the actual flight may diverge from the filed flight plans because of flight crew preferences or ATC interventions. The aircraft might also be rerouted to avoid severe weather conditions, which causes the actual flight to deviate from its prescribed flight plan [52]. Overall, the aircraft intent uncertainty is shaped by the difference between the pilot/FMS model applied to the TP and the actual strategy of guidance applied by the pilot/FMS throughout the flight [53].

#### Atmospheric uncertainties

Atmospheric properties like temperature, humidity, and wind conditions (speed and direction) are commonly implemented in aircraft trajectory predictions as they could have a significant impact on the performance of the aircraft and thus the evolution of the flight. However, as with any other measurement, the measurement of the atmospheric properties is subjected to inherent inaccuracy which should be taken into account when modelling the uncertainty. This also accounts for weather forecasts that, despite the increasing accuracy of these forecasts, inevitably consists of an element of uncertainty.

#### Modelling uncertainties

The use of an aircraft performance model to compute the predicted trajectories introduces uncertainties that are caused by the simplifications and assumptions made to represent the motion of the aircraft by a mathematical model. The selection of an accurate aircraft performance model would contribute to the improvement of the accuracy of the predictions, especially during the climb and descent phases which are considered to be the most complex from a modelling perspective. Currently, the Eurocontrol BADA models are the most accurate APMs that are publicly available, which is why they have been widely adopted by many studies. Overall, this category of uncertainty covers all modelling implementation errors and the required assumptions to formulate the mathematical expression of the motion of the aircraft [51].

#### Flight technical uncertainties

The flight technical errors are inevitably introducing uncertainty in the predictions. These discrepancies represent the lack of adherence to the planned track of the aircraft. It defines the difference between the intended and actual flight due to the performance of the autopilot/FMS. These impacts cannot be accounted for in the TP as it is not related to any modelling simplification or assumption. It can be assumed that the influence of this source of uncertainty is negligible compared to other sources of uncertainty discussed above [53].

The sources of uncertainties discussed above all impact the predictive capability of a TP. When using a deterministic approach, these uncertainties are not addressed and a nominal value is selected to represent the parameters described above. This would result in a single predicted trajectory that does not contain any information that could be used to state the level of confidence that is associated with the predicted outcome. In order to account for the uncertainties defined above, a stochastic or probabilistic approach is required. A probabilistic approach takes into account the uncertainty that is associated with the input data, and eventually computes a predictive distribution that provides information regarding the level of confidence that is associated with the predictions.

### 3.2. Uncertainty characterisation

Once the stochastic factors are identified, the uncertainty of these factors should be characterised. Commonly, the uncertainty of a variable could be characterised by representing the variable by a probability density function (PDF), and many studies have adopted the Gaussian distribution to represent the parameters. The symmetric Gaussian distribution could be used to represent variables of which a nominal value is known. This nominal value would represent the mean of the distribution, and the probability decreases for values further away from this nominal value. However, the Gaussian distribution might not always be suitable for application since the support of this distribution is infinite. The selection of appropriate PDFs could be based on a prior belief in the parameter of interest. Certain parameters might have a known lower and upper bound, which implies that using a Gaussian distribution would not provide a reasonable representation of the parameter. A distribution with finite support might be more appropriate to model that particular input variable. In case when the parameter of interest is bounded by a lower and upper bound and the probability does not vary across the specified interval of possible values, the uniform distribution could be used to effectively characterise the parameter. Casado et al. [51] suggest the use of the uniform distribution for the forecasts of local temperature and pressure, in case these forecasts only provide minimum and maximum values. More complex behaviour of variables could be characterised by the Beta distribution which is a flexible distribution that is defined by two shape parameters that could be adjusted to represent different behaviours.

In another study, Casado et al. [53] specified various stochastic factors that affected the evolution of the trajectory of an aircraft. Eventually, three different distributions were selected to represent the variables. A uniform distribution was used to represent the initial mass of the aircraft. Certain parameters that described the aircraft intent (cruise flight level, descend speed) were modelled as normal variables. Drag coefficients and fuel consumption coefficients, as defined by the APM, were represented by triangular distributions that clearly define the most likely value of the variable. The selection of the particular distributions was based on made assumptions and simplifications and not supported by any observational data.

Álvaro Rodríguez-Sanz et al. [54] used a slightly different approach. Instead of defining a distribution that represents the values of the parameter of interest, this study modelled the inputs as the variable plus a precision error. The nominal value of the input parameter was obtained from a deterministic model, while the precision error for each parameter was drawn from a selected statistical distribution. For example, the temperature parameter was modelled by a nominal value obtained from the ISA model, while the precision errors were represented by a Gaussian distribution with mean  $\mu = 0^\circ$  and a standard deviation  $\sigma = 1^\circ$ .

While the studies above determined the selection of statistical distribution based on theory or prior belief, Rudnyk et al. [55] characterised the stochastic factors by PDFs that were obtained from surveillance data, weather forecasts, and air traffic controller's inputs. The parameters of a specific distribution were estimated by using the Maximum Likelihood Estimate (MLE). The MLE estimates the parameters of a distribution that makes the observed data most probable. After a distribution was selected and its parameters were estimated, a goodness of fit test was applied to evaluate how well the sample data fits the selected distribution. For this purpose, the Kolmogorov-Smirnov (K-S) test was applied. The K-S test computes the distance between a hypothetical cumulative distribution and the empirical cumulative distribution obtained from the data. The lower this distance, the better the data fits the selected distribution.

### 3.3. Uncertainty propagation

The uncertainties of the input parameters are propagated through the predictive model which allows for a more extensive analysis to identify principal contributors to the output's uncertainty. The propagation of uncertainty involves the use of computational tools to identify the joint effect of the stochastic factors on the prediction of the quantity of interest. The uncertainty of the predictions of the target variables then is represented by a posterior predictive distribution [56]. Probably one of the most well-known methods that incorporates the propagation of uncertainty is the Monte Carlo (MC) method. This method was also applied by the studies described in the previous section. The Monte Carlo approach utilises the probabilistic representations of the stochastic factors to draw the inputs of the prediction model. The inputs are sampled randomly from their corresponding distribution in order to incorporate the uncertainty in the model. For each combination of selected input values, a deterministic problem is solved. In aircraft trajectory predictions, this deterministic problem is represented by the mathematical formulation of the motion of the aircraft. The obtained results, from a number of simulations with different inputs, are aggregated to obtain a distribution of outcomes [54]. Other methodologies that are commonly used to model uncertainty in predictive models are Particle Filtering, Gaussian Process Regression, and Polynomial Chaos Expansion. These techniques and their applications will be discussed extensively in Chapter 4.

### 3.4. Uncertainty management

Uncertainty management generally refers to activities that aid in the evaluation and quantification of the uncertainty in the final predictions [56]. McKay [49] specified that prediction uncertainty relates to the variability in the output associated with input uncertainty and that it is characterised by a prediction probability distribution. In this definition, the model structure is assumed to be known and fixed. Hence, the prediction uncertainty focuses on the impact of input uncertainty rather than structural model uncertainty. As a result of the uncertainty analysis, the prediction distribution attempts to describe the range of possible outcomes together with their corresponding probability [57]. The output uncertainty is commonly expressed by the standard deviation of the prediction distribution. Overall, the output distribution could be used to:

- describe the range of potential outputs at some level of confidence
- measure the probability that the output exceeds a particular threshold value

Commonly, a sensitivity analysis (SA) is performed in combination with the uncertainty analysis. While an uncertainty analysis aims to compute an output distribution that quantifies the output uncertainty due to input uncertainty, a sensitivity analysis aims to describe the effect of changes in model input on the output values of the model. Therefore, the sensitivity analysis could contribute to the identification of the most influential parameters used in a TP. A distinction is made between local and global sensitivity analysis [58].

#### 3.4.1. Local sensitivity analysis

A local SA only varies one input parameter each time, while keeping the other inputs at their reference values. This procedure then is repeated for each parameter in order to identify to which extent each parameter affects the uncertainty in the outputs. The sensitivity index  $S_i$  in a derivative-based local SA is computed by taking the partial derivative of the output  $Y$  with respect to the  $i^{th}$  input  $X_i$  (Equation 3.1).

$$S_i = \frac{\partial Y}{\partial X_i} \quad (3.1)$$

The sensitivity index characterises the effect on the output variable  $Y$  of a perturbation on an input variable  $X_i$  from its reference value [59]. Commonly, the perturbation could be defined as a percentage from the nominal value. It should be noted that the obtained measure of sensitivity is only valid near the chosen nominal value of the parameter. For non-linear systems, the sensitivity index should be computed for different points in the samples space of the parameter in order to obtain a more comprehensive view of the input-output relationship. The main limitation of the local SA is that it does not allow simultaneous changes of input parameters. The local SA analyses each parameter individually

and thus neglects the interaction between parameters. To overcome these limitations, a global SA could be applied.

### 3.4.2. Global sensitivity analysis

In a global SA, all input parameters are varied at the same time, which allows the evaluation of the contributions of each individual parameter as well as interactions between these parameters on the output variable. A common technique in the application of a global SA is based on the computation of the Sobol indices [59]. The Sobol method is a variance-based SA in which the variance of the output is decomposed into fractions that correspond to particular contributions of inputs or subsets of the inputs. The first-order Sobol index is a measure of the contribution of one individual input parameter to the output variance. The first-order index is computed with Equation 3.2.

$$S_i = \frac{V_i}{V} = \frac{\text{Var}(\mathbb{E}(Y | X_i))}{\text{Var}(Y)} \quad (3.2)$$

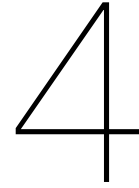
where  $\mathbb{E}(Y | X_i)$  defines the mathematical expectation of the output distribution conditioned on the  $i^{\text{th}}$  input parameter. The higher-order indices, like  $S_{ij}$  could be computed similarly where the output distribution should be conditioned on multiple input parameters ( $Y | X_i, X_j$ ). The higher the sensitivity indices, the greater the influence of that particular set of input parameters on the output variable [60].

While the first-order indices only describe the effect of the individual parameter, the total sensitivity indices also incorporate the effect of the interactions between input parameters. The total sensitivity index  $S_{T_i}$  for the  $i^{\text{th}}$  parameter is computed by adding all respective lower-order effects. For example, if only three input parameters are included in a model ( $X_1, X_2, X_3$ ), then  $S_{T_1}$  is computed with Equation 3.3.

$$S_{T_1} = S_1 + S_{12} + S_{13} + S_{123} \quad (3.3)$$

It is important to calculate both the first-order indices as well as the total-order indices. A low first-order sensitivity index does not necessarily mean that the parameter is unimportant. The interaction of this parameter with other variables might significantly contribute to the variance in the output. Besides, the difference between the first-order effect and the total-order effect represents the contribution of the interactions between parameters on the variability in the output. The study of Sankararaman and Daigle [56] applied the variance-based global SA to the uncertainty analysis in the prediction of the altitude of an aircraft throughout its trajectory. The results showed that the uncertainty of speed commands during the take-off phase contributed to approximately 90% of the total variance in the altitude predictions.





# Probabilistic approach to trajectory predictions

This chapter discusses a variety of techniques that employ a probabilistic framework in a predictive analysis. The techniques described in this chapter are based on the principle of Bayesian statistics, which will be discussed in Section 4.1. The most common probabilistic method used for predictive analytics is the Monte Carlo method, which is briefly described in Section 4.2. Alternative model-based methods like Polynomial Chaos Expansion and Sequential Monte Carlo methods are described in Section 4.3 and 4.4 respectively. A purely data-driven approach called Gaussian Process Regression is explained in Section 4.5. Ultimately, Section 4.6 reviews the discussed methods on their applicability to the predictions of aircraft trajectories using a probabilistic approach.

## 4.1. Bayesian statistics

Before the probabilistic predictive methods are discussed, it is important to point out a key statistical theory that all these methods are based upon. The theory behind the probabilistic approach of uncertainty modelling refers to Bayesian statistics, which is the polar opposite of the more classical Frequentist statistics. Both approaches provide a different interpretation of probability. The frequentist approach defines probability as the limiting relative frequency in many trials. For example, if a coin is tossed  $N$  times (where  $N$  is a large number), and  $N/2$  of these tosses land on heads, then the probability of head is approximately 50% according to the Frequentist approach [61]. On the contrary, the Bayesian interpretation of probability is not based on repetitive trials. In Bayesian statistics, the probability of an event is based on a state of known information, knowledge or the quantification of a prior belief. Referring back to the coin toss example, the outcome of a single trial of the coin toss could be modelled as a random variable following a Bernoulli distribution with parameter  $p$ . The Bernoulli distribution is a discrete PDF that takes the value 1 (heads) with probability  $p$  and 0 (tails) with probability  $1 - p$ . From a frequentist perspective, the inferred value of the parameter  $p$  is said to be fixed or deterministic. On the contrary, from a Bayesian perspective, this parameter  $p$  is also considered to be a random variable that follows a specified distribution that could be defined based on prior knowledge or belief. In a statistical model, the prior belief is commonly referred to as the *a priori* information, which represents known information before the data have been observed. The Bayesian approach provides a probabilistic framework to combine the *a priori* information with the information obtained from the data to eventually compute a refined distribution: the so-called *a posteriori* distribution. Effectively, the prior distribution is being updated to a posterior distribution with the aid of data. The principle of Bayesian statistics could be expressed mathematically by using Bayes' Theorem (Equation 4.1).

$$P(A | B) = \frac{P(B | A)P(A)}{P(B)} \quad (4.1)$$

Bayes' Theorem expresses that the conditional probability of event  $A$  given event  $B$  is equal to the

probability of event B given event A multiplied by the marginal probability of event A divided by the marginal probability of event B [62]. As mentioned previously, Bayesian statistics commonly involves probability distributions rather than fixed point probabilities. The main goal of the application of Bayesian statistics is to represent prior uncertainty regarding model parameters by a probability distribution and to update that distribution, with the help of data, to a posterior distribution that contains less uncertainty. Bayes' Theorem could be expressed using probability distributions as defined by Equation 4.2.

$$f(\theta | \text{data}) = \frac{f(\text{data} | \theta)f(\theta)}{f(\text{data})} \quad (4.2)$$

where  $f(\theta | \text{data})$  represents the updated posterior distribution for the parameter  $\theta$ .  $f(\theta)$  represents the prior distribution of the parameter and  $f(\text{data})$  is the marginal probability of the data, also commonly referred to as the evidence [62]. Furthermore,  $f(\text{data} | \theta)$  is the sampling density function that is proportional to the likelihood function that quantifies the extent to which the data supports the prior belief on the parameter. The denominator, which is computed by Equation 4.3, acts as a scaling constant such that the posterior distribution defines a proper distribution that integrates to 1 over its domain.

$$f(\text{data}) = \int f(\text{data} | \theta)f(\theta)d\theta \quad (4.3)$$

The integral stated above is usually computationally expensive and time-consuming. Since the outcome of the integral only acts as a scaling constant, the posterior distribution is usually expressed using the proportionality to the likelihood and the prior distribution as expressed by Equation 4.4.

$$\text{Posterior} \propto \text{Likelihood} \times \text{Prior} \quad (4.4)$$

where the " $\propto$ " symbol describes "proportional to".

Figure 4.1 illustrates the Bayesian principle. This graph contains the prior distribution, the likelihood distribution, and the posterior distribution. The prior information (dashed line) clearly shows that the parameter almost certainly lies within -4 and 4, and is most likely to be between -2 and 2. The data, represented by the likelihood distribution (dotted line), is shifted to the right and favours values between 0 and 3. According to the data, values outside this interval are less likely and contradicts the prior information. The posterior distribution (solid line) combines both distributions to generate the final distribution.

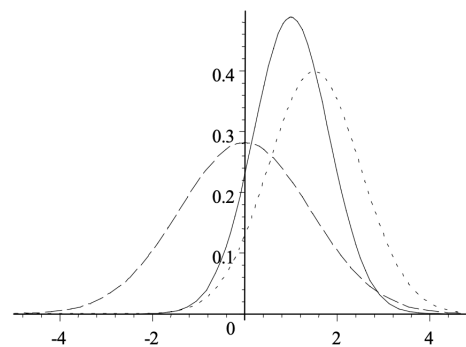


Figure 4.1: Illustration of Bayesian statistics showing the prior distribution (dashed), the likelihood function (dotted), and the posterior distribution (solid) [3]

As could be observed, the prior information is centred around 0 while the likelihood is centred around 1.5. The posterior distribution lies in between these two distributions and is slightly more shifted towards the likelihood distribution. The reason for this is that Bayes' Theorem recognises the strength of the source of information, which is represented by the narrowness of the distribution. The likelihood function clearly shows less variance, which is why the posterior distribution prioritises this source of information [3]. In this example, the frequentist estimate of the parameter would be 1.5 which represents the MLE. The Bayesian estimate, that incorporates prior knowledge and information, would be

approximately 1.

The formulation of prior information is a key aspect of Bayesian statistics. However, obtaining an informative prior might not always be possible. For example, in complex applications where the formulation of the dependencies between parameters might be out of reach due to limited knowledge of the problem. If no sufficient prior information is known, it is desired to obtain a prior distribution that has minimal influence on the inference. These priors are called non-informative priors. For example, a uniform prior distribution is a well-known non-informative prior which assigns equal probabilities to a range of values within a specified interval. Consonni et al. [63] provide further information on various non-informative priors.

The main difference between Frequentist and Bayesian statistics is how both approaches measure uncertainty in parameter estimation. As discussed, the Frequentist approach obtains point estimates of unknown parameters which are commonly based on the MLE. From here on, the derived parameter is said to be fixed and no probabilities are assigned to other potential values for the parameter in question. Frequentists rely on the construction of confidence intervals around the estimate to measure uncertainty. These confidence intervals simply reflect the probability of obtaining an interval estimate that includes the particular parameter under repeated trials. Hence, a confidence interval of 95% only implies that 95% of the constructed confidence intervals will contain the true parameter. It would be incorrect to state that a confidence interval covers the true parameter with a probability of 95%. In the Bayesian approach, however, a full posterior distribution of the parameter of interest is derived. This allows for more extensive statistical analysis to measure and quantify the uncertainty of the estimation [62]. Since this thesis project focuses on modelling and quantifying uncertainty in predictions, using the Bayesian approach would be a logical choice.

## 4.2. Monte Carlo methods

As mentioned in section 3.3, one of the most common probabilistic methods used to incorporate uncertainty in a model is the simulation-based Monte Carlo (MC) method. The MC processes are used to estimate the probability of different outcomes of a model that is subjected to various uncertain inputs. The MC method is based on Bayesian statistics and contains a set of methods used for randomly sampling variables from their corresponding probability distributions. After the inputs are drawn from their distributions, the deterministic model is simulated many times in order to arrive at an ensemble of outputs. These outputs are aggregated to estimate the posterior distribution [64]. The MC method is fairly easy to implement which has made it the method of choice for several studies. This method has also been used as a common benchmark model to compare the results to the outcomes of different methodologies [53]. However, the main drawback of this approach is the fact that it is computationally expensive and time-consuming [53]. This is caused by the required number of simulation runs to obtain accurate estimations. The MC method eventually computes an approximation of the posterior distribution and hence is subjected to approximation errors. These relative approximation errors ( $e_{appr}$ ) decrease when the number of runs ( $N$ ) is increased according to Equation 4.5.

$$e_{appr} = \frac{1}{\sqrt{N}} \quad (4.5)$$

Hence, in order to reduce the error by half, the number of runs is required to increase by four. Rudnyk et al. [55] assumed a relative error of 0.01, which required 10,000 simulations of the trajectory of an aircraft. The computational cost related to the required number of simulations is a major disadvantage of the classical Monte Carlo approach.

## 4.3. Polynomial Chaos Expansion

Polynomial Chaos Expansion (PCE) is a relatively new stochastic technique applied in UQ that captures the uncertainty related to the input parameters through a basis of polynomials. These input uncertainties are propagated to the model outputs with only a limited number of simulation runs [65]. The PCE is based on the principle of representing an arbitrary random variable of interest (output) as a function of other random variables (inputs), where the function is represented by a polynomial expansion. Just as the classical Monte Carlo approach, it is required to specify the probability density functions of the

input random variables [66]. A comprehensive description of the principles behind the PCE technique could be found in the tutorial by O'Hagan [66].

The principle of PCE has not been used extensively in the field of aircraft trajectory prediction. Even though this model presents considerable computational advantages over the classical Monte Carlo approach, it is known to be more difficult to implement. Casado et al. [53] applied the PCE method to quantify the uncertainties associated with the prediction of aircraft trajectories. Several sources of uncertainty were identified and eventually expressed by univariate polynomial descriptions. These expressions were used to build a multivariate polynomial expression that represented the variability of aircraft state variables (e.g. aircraft mass, speed, heading) along a predicted trajectory. The mean and standard deviation of the aircraft state variables were computed and compared to a benchmark model that applied the Monte Carlo approach. The results showed negligible differences between the outcomes of both methods. The study highlighted the computational efficiency of PCE, where PCE obtained similar results while being around 200 times faster than the Monte Carlo method.

#### 4.4. Sequential Monte Carlo methods

Data analysis in real-world applications often involves the estimation of unknown variables given a sequence of observations on quantities that are related to the variable of interest. Often, these observations arrive sequentially in time and examples include the tracking of the aircraft position given radar measurements, or the identification of a communication signal given noisy measurements that arrive sequentially in time. The Bayesian framework combines prior information regarding the observable and the likelihood functions that relate the observations to the unknown parameters. The resulting posterior distribution could be approximated using Bayes' Theorem. In processes where more observations become available over time, it would be more convenient to update the posterior distribution than to recalculate from scratch that requires all data to be stored. A common method that uses this principle of approximating a posterior distribution sequentially in time is the Sequential Monte Carlo method (SMC). The SMC methods comprise a set of simulation-based methods that provide convenient approaches to estimating a posterior distribution from partial observations [67]. One of the well-known applications of SMC methods is the use of particle filters. The particle filtering approach sequentially processes the received observations. Such filters commonly work in two stages: prediction and update. The prediction stage utilises the system model to predict the posterior distribution function of the state of the system. The state of the system is commonly subjected to disturbances (process noise). Hence, the prediction usually deforms and spreads the posterior distribution function. The update stage aims to make use of the latest observations to modify and refine the posterior distribution [68].

##### 4.4.1. Recursive Bayesian estimation

SMC methods are based on the principle of Recursive Bayesian estimation where a probabilistic framework is applied to estimate a posterior distribution recursively over time by using incoming measurements. As SMC methods are simulation-based, the definition of a state-space model is required that could be used to simulate the evolution of the states of the aircraft model. Hence, the starting point in SMC is defining a discrete-time model of the nonlinear dynamics of the aircraft and the observed measurements. The state-space model that is used to simulate the state evolution of the aircraft has the following form:

$$\begin{aligned} x_t &= f(x_{t-1}) + \omega_{t-1} \\ y_t &= h(x_t) + v_t \end{aligned} \tag{4.6}$$

where  $x_t$  and  $y_t$  contains the set of system states and measurements at time  $t$  respectively. The state vector comprises all relevant information that is necessary to describe the motion of the aircraft, while the observations might comprise weather forecasts or aircraft positions obtained from radar measurements. The state transition function and observation function are represented by  $f(\cdot)$  and  $h(\cdot)$  respectively. The state-space model is completed with the addition of process noise  $\omega_{t-1}$  and observation noise  $v_t$ . This system of equations could be transformed into a probabilistic framework as expressed below.

$$\begin{aligned} x_t &\sim p(x_t | x_{t-1}) \\ y_t &\sim p(y_t | x_t) \end{aligned} \quad (4.7)$$

Here,  $p(x_t | x_{t-1})$  represents a PDF that models the stochastic evolution of the states of the aircraft over time. This transition probability function is a key feature of a Markov process, which describes that the current state at time  $t$  is only dependent on the state at the previous time step  $t - 1$ .  $p(y_t | x_t)$  is a PDF that models the distribution of the observations given the current state at time  $t$  [19]. The principle of recursive Bayesian estimation is to derive the posterior distribution function, given the set of measurements, denoted by  $p(x_t | y_{1:t})$ . This requires the assumption that the initial distribution of the state vector  $p(x_0)$ , also known as the prior, is known. The posterior distribution function is approximated in two stages: prediction and update. The prediction stage involves the state transition probability function defined by Equation 4.7. In Markov processes, the Chapman-Kolmogorov equation could be used to express the state prediction equation (Equation 4.8) [69].

$$p(x_t | y_{1:t-1}) = \int p(x_t | x_{t-1}) p(x_{t-1} | y_{1:t-1}) dx_{t-1} \quad (4.8)$$

As soon as a following measurement  $y_t$  becomes available at time  $t$ , the prior distribution could be updated by using Bayes' Theorem for probability density functions according to Equation 4.9.

$$p(x_t | y_{1:t}) = \frac{p(y_t | x_t) p(x_t | y_{1:t-1})}{p(y_t | y_{1:t-1})} \quad (4.9)$$

When combining Equation 4.9 and Equation 4.8, the recursive form of the posterior distribution (update equation) could be expressed by Equation 4.10.

$$p(x_t | y_{1:t}) = \int \frac{p(y_t | x_t) p(x_t | x_{t-1})}{p(y_t | y_{1:t-1})} p(x_{t-1} | y_{1:t-1}) dx_{t-1} \quad (4.10)$$

The integral expressed above cannot typically be computed analytically and makes direct sampling from this distribution impossible. This is where particle filtering comes into play where the SMC sampling method is applied to approximate the optimal Bayesian solution [69].

#### 4.4.2. Particle filtering methods

The particle filter uses recursive Bayesian estimation based on importance sampling in order to approximate the posterior distribution. The idea behind particle filtering is to represent the desired posterior distribution function by a specified set of samples with corresponding weights. These samples are represented by a set of particles, where the weight of that particle is based upon the likelihood of that particle being drawn from the posterior distribution. When a large number of particles are drawn, the particle filter approximates the target distribution by sampling the particles from a proposal distribution that updates these particles recursively when new measurements arrive. The set of  $N$  particles could be represented by  $\chi$  as follows:

$$\chi = \{x_t^{(i)}, w_t^{(i)}\}_{i=1}^N \quad (4.11)$$

where  $x_t^{(i)}$  defines the  $i^{th}$  possible state at time  $t$ , while  $w_t^{(i)}$  represents the corresponding normalised weight that is assigned to that particular state [70]. This set of particles then is used to approximate the posterior density function empirically (Equation 4.12).

$$p(x_t | y_{1:t}) \approx \sum_{i=1}^N w_t^{(i)} \delta(x_t^{(i)}) \quad (4.12)$$

where  $\delta(\cdot)$  is the Dirac Delta function centred around  $x_t^{(i)}$ , which is used to construct the empirical distribution according to the normalised weights associated with these possible states. When direct sampling from a target distribution  $p(x)$  is intractable, the particle filter samples from a proposal distribution  $\pi(x)$ , also described as the importance function. The non-normalised weights, computed by

Equation 4.13, represent how close the support of the proposal distribution fits the target distribution to be estimated.

$$w^{*(i)} = \frac{p(x)}{\pi(x)} \quad (4.13)$$

Subsequently, the weights are normalised by dividing each weight by the total sum of weights, such that the sum of normalised weights equals one. In sequential importance sampling, the particles are drawn from the proposal distribution  $\pi(x)$ . In the literature, the most common choice for the proposal distribution is called the prior importance function  $p(x_t^{(i)} | x_{t-1}^{(i)})$ . Djuri et al. [70] present the following two important steps that are required to update the weights of the particles (Equation 4.14).

$$\begin{aligned} x_t^{(i)} &\sim p(x_t^{(i)} | x_{t-1}^{(i)}) \\ w_t^{(i)} &\propto w_{t-1}^{(i)} p(y_t | x_t^{(i)}) \end{aligned} \quad (4.14)$$

The particle update equations expressed above start with drawing the particles from the proposal distribution. Hereafter, the corresponding weights are computed and updated by using the lower equation. Each update step of the particles requires the normalisation of the weights, such that the sum of the weights is equal to one. As could be observed, the updated weight is dependent on  $p(y_t | x_t^{(i)})$  that involves the likelihood of the measurements to be related to the particular possible state.

A common problem in particle filtering is that after several iterations of the predicting and updating stages, the majority of the weights will be concentrated on a few particles and most particles will be assigned to negligible weights. This is called sample degeneracy which degrades the performance of the particle filter [71]. This degeneracy could be avoided by combining a proper choice for the importance function with re-sampling. The principle of re-sampling is to neglect particles with negligible weights and instead replace those with particles in the proximity of highly weighted particles. After the re-sampling step, all particles are weighted equally with  $1/N$ .

#### 4.4.3. Applications of particle filtering

The method of particle filtering can be applied to a large variety of models to estimate unknown parameters and infer predictions. The study of Sun et al. [72] applied the particle filtering method to estimate the aircraft mass and thrust settings right after take-off during the initial phase of the climb. A point-mass aircraft performance model was defined to model the non-linear evolution of the states of the aircraft. This study focused on a short segment (within 30 seconds) right after take-off which allowed the assumption that the mass and thrust settings were constant during that short period of time. The prior belief related to the mass and thrust setting of the aircraft was incorporated by specifying an initial state distribution  $p(x_0)$ . Both states were assumed to originate from uniform distributions, where the mass was limited by the Operating Empty Weight (OEW) and the Maximum Take-Off Weight (MTOW) of the specific aircraft in question. The observations related to other states of the aircraft were primarily derived from ADS-B broadcasts, where observation noise was implemented in the state-space model by considering the ADS-B accuracy standards. In order to test and validate the results from the estimations of the mass and thrust settings, simulated, real, and measurement flights were used. The proposed recursive Bayesian estimation framework showed its potential to accurately estimate the mass of the aircraft with a mean absolute error of 4.3% of the actual true aircraft mass. The accurate estimation of the mass could contribute to a more accurate prediction of other states of the aircraft throughout its trajectory.

Lymperopoulos and Lygeros [19] formulated the aircraft trajectory prediction as a Bayesian estimation problem, where they applied the particle filtering approach. A stochastic non-linear aircraft model was specified where partial observations arrived every 30 seconds from radar measurements. The stochastic dynamics arose from the uncertainty related to wind conditions that potentially affect the flight and the uncertainty caused by the unknown mass of the aircraft. The results from the particle filter were compared to a simulated trajectory that was considered as the real trajectory. The study focused on the climb phase as this was found to be the most challenging part of the flight due to rapid changes in

wind conditions between different flight levels. Besides, the mass of the aircraft plays a crucial role in the climb performance of the aircraft. The results were assessed on the spatial and temporal errors as defined in section 2.3. The results discovered that the SMC method has no problems in capturing the non-linear flying dynamics of the aircraft. As new measurements arrive, the particle filter algorithm converges to the real trajectory and provide increased accuracy in the predictions of the future position of the aircraft. Conde et al. [73] also point out the interest of the re-sampling process, which contributed to the reduction in uncertainty as particles with negligible weights are not propagated through the entire computation.

## 4.5. Gaussian Process Regression

The methods discussed in the previous sections rely on the simulation of a model that represents a mathematical formulation of the flight dynamics of the aircraft. However, as mentioned in section 2.2, data-driven approaches could be used to compute predictions based on historical observations by exploiting the available data on flown trajectories. Gaussian Process Regression (GPR) is such a machine-learning approach that exploits the available data to compute the predictions using a Bayesian approach to regression techniques.

### 4.5.1. Gaussian Process background

Regression is a common statistical analysis that aims to describe the relationship between a continuous dependent variable  $y$ , and a set of independent variables defined by the input vector  $\mathbf{x}$ . The relationship between the dependent and independent variables could be exploited to generate predictions on the variable of interest. A common regression model takes the following form, as defined by Equation 4.15.

$$y = f(\mathbf{x}) + \epsilon \quad (4.15)$$

where  $f(\mathbf{x})$  defines the underlying regression function that should be estimated, and  $\epsilon$  represents the noise term with which the dependent variable is distributed around the regression function [74]. Under GPR, it is assumed that the regression function follows a Gaussian Process (GP) prior. This prior expresses the modelling assumptions and essential features of the function, such as periodicity and the smoothness of the function [75]. Mathematically, a GP could be expressed as a collection of random variables indexed by a continuous multivariate variable  $\mathbf{x}$  such that any finite selection of random variables has a multivariate Gaussian distribution. This implies that a GP could be fully expressed by the mean function  $m(\mathbf{x})$  and the covariance function  $k(\mathbf{x}, \mathbf{x}')$ . While a common regression model aims to estimate a variable, GPR exploits the regression model to estimate a function. Hence, the mean and covariance of the GP prior are functions defined by Equation 4.16 and Equation 4.17.

$$m(\mathbf{x}) = \mathbb{E}[f(\mathbf{x})] \quad (4.16)$$

$$k(\mathbf{x}, \mathbf{x}') = \text{Cov}[f(\mathbf{x}), f(\mathbf{x}')] \quad (4.17)$$

The combination of the mean function and the covariance function (or kernel) allows for the representation of the GP, as defined by Equation 4.18.

$$f(\mathbf{x}) \sim \mathcal{GP}(m(\mathbf{x}), k(\mathbf{x}, \mathbf{x}')) \quad (4.18)$$

Studies that applied GPR often assume the mean function to be zero and the noise term to be drawn independently from a Gaussian distribution with mean zero and noise variance  $\sigma_n^2$ . The combination of these two assumptions could be used to derive the distribution of the dependent variable  $y$  (Equation 4.19) [76].

$$y \sim \mathcal{GP}(0, k(\mathbf{x}_i, \mathbf{x}_j) + \sigma_n^2 \delta_{ij}) \quad (4.19)$$

where  $k(\mathbf{x}_i, \mathbf{x}_j)$  denotes the covariance between two input vectors  $\mathbf{x}_i$  and  $\mathbf{x}_j$ .  $\delta_{ij}$  represents the Kronecker Delta function that is equal to one when  $i = j$  and zero otherwise. The covariance matrix in a GP with  $N$  observations could be expressed as follows:

$$K(X, X) = \begin{bmatrix} k(\mathbf{x}_1, \mathbf{x}_1) & k(\mathbf{x}_1, \mathbf{x}_2) & \dots & k(\mathbf{x}_1, \mathbf{x}_N) \\ k(\mathbf{x}_2, \mathbf{x}_1) & k(\mathbf{x}_2, \mathbf{x}_2) & & k(\mathbf{x}_2, \mathbf{x}_N) \\ \vdots & \ddots & \ddots & \vdots \\ k(\mathbf{x}_N, \mathbf{x}_1) & k(\mathbf{x}_N, \mathbf{x}_2) & \dots & k(\mathbf{x}_N, \mathbf{x}_N) \end{bmatrix} + \sigma_n^2 I_N \quad (4.20)$$

where  $I_N$  represents an identity matrix of size  $N$ .

#### 4.5.2. Model selection

The prior information incorporated in this Bayesian technique is entirely captured by the selection of the covariance/kernel function. These kernels fully determine the shape of the prior and posterior of the GP. These kernels incorporate assumptions on the function to be estimated by defining the similarity between data points. The similarity between these data points is expected to be a key driver for the estimation of the target variable as it is assumed that two dependent variables will be similar when they are observed at similar data points. A distinction is made between stationary and non-stationary kernels. Stationary kernels only depend on the distance between two data points and do not take into account the absolute value of these points, while non-stationary kernels do consider the specific values of the data points [77].

##### Squared exponential kernel

One of the most commonly adopted kernel function is the stationary squared exponential function as expressed by Equation 4.21 [78].

$$k(\mathbf{x}_i, \mathbf{x}_j) = \sigma_f \exp\left(-\frac{\|\mathbf{x}_i - \mathbf{x}_j\|}{2\ell}\right) \quad (4.21)$$

The kernel above is also commonly described as the Radial Basis Function (RBF). This specific kernel function contains two parameters:  $\sigma_f$  and  $\ell$ . These parameters are called the hyperparameters of the GPR model.  $\sigma_f$  defines the amplitude that describes the maximum assigned covariance between two input vectors, while  $\ell$  is the length scale parameter that defines the rate of decay of the covariance as the distance between the input vectors gets larger. The Euclidean distance  $\|\cdot\|$  is used as a measure of similarity between the input vectors. This kernel is infinitely differentiable, which makes the function rather smooth. Hence, this would be a promising kernel in the application of trajectory predictions, which could be considered as a smooth function without abrupt changes of the dependent variable, being either the latitude, longitude or altitude of the aircraft.

##### Rational quadratic kernel

The rational quadratic kernel could be considered as a mixture of RBF kernels that defines different characteristic length scales. GP priors that use this kernel are expected to encounter functions that vary smoothly across different length scales. The rational quadratic kernel is expressed by Equation 4.22 [77].

$$k(\mathbf{x}_i, \mathbf{x}_j) = \sigma_f \left(1 + \frac{\|\mathbf{x}_i - \mathbf{x}_j\|}{2\alpha\ell^2}\right)^{-\alpha} \quad (4.22)$$

The rational quadratic kernel includes an additional hyperparameter  $\alpha$  which is known as the scale mixture parameter. When  $\alpha$  approaches large values, the rational quadratic kernel converges to the squared exponential kernel.

##### Other kernels

Rasmussen and Williams [77] describe a multitude of kernel functions that could be used to represent a large variety of functions. A more rough function could be obtained with the Matérn kernel that incorporates an additional hyperparameter that allows for the adjustment of the smoothness of the function. Other functions might need to represent periodic behaviour which requires the inclusion of a cosine or sine component in the covariance function. For this purpose, the exponential sine squared kernel would be more appropriate. To model sudden changes in the behaviour of the function, a combination

of kernels could be combined to allow for sudden changes. Overall, the squared exponential kernel and the rational quadratic kernel seem to be the most promising kernels that could be used to reconstruct a function of the flown trajectory of an aircraft. Both kernels are stationary and provide smooth functions, and neighbouring input vectors are considered to cause motion in similar directions which applies to the expression of the aircraft trajectory.

The learning process of GPR comprises the tuning of the hyperparameters, such that the selected parameters maximise the posterior probability. This is commonly done by maximising the marginal log-likelihood with respect to the hyperparameters [79]. A gradient-based optimiser could be used to efficiently find the maximum of the marginal log-likelihood.

### 4.5.3. Predictions based on Gaussian Process Regression

The objective of the use of GPR is to estimate the value of a function  $f$  evaluated at any set of new inputs  $\mathbf{x}^*$ . The joint distribution of the observed values  $y$ , and the predicted values  $y^*$  can be expressed by Equation 4.23 [78].

$$\begin{bmatrix} y \\ y^* \end{bmatrix} \sim \mathcal{N} \left( 0, \begin{bmatrix} K(X, X) & K(X, X^*) \\ K(X^*, X) & K(X^*, X^*) \end{bmatrix} \right) \quad (4.23)$$

Hence, the posterior predictive distribution of the dependent variable is also a multivariate Gaussian distribution, given by:

$$\begin{aligned} y^* | X^*, X, f &\sim \mathcal{N}(\mu, \Sigma) \\ \mu &= K(X^*, X) K(X, X)^{-1} f \\ \Sigma &= K(X^*, X^*) - K(X^*, X) K(X, X)^{-1} K(X, X^*) \end{aligned} \quad (4.24)$$

Since GPR follows a Bayesian probabilistic approach, the predictions on particular variables are represented by a predictive distribution. Usually, the best estimate of the variable is considered as the mean of this distribution, while the uncertainty of the prediction is associated with the variance of this particular distribution. The computational complexity of Equation 4.24 arises from the inversion of the covariance matrix. This grows as  $\mathcal{O}(N^3)$  in the number of observations  $N$ . Rong et al. [78] applied a technique called the Cholesky decomposition which reduced the overall computational complexity to  $\mathcal{O}(N^2)$ . This technique relies on the decomposition of a matrix and is commonly used in linear algebra to speed up matrix operations.

### 4.5.4. Applications of Gaussian Process Regression

GPR models have been widely applied to a variety of studies and proved to be a well-suited model for applications with noisy measurements, such as positional sensor data obtained from moving vehicles. Tran and Firl [80] applied GPR to model road traffic situations near intersections by specifying the vehicle speed in  $x$ - and  $y$ -direction as two independent Gaussian Processes. The same approach was followed by Goli et al. [79], who address the problem of long-term position prediction of vehicles in a road transportation system. A pair of GPR models was constructed to map the two-dimensional position vector into the speeds in both directions. These velocities were represented by Gaussian Processes that were a function of the positional information. The complete model aims to learn motion patterns from historical trajectories, to eventually predict the future positions of vehicles in a specified environment. Their study also identified the importance of trajectory clustering to improve the performance of the trajectory pattern learning performance of the model. Training a GPR model on a subgroup of trajectories showed better performance in the sense of processing time and prediction results. The trajectories were clustered using the K-means clustering algorithm. Rong et al. [78] used a GP to define a distribution of the lateral position of a ship along its trajectory. As observational data arrived, the GP allowed predicting the lateral position conditionally on newly observed data and prior observations. Both studies described above used the squared exponential covariance function to specify the characteristics of the function to be estimated. Even though GPR has been a popular framework to model and predict vehicle motion [78–80], no literature was found on the prediction of aircraft trajectories using this technique. However, a few studies have applied the method to predict certain aircraft parameters.

Naturally, the mass of the aircraft plays a crucial role in aircraft performance and affects a variety of characteristics, ranging from the flown trajectory to the fuel burn during the flight. The take-off mass of the aircraft is usually not available, which motivated Chati and Balakrishnan [76] to propose a model to statistically predict the take-off mass of the aircraft using a GPR model. In another study, Chati and Balakrishnan [74] examined the performance of the engine of the aircraft by statistically analysing and modelling the engine fuel flow rate using GPR. The fuel flow rate is an important performance parameter of the engine, but is commonly proprietary to the airline and thus is not easily accessible for researchers. Therefore, the proposed model could be helpful to studies that only have limited information available. The study exploited flight track data to predict the fuel flow rate, and the results were compared to the deterministic BADA model. The GPR model showed a significant improvement in predictive performance with a 50% reduction in the mean error between the true- and predicted fuel flow rate. Both studies have shown the relevance of the use of GPR to predict parameters, like the aircraft mass and fuel flow rate, which are usually not publicly available. The estimation of such parameters, that would otherwise be unknown, could contribute to the more accurate prediction of aircraft performance and flown trajectories.

The studies outlined above have shown several advantages of the use of GPR models to predict the motion of a vehicle. GPR has proven to be a powerful, robust technique for regression problems. One of the major advantages is the non-parametric nature of this technique, in which no underlying assumptions of the functions or independent variables have to be specified. The function to be estimated could conveniently be specified by only making use of a mean function and covariance function. Other advantages arise from its applicability to trajectory predictions that are subjected to uncertainties. The GPR model provides good analytical properties by constructing a prediction distribution which allows for the analysis of the uncertainties of the predictions.

#### **4.6. Review of probabilistic prediction techniques**

Using probabilistic prediction techniques rather than deterministic methods allows for the propagation of input uncertainty through the model to represent the outputs as a prediction distribution. In aircraft trajectory predictions, representing the predicted trajectory as a distribution of likely trajectories allows for a more extensive evaluation of prediction uncertainty. This is in contrast to the deterministic approach that simply computes the most likely trajectory.

Simulation-based techniques, like the Monte Carlo approach, require the input parameters to be specified as probability density functions. The input parameters are then sampled from their corresponding distribution, and a deterministic model is solved numerous times to obtain a distribution that represents the outcome of the deterministic model. Hence, the Monte Carlo approach is only partially stochastic as it solves a deterministic model for different inputs, where the deterministic model is represented by the point-mass model of the aircraft. For the purpose of this project, it is required to have a fully stochastic model that not only includes probabilistic inputs but also the stochastic evolution of the states of the aircraft throughout the flight. Therefore, Sequential Monte Carlo methods would be more appropriate.

Sequential Monte Carlo methods, also known as particle filtering, have been widely applied for the purpose of tracking and predicting the positions of moving objects in a non-linear system. Particle filters use a selection of particles to represent a distribution of a given stochastic process, where each particle is assigned to a computed weight representing the likelihood of being drawn from the distribution. The prediction of states is sequentially updated by propagating these particles. The predictions are sequentially updated using the last received observation, without the need to reprocess older observations. The ability of these methods to predict a multitude of states of a non-linear system with arriving observations sequentially in time show the promising applicability to aircraft trajectory predictions.

As previously mentioned, the increasing availability of data has provided the opportunity to employ data-driven techniques that exploit the available data to learn patterns from historical observations. These patterns are used to compute predictions by using machine learning approaches. In the context

of uncertainty modelling, the non-parametric Gaussian Process Regression (GPR) has been applied in a variety of applications. This technique provides several advantages, in contrast to other variants of regression methods. First of all, GPR is non-parametric which means that the underlying function to be estimated does not have to be defined. Besides, unlike the Monte Carlo simulation-based methods, the use of GPR does not require the quantification of the distribution of the input variables, which might be difficult in certain situations. This method is highly flexible and prior knowledge could be included by specifying the covariance function that describes certain properties of the function to be estimated.

For this project, it has been decided to apply GPR to predict the aircraft trajectories by exploiting historical data. To improve the performance of the model, this method will be applied to subsets of trajectories that are identified from clustering techniques. Furthermore, because of the proven applicability of particle filtering in trajectory predictions, the particle filtering technique will be applied as a benchmark model to be used for comparison and validation of the results. Both particle filtering and GPR propagate the uncertainties in the input parameters through the model to eventually compute a predictive distribution of the predicted trajectories. These distributions are used to evaluate the uncertainty and accuracy of the models.



# 5

## Research approach

This chapter discusses the main research question of this project and the associated sub-questions. The project is broken down into three phases and each phase covers certain sub-questions that collectively contribute to structurally provide an answer to the main research question (Section 5.1). In order to ensure the feasibility of the project, the research scope is defined by setting a number of limitations and assumptions (Section 5.2).

---

### 5.1. Research questions and project breakdown

As described in Chapter 1, the main objective of this research project is to utilise a probabilistic approach to predict the four-dimensional trajectory of an aircraft while taking into account the uncertainty that is associated with the evolution of the flight. While the majority of studies evaluated in the literature review aim to obtain the most accurate predictions, the use of a probabilistic approach allows for a more extensive evaluation of the uncertainty of the predictions. This research objective is translated to the main research question stated below.

**“How could stochastic methods be applied to quantify and model the uncertainties associated with the aircraft 4D-trajectory prediction, and to what extent do these uncertainties affect the predictive capability?”**

The project is broken down into three different phases to structurally arrive at an answer to the main research question defined above.

#### Phase 1: Collection and preparation of data

This first phase concerns the collection of the available data, which originates from different data sources. Different sources of data should be merged to generate a final dataset that eventually is used as input to the probabilistic predictive models. This final dataset includes numerous flight trajectories and other features that describe the state of the aircraft throughout the evolution of the flight. To effectively train the predictive models on the dataset, the trajectories are clustered in groups that contain trajectories with similar space and time characteristics. This is an essential step in the preparation of the final dataset in order to more efficiently train the predictive models. Furthermore, the trajectories are segmented into different flight phases: climb, cruise, and descent. Other pre-processing tasks might include: handling missing values, transforming categorical features to numerical values and filtering outliers. After all data preparation steps, a final dataset is constructed that is used to train the predictive models. The following sub-questions are relevant during this phase of the project:

1. Which parameters are relevant to the evolution of a 4D-trajectory of an aircraft and thus should be included as inputs to the predictive model?
  - (a) Which sources of data could be used to aggregate the trajectory data and how should this data be pre-processed?

- (b) How could the trajectories be clustered into different groups with similar space- and time characteristics?

### Phase 2: Application of the predictive models

Once the final dataset with the relevant features of the trajectories is constructed, the predictive models are applied. These models will be applied to the clusters of trajectories identified from the clustering technique applied during the previous phase. From the literature review, two predictive models have been selected. The model-based Sequential Monte Carlo method that utilises an aircraft performance model, and the data-driven Gaussian Process Regression that fully exploits the generated dataset. The generated dataset will be used to both train and test the predictive models, hence the following sub-question will be answered throughout this phase:

2. How could the established predictive models be trained, tested, and validated?

### Phase 3: Analysis of the results

The probabilistic approaches to the prediction of aircraft trajectories generate a predictive distribution of possible future trajectories assigned to different probabilities. This probability distribution is used to evaluate and analyse the uncertainty associated with the predictions. The main goal of this phase is to evaluate the effects of the input parameters on the predictive capability of the applied models. These models will be assessed on the accuracy and uncertainty of the predictions. The following sub-questions play a crucial role in the analysis of the results:

3. How could the predictive capability be quantified?  
 4. Which parametric uncertainties have the greatest effect on the predictive capability of the 4D-trajectory of the aircraft?  
 5. How does the predictive capability evolve for increasing look-ahead times?

A visual representation of the breakdown of the project into the three described phases is shown in Figure 5.1.

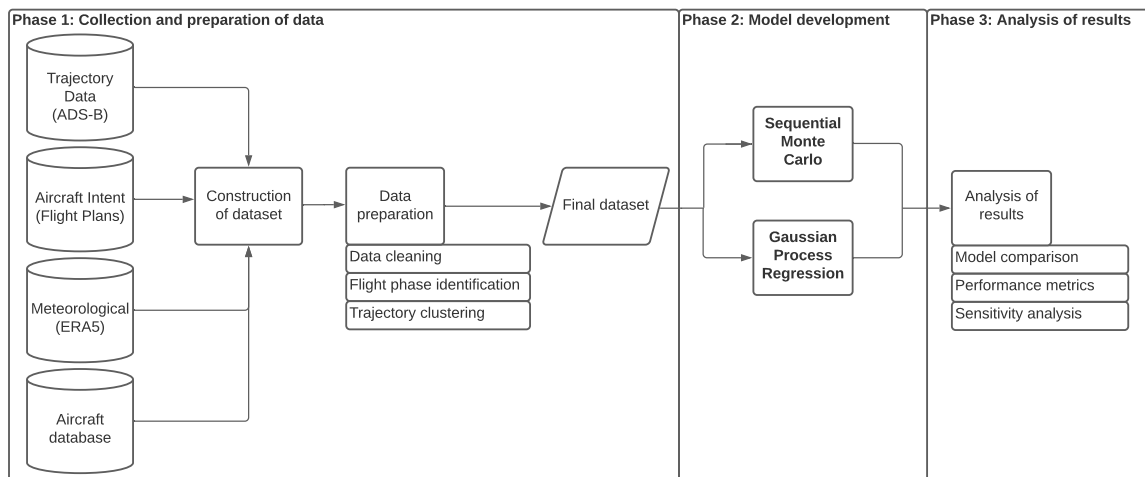


Figure 5.1: Breakdown of the project into three phases

## 5.2. Research scope

Now that the research objective and framework has been established, further demarcation of the project is done by defining the research scope. In order to ensure the feasibility of the project, several assumptions and limitations of the project are introduced. The scope of this research project ensures that the project is feasible to be carried out in the given time span. Furthermore, the available processing capacity is taken into account when considering the amounts of data to be included.

The time span of this project is approximately seven months, and the work is broken down into three phases as discussed above. First of all, ADS-B data, aircraft intent data (obtained from filed flight plans), and meteorological data are merged together to generate an initial dataset that is used to train the predictive models. The data from flight plans were only available for a selection of months, and the most recent month of data (June 2018) was used for this project. Hence, the initial dataset covers flights operated in this particular month. An extensive description of the utilised sets of data and the generation of the initial dataset is found in Chapter 6.

The predictions focus on single trajectories and will neglect the interaction between different aircraft in the airspace. Hence, the detection and resolution of potential conflicts is not considered in this research project. Besides, the prediction of trajectories is segmented into different flight phases: climb, cruise, and descent.

As mentioned previously, two different probabilistic prediction methods will be applied: the model-based SMC and the data-driven GPR. Different variants to the GPR could be applied in which the co-variance/kernel functions could be selected.



# 6

## Data collection and preparation

This chapter elaborates on the first phase of the project that involves the collection and preparation of the data. This results in a final dataset that is used in subsequent phases of the project to develop the predictive models. Initially, the collection of data, originating from different sources, is described (Section 6.1). Then, the steps performed to couple the available datasets are described (Section 6.2). Subsequently, the preparation of the final dataset is discussed, which involves activities like data cleaning, interpolating variables, appending features (Section 6.3). An overview of the final dataset and the exploration of the dataset is provided in Section 6.4. Ultimately, the application of the clustering algorithm to identify subsets of clusters with similar spatial characteristics is discussed (Section 6.5).

### 6.1. Available datasets

The literature review highlighted that the prediction of an aircraft trajectory is usually performed with three main building blocks. The model-based approach uses an aircraft performance model to simulate the evolution of the flight. Besides, the aircraft intent and the meteorological conditions are significant factors that should be considered to accurately predict the aircraft trajectories. This section explores the different sources of data that were used to construct a final dataset to be used for the development of the predictive models.

#### 6.1.1. Trajectory data from ADS-B

The trajectory data is obtained from ADS-B datasets. ADS-B data is automatically transmitted by the aircraft to surrounded ground stations and provides information concerning the state of the aircraft in terms of position and speed. The flown trajectory of the aircraft could be reconstructed by sequencing the position updates over time. Table 6.1 provides an overview of the features included in the ADS-B flight data.

Table 6.1: Features of the ADS-B dataset

Variable	Unit
Unix timestamp	s
ICAO	-
Latitude	deg
Longitude	deg
Altitude	ft
Ground speed	kts
Track	deg
Rate of Climb	ft/min
Callsign	-
Flight ID	-

The Flight ID specified in Table 6.1 is a unique code linked to each flight. A previous research project has applied the DBSCAN clustering technique to extract continuous flights from the ADS-B dataset and assign the unique codes to the identified trajectories [34]. The ADS-B dataset of June 2018 includes a total of 253431 (partial) trajectories, which corresponds to an average of around 8448 daily flights.

Figure 6.1 visualises hundred partial flight tracks from the ADS-B dataset. These tracks were reconstructed from the ADS-B data by ordering the positions of the flight sequentially over time. As could be observed, the data covers the flight paths in and around the Flight Information Region (FIR) of the Dutch airspace.



Figure 6.1: Data coverage of a sample of hundred trajectories flown on 01-06-2018

### 6.1.2. Aircraft intent data from filed flight plans

The flight plan data, released by Eurocontrol, are used to express the aircraft intent which is implemented in the predictions of the aircraft trajectories. Eurocontrol releases different sets of flight data for Research and Development purposes. These data originate from filed flight plans (FP) that are submitted by the aircraft operator that executes flights in and over Europe. All flights operating under Instrument Flight Rules (IFR) are required to submit an FP to the Network Manager (NM) of EUROCONTROL. The available data is distributed over different datasets. An overview of the datasets used throughout this project is found in Figure 6.2.

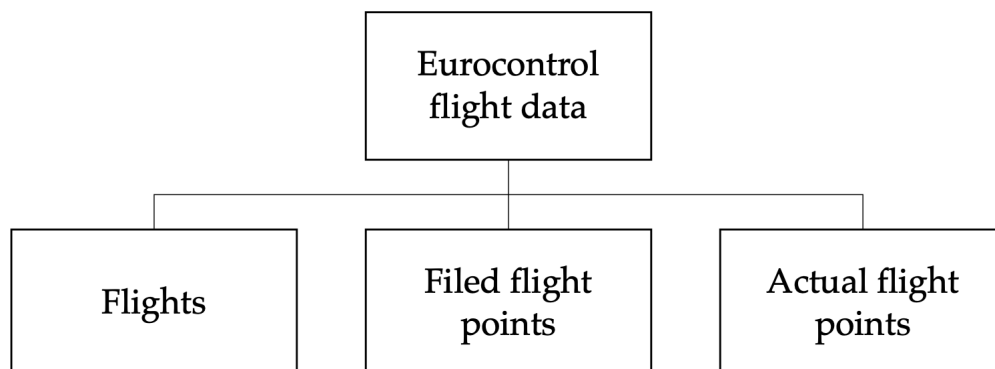


Figure 6.2: Overview of datasets from Eurocontrol

The flights file includes flight details from the FPs. These details comprise, among others, departure-

and arrival airport information, actual- and filed arrival times, requested flight level, market segments (e.g. cargo, low-cost operations), and aircraft-specific information like the registration and type of the aircraft. The most important dataset used is the filed flight points dataset, which comprises a sequence of waypoints filed by the aircraft operator that defines the planned flight path of the aircraft for its flight. Table 6.2 below describes the variables found in this dataset.

Table 6.2: Features of the flight points dataset

Variable	Unit	Description
ECTRL ID	-	Unique numeric identifier for each flight
Sequence number	-	Number of the waypoint crossed by the flight (in chronological order)
Time Over	-	Time at which waypoint is crossed
Flight Level	100 ft	Altitude in flight levels of waypoint
Latitude	deg	Latitude of waypoint
Longitude	deg	Longitude of waypoint

As shown in Figure 6.2, the flight plan data provided by Eurocontrol contain both the filed waypoints as well as the actual waypoints, where the actual version of the data contains updates of the flown flight path from radar observations.

### 6.1.3. Meteorological data from ERA5

The meteorological data were downloaded from the ERA5 database from ECMWF. This dataset is publicly available and provides hourly estimations of a large variety of meteorological variables. The ERA5 dataset stores these variables with a spatial resolution of 30 km over 37 different pressure levels ranging from the Earth's surface to an altitude of 80 km. The pressure ( $P$ ) at different levels was converted to altitude in feet with Equation 6.1 presented below<sup>1</sup>.

$$h_{alt} = \left( 1 - \left( \frac{P}{1013.25} \right)^{0.190284} \right) \times 145366.45 \quad (6.1)$$

Generally, cruise altitudes of commercial airlines will not exceed 45000 ft. Hence, a total of 26 pressure levels higher than 125 hPa were selected. Even though the data is available on an hourly basis, it was decided to only select observations every two hours to limit the dataset dimensions and reduce the required processing capacity. Since the available ADS-B data covers a sub-region of Europe, the extraction of meteorological data is also limited to this region with longitudes ranging from -10 to 30 degrees and latitudes ranging from 30 to 70 degrees. These boundaries ensure that all flights from the ADS-B data are covered and could be aggregated with the selected meteorological parameters. The selected longitudes and latitudes results, with the given spatial resolution, in a horizontal grid of 161 by 161 locations where the parameters of interest are measured. Table 6.3 provides an overview and explanation of the selected meteorological parameters extracted from the ERA5 dataset.

Table 6.3: Features of the ERA5 dataset

Variable	Unit	Description
U-component of wind	m/s	Eastward horizontal component of the wind (positive when moving towards the east)
V-component of wind	m/s	Northward horizontal component of the wind (positive when moving towards the north)
Vertical velocity	Pa/s	Speed of air motion in upward or downward direction (positive values indicate downward motion)
Temperature	K	Temperature in the atmosphere

Reanalysis data were extracted from the ERA5 database. The reanalysis combines previous weather forecasts with newly available observations to produce an optimal estimate of the atmosphere's state.

<sup>1</sup><https://www.weather.gov/media/epz/wxcalc/pressureAltitude.pdf>

ERA5 also provides uncertainty estimations at a lower spatial- and temporal resolution. This uncertainty estimate is sampled by a 10-member ensemble. The 10-member ensemble will not be included in the predictive analysis as this would significantly increase the required processing capacity. However, the data could be included for the analysis of individual flights in order to explore the effect on the predictive analysis.

The data extracted from the ERA5 database is formatted in grids of latitudes and longitudes for each selected pressure level and timestamp. Hence, four dimensions should be taken into account to generate interpolation models to link the meteorological data to the ADS-B data. This process is discussed in the subsequent section.

## 6.2. Coupling data sources

As discussed in the previous sections, various sources of data are used to eventually construct a final dataset that will be used for predictive modelling purposes. In order to merge different sources of data, several steps have to be performed. Most importantly, common features between datasets should be explored to identify possibilities to link the datasets together.

### 6.2.1. Merging the flight plan data with the ADS-B data

In order to merge the flight plan data to the ADS-B data, common features in both datasets should be explored to link both datasets. For this purpose, the ICAO code that uniquely identifies a particular aircraft was used in combination with a rounded timestamp of the data point from the ADS-B dataset and the actual flight points from Eurocontrol. In both datasets, the timestamp of the particular observation was rounded to the nearest 10-minute mark. When these features are used, the unique code that Eurocontrol assigns to each flight (CTRL ID) could be added to the ADS-B data. The inclusion of this feature allows for the addition of valuable flight-specific information from the flight plans to the ADS-B dataset.

In order to implement the aircraft intent in the final dataset, the next three waypoints from the filed flight plans will be assigned to each observation from the ADS-B dataset. These next three waypoints indicate the expected trajectory of the aircraft, as it provides positional information with respect to the planned trajectory.

#### Selecting the next three waypoints

The selection of the following three waypoints for a given observation in the ADS-B data was performed by initially identifying a feature of the dataset that expresses the progress of the flight. For this purpose, the great circle distance between the position of the aircraft and the position of the departure airport was used. The larger this distance, the further the flight has progressed in its trajectory. This distance was computed for both the ADS-B data as well as the flight plan data, such that each observation and each waypoint includes the corresponding distance from the departure airport. This distance was computed using the Haversine equation, which calculates the great-circle distance between two points on a sphere. By comparing the distance from the departure airport of the ADS-B observation, the corresponding following waypoints could be selected from the flight plan. An example is shown below, where Table 6.4 provides a sample observation from the ADS-B dataset in which the position of the aircraft is displayed together with the distance from the departure airport at a given timestamp.

Table 6.4: Sample observation from ADS-B dataset

Timestamp	Latitude	Longitude	Altitude	Distance
2018-06-29 00:58:38	53.6445	10.6517	35000	4863.67

The observation from the ADS-B dataset in Table 6.4 could be supplemented with the data from the filed flight plans by considering the distance from the departure airport and select the appropriate waypoints from the flight plan. A sample flight plan that concerns the particular flight from the ADS-B data described above is shown in Table 6.5.

Table 6.5: Sample of a filed flight plan

Sequence number	Time Over	Latitude	Longitude	Flight Level	Distance
127	2018-06-29 00:39:16	54.3056	11.0053	350	4798.22
128	2018-06-29 00:45:39	53.6095	10.0664	320	4851.57
129	2018-06-29 00:52:08	52.8817	9.1275	320	4906.75
130	2018-06-29 00:58:53	52.1214	8.18861	320	4963.84
131	2018-06-29 01:05:49	51.3261	7.24945	320	5022.99

When comparing the distance from the ADS-B data to the distance column from the planned waypoints in the filed flight plan, it could be observed that the next planned waypoint should be assigned to the waypoint with sequence number 129. Hence, the observation from Table 6.4 would be supplemented with the information related to the next three waypoints, being waypoints 129, 130, and 131. This means that, according to the planned waypoints, the aircraft is expected to decrease to a lower flight level while travelling in a southwesterly direction (indicated by the decreasing longitude and latitude).

The distance from departure airport was selected as it would most optimally assign the next three expected waypoints in case the actual flight would be diverted or delayed. Using the cumulative distance flown, rather than the distance from departure airport, would potentially allocate incorrect future waypoints in case of divergences as more/less distance might be covered by the flight than anticipated by the flight plan. Besides, if the timestamp would be used to select the next waypoint in the example above, the next waypoint would have been waypoint 130. This means that certain waypoints, that have not been traversed yet, would be skipped.

Each observation from the ADS-B dataset is supplemented with information related to the following three waypoints. Each waypoint includes the three spatial components (altitude, longitude, latitude) and a time component. The time component ( $t_{wp}$ ) was set to the difference between the time since planned take-off and the time since actual take-off as shown by Equation 6.2.

$$t_{wp} = T_{planned} - T_{actual} \quad (6.2)$$

where  $T_{planned}$  represents the total flight time since take-off obtained from the filed flight plan, whereas  $T_{actual}$  defines the actual flight time since take-off extracted by subtracting the actual take-off time from the timestamp component of the ADS-B dataset. This parameter would indicate how the actual trajectory, reconstructed from the ADS-B data, temporally aligns with the waypoints from the flight plan. A negative time component ( $t_{wp}$ ) indicates that the actual flight took more time to reach the particular waypoint than anticipated by the FP.

### 6.2.2. Merging the meteorological data with the ADS-B data

The parameters from the ERA5 dataset are obtained in horizontal grids, where the region of interest is divided into 161 latitudes and 161 longitudes. It is assumed that the parameters of interest behave linearly in both the spatial and temporal domain. Therefore, four-dimensional linear interpolation models were generated to be able to fit the ERA5 data to the observations from the ADS-B dataset.

## 6.3. Preparation of the dataset

Once all data sources are merged into one dataset, further preparation steps are required in order to finalise this set of data. These steps include the filtering of data, treatment of outliers, treating missing values, adding other relevant features to the dataset, and converting categorical data to numeric data that could be processed by the predictive models.

### 6.3.1. Filtering the dataset

The constructed dataset was filtered in order to obtain a reliable, concise dataset. First of all, flight trajectories with less than 30 data points were disregarded from the dataset. Flights should have a sufficient number of data points to effectively train the predictive models and apply the clustering

algorithms to detect spatial and temporal similarities between different trajectories. Furthermore, incomplete observations where various features were missing were removed from the dataset as they could not provide any additional value to the analysis.

### 6.3.2. Flight phase computation

The predictive analysis will focus on individual segments of the flights. Therefore, the flight data should be segmented into different flight phases, being level, climb, cruise, or descent. To distinguish these different flight phases from the partial trajectories of the ADS-B data, a Python library developed by Sun et al.[34] was applied. This library includes several functions, where one of them applies fuzzy logic methods to segment (partial) trajectories into different flight phases by using three input parameters: rate of climb, altitude, and ground speed. Fuzzy logic is applied to compute the probability of each phase, and the most probable phase is assigned to the time-series data. Before applying this function, the relevant parameters had to be interpolated in order to compute the missing values in the original ADS-B dataset. For this purpose, linear interpolation over time was used.

### 6.3.3. Adding features to the dataset

As mentioned in the previous section, certain features had to be added to the datasets in order to be able to couple the various datasets to each other. The time since take-off was added to couple the FP data to the ADS-B data. Besides, in order to compute the distance from the departure airport, the geographical position of the departure airport was added. Next to the addition of these variables, the categorical variables from the dataset were converted to numerical features which is required for the application of the predictive models. One-hot encoding was applied to convert the aircraft type and the aircraft operator to numeric, binary variables. This machine learning process requires the definition of certain features that contribute to the classification of the categorical variable. Subsequently, one-hot encoding assigns either a 1 or 0 to the selected feature to indicate whether it applies to the categorical variable of interest. The aircraft types were categorised based on their ICAO Wake Turbulence Category (WTC), which is dependent on the maximum certified take-off mass as described by Table 6.6 below. The mass of the aircraft plays a significant role in the evolution of an aircraft trajectory, as it directly impacts the performance parameters of the aircraft like the climb- and cruise speed.

Table 6.6: Categorising aircraft types by their Wake Turbulence Category (WTC)

Maximum certified take-off mass	WTC
$\geq 136.000$ kg	Heavy (H)
$>7.000$ kg, $<136.000$ kg	Medium (M)
$\leq 7.000$ kg	Light (L)

The aircraft operator, being the airline that operates the flight, is classified based on their type of operation which is represented by the market segment that the airline operates in. A total of five different market segments are defined by the flights file from the Eurocontrol flight plan data:

- All-cargo
- Business aviation
- Unscheduled (e.g. charter)
- Low-cost
- Traditional scheduled

An individual trajectory from one airport to the other might be flown with different speed- and altitude profiles preferred among different airlines. These variations in speed- and altitude profiles might result from varying cost indices set by the operator of the aircraft. This cost index represent the ratio of fuel costs to all other costs associated to the operation of the flight. A lower cost index results in lower speeds, and generally increased cruise altitudes. These cost indices, however, are not publicly available and might still vary between flights operated by the same airline. In order to differentiate among

different airlines, the segmentation of the market was selected to classify the type of operations of the airlines.

## 6.4. Overview of final dataset

Figure 6.4 below provides a schematic overview of the process concerning the construction of the final dataset from four different sources of data. ADS-B data was used to reconstruct the trajectories and includes the evolution of relevant state variables of the aircraft over the progression of the flight. Secondly, the aircraft intent is expressed in the dataset by including the next three waypoints from the filed flight plans prior to the flight. Each waypoint is represented by a three-dimensional position in a Cartesian reference frame together with a temporal component representing the difference in time between the actual flight and the flight plan when crossing a particular waypoint. Further flight-specific information is extracted from the flights database obtained from Eurocontrol. Ultimately, the meteorological parameters, obtained from the ERA5 database, were added to the dataset by using a linear interpolation model.

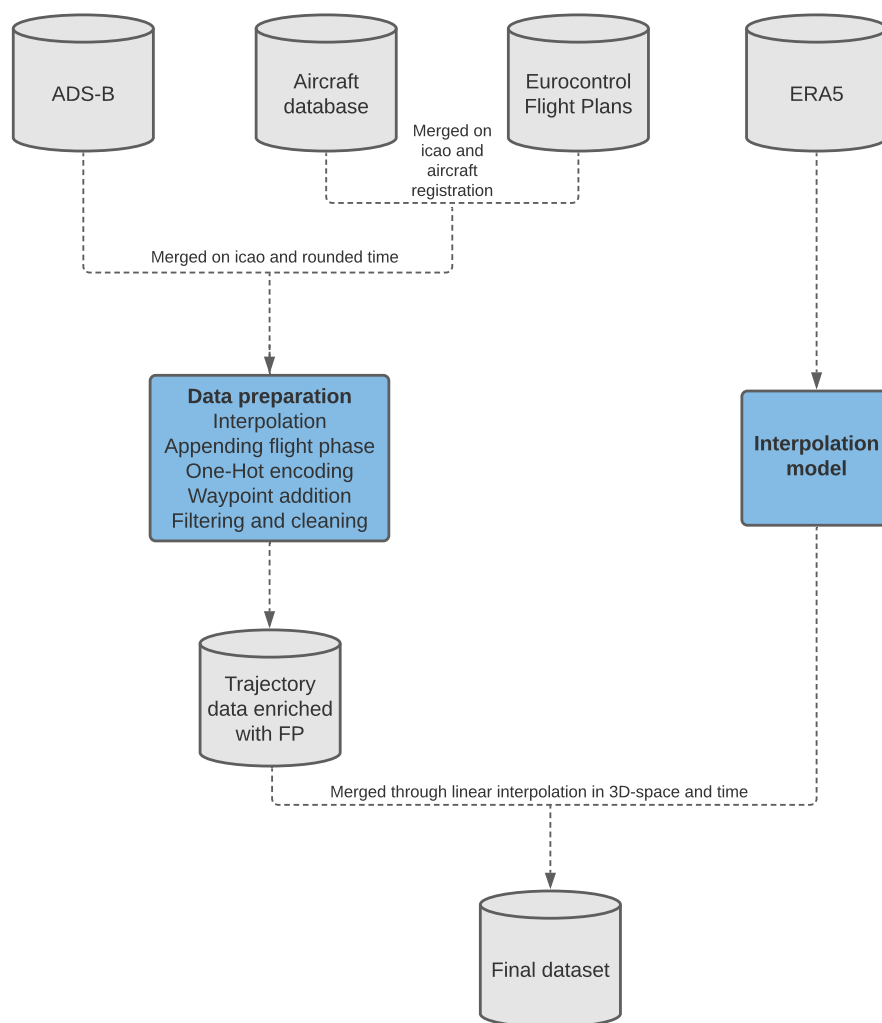


Figure 6.3: Process flow of the construction of the final dataset

The final dataset includes different features that are used to train the predictive models. Part of the data is used to enrich the trajectory data, such that each point of the trajectory contains enhanced information. The dataset also includes more general information that is applicable to the trajectory in its entirety, such as the type of aircraft, airline, market segment, and departure- and arrival airport. An

overview of the features included in the final dataset is shown in Table 6.7.

Table 6.7: Features of the final dataset

<b>Feature</b>	<b>Unit</b>
ECTRL ID	Eurocontrol
Timestamp	ADS-B
Time since take-off	Eurocontrol
Latitude	ADS-B
Longitude	ADS-B
Altitude	ADS-B
Ground speed	ADS-B
Track	ADS-B
Rate of Climb	ADS-B
Wind velocity (u)	ERA5
Wind velocity (v)	ERA5
Vertical wind velocity	ERA5
Temperature	ERA5
Waypoint Latitude	Eurocontrol
Waypoint Longitude	Eurocontrol
Waypoint Altitude	Eurocontrol
Waypoint Time	Eurocontrol
Flight phase	Generated
Aircraft type	Aircraft database
Airline	Eurocontrol
Market segment	Eurocontrol
Wake Turbulence Category	ICAO
Departure airport	Eurocontrol
Arrival airport	Eurocontrol

The final dataset comprises a total of 154827 (partial) trajectories, which are evenly distributed over the weeks of the month of June 2018. A total of 7667 different flight legs was observed. The figures below depict the most frequent occurrences of departure and arrival airports. As the ADS-B dataset includes flights centred around the Dutch airspace, the most frequently occurring airport is Schiphol Amsterdam, which takes the most significant part of the dataset. However, the flight legs between Frankfurt and London Heathrow were observed most frequently.

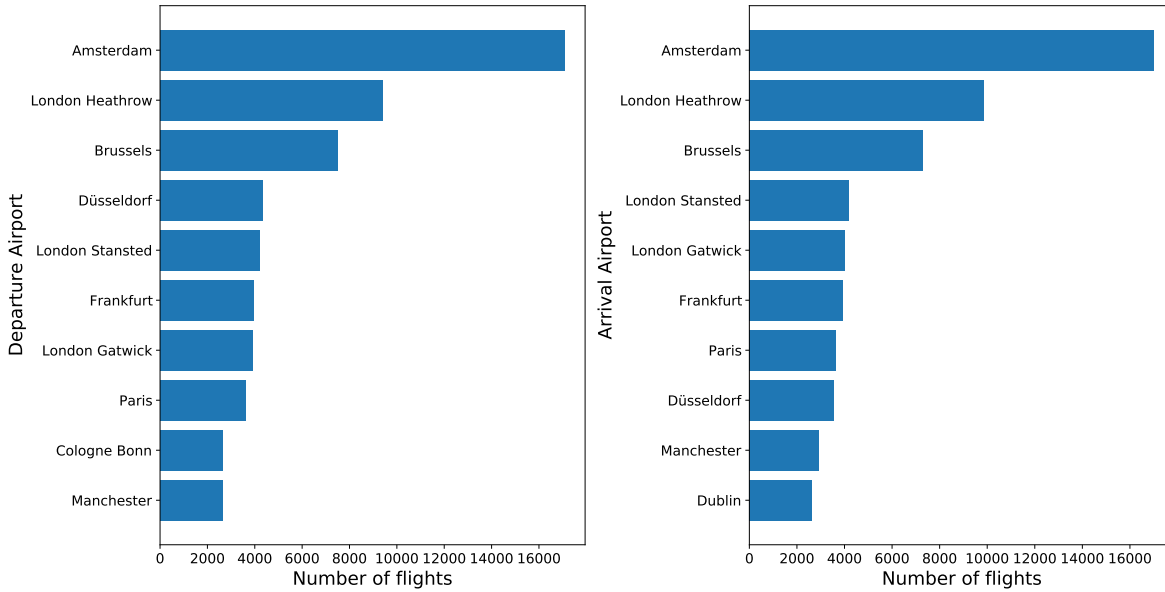


Figure 6.4: Ten most frequent occurrences of departure- (left) and arrival (right) airports

The ADS-B dataset was aggregated with the aircraft type and airline obtained from a separate dataset. Figure 6.5 visualises the ten most common airlines and aircraft types found in the final dataset. Many of the flights are operated by the low-cost airlines Ryanair and Easyjet, while full-service carriers like British Airways and KLM also have a significant share in the dataset. As could be observed, the vast majority of flights is operated by narrow-body aircraft types like the B737-800, A320, and the A319.

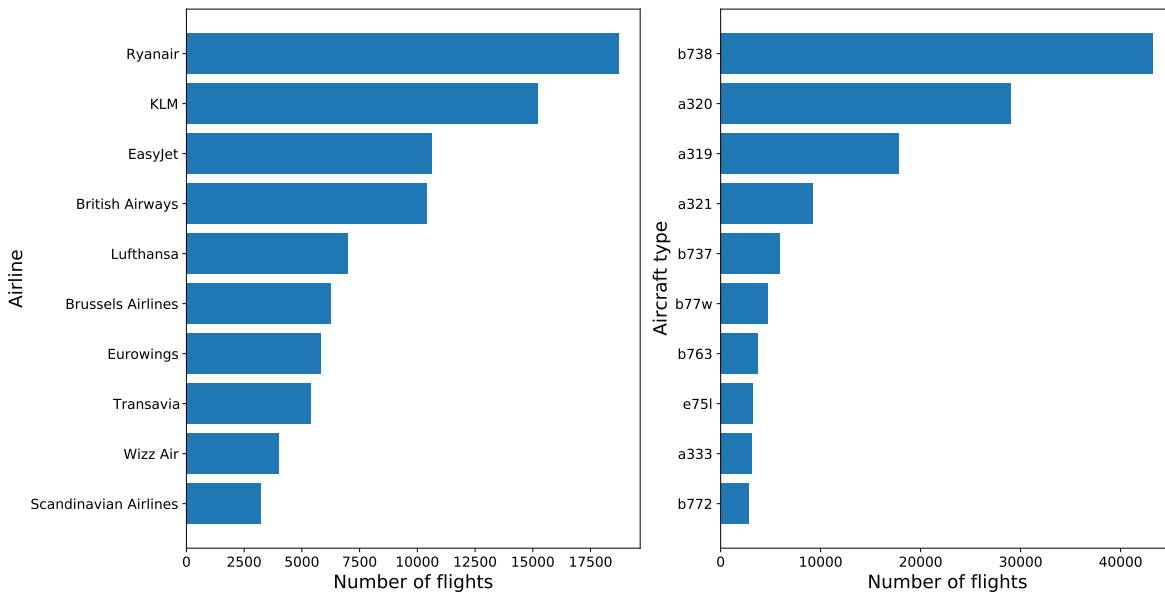


Figure 6.5: Ten most frequent occurrences of airlines (left) and aircraft types (right)

As mentioned, the trajectories have been segmented based on the flight phase. As could be observed from Figure 6.6, the majority of the observations in the final dataset concerns either the climbing or cruising phase of the flight.

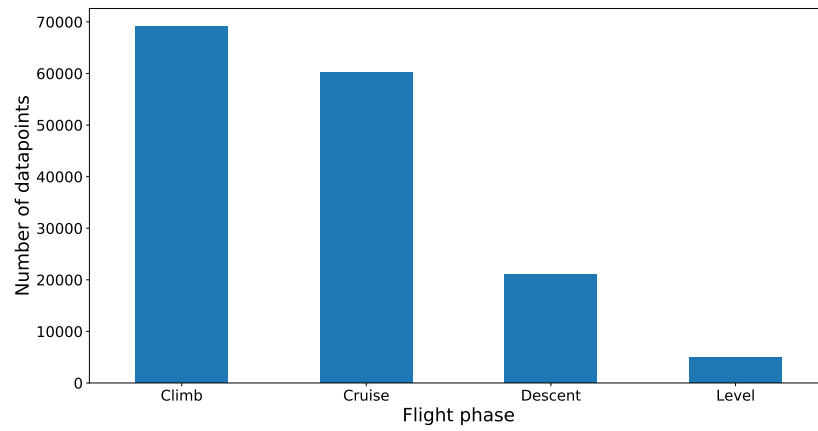


Figure 6.6: Flight phase segmentation of trajectories

## 6.5. Clustering trajectories

The final dataset includes a variety of features that describe the trajectory of the aircraft. The final step before exploiting the dataset to develop the predictive models is to cluster the trajectories. The clustering of trajectories contributes to the identification of subsets of trajectories that have similar spatial patterns. The predictive models could be developed more efficiently based on these subsets of data, since the historical patterns found in the trajectories might vary among different types of trajectories. Hence, the predictive models will be trained based on each cluster of trajectories that show similar patterns. The clustering of trajectories will be performed by using the DBSCAN algorithm, which is able to identify clusters with varying densities and different shapes. Furthermore, DBSCAN is able to identify outliers, which do not belong to a particular cluster. In this section, the DBSCAN algorithm will be trained using one week of data. This subset of data is expected to be sufficient as it includes a sufficient number of trajectories. Furthermore, the spatial characteristics of trajectories is not expected to vary over different weeks of the month of available data. The results of the DBSCAN application will be evaluated by visually inspecting the clustered trajectories.

In order to apply the DBSCAN algorithm, each trajectory should be expressed by a number of features. The trajectories will be grouped based on their spatial similarities, thus the features included in the clustering algorithm define the three-dimensional position of the aircraft (latitude, longitude, and altitude). The latitude and longitude are converted to a Cartesian reference frame in order to have all variables on a linear scale. This conversion resulted in  $x$  and  $y$  coordinates expressed in metres relative to a random origin. Furthermore, each trajectory should be of equal length, which requires all trajectories to be resampled into the same number of data points. Each trajectory has been divided into 30 intervals, where the mean of the three-dimensional position was taken as the particular datapoint. The resampled trajectories are formed from the Eurocontrol dataset that includes the actual flight points of the flown trajectory. Unlike the created final dataset, that includes trajectories reconstructed from ADS-B data, the actual flight points cover the entire trajectory from departure airport to arrival airport. Eventually, each trajectory is represented by an array of 90 features, which represents the position of the aircraft over 30 subsequent points in time. These data points are equally spaced over the time span of the data coverage. An example of trajectory data input is shown below.

$$T_i = [x_i^{(1)} \dots x_i^{(30)}, y_i^{(1)} \dots y_i^{(30)}, alt_i^{(1)} \dots alt_i^{(30)}]$$

In order to transfer all variables to the same range, the features are normalised using the Min-Max normalisation formula expressed by Equation 6.3 below. This normalisation converts the feature  $x$  to a normalised variable  $x'$  in the range 0-1.

$$x' = \frac{x - \min(x)}{\max(x) - \min(x)} \quad (6.3)$$

In order to distinguish trajectories from each other, a distance metric should be introduced such that trajectories with similar spatial characteristics are clustered into the same subset. A broad variety of distance metrics exist and for this purpose the Chebyshev distance will be used. The Chebyshev distance is equal to the maximum difference between elements of two arrays. Element-wise comparison between two arrays is used to compute the absolute difference between the arrays, and the maximum of these differences is then defined as the Chebyshev distance. Mathematically, the Chebyshev distance ( $D_{\text{Chebyshev}}$ ) between two trajectories  $T_1$  and  $T_2$  is expressed by Equation 6.4.

$$D_{\text{Chebyshev}}(T_1, T_2) = \max_i (|T_1^{(i)} - T_2^{(i)}|) \quad (6.4)$$

### 6.5.1. Application of DBSCAN to an initial subset of the data

In order to evaluate the performance of the DBSCAN application, an initial subset of the data is used to train and evaluate the algorithm. This initial subset comprises flights either departing or arriving at Amsterdam (EHAM), London Heathrow (EGLL), or Paris (LFPG). This dataset only comprises 387 different flights and could be used as a sample set to effectively evaluate the application of the algorithm. Apart from the selection of an appropriate distance metric, DBSCAN requires two additional parameters to be selected discussed in Section 2.2.2: MinPts and  $\epsilon$  ( $\epsilon$ ). MinPts specifies the minimum

number of trajectories that could form a cluster. Setting this parameter too small will result in many clusters, that could potentially include outliers that should not be assigned to a cluster. On the contrary, increasing this parameter would decrease the number of clusters formed by the algorithm. The selection of the MinPts parameter is an iterative process that is adjusted based on visual inspection of the clustering results as well as the evaluation of clustering performance metrics. Initially, MinPts is set to 15 trajectories, indicating that each identified cluster includes at least 15 flights.

The optimum value of eps is found by computing the average distance to the nearest  $k$  points for each point. The computed distances are sorted in ascending order and the results are plotted over all data points [81]. In this procedure,  $k$  is set to the MinPts parameter as defined above (MinPts = 15). Figure 6.7 depicts the average computed distance to the 15 nearest trajectories for each trajectory. The optimal value for epsilon is found in the region of greatest curvature, where the most profound difference is found when increasing epsilon. As could be observed from Figure 6.7, this effect is observed around an epsilon of 0.2. The DBSCAN algorithm will be applied for various values of epsilon in the range between 0.1 and 0.4.

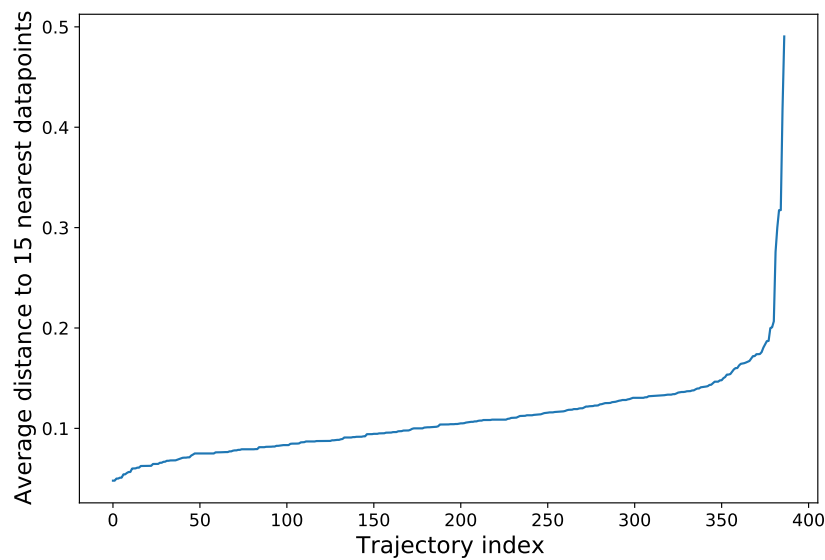


Figure 6.7: Average distance of Nearest Neighbours to determine optimal value for epsilon

Epsilon values will be varied ranging from 0.1 to 0.4 in steps of 0.02. Besides, the MinPts variable will be varied from 4 to 50 in steps of 2. The clustering performance will be evaluated by computing the Silhouette score. This score is commonly used to evaluate the performance of a clustering algorithm when the ground truth remains unknown. The Silhouette score is used as a measure to define how similar a clustered object is to its assigned cluster compared to other clusters. The Silhouette score of trajectory  $i$   $S_i$  is computed using Equation 6.5.

$$S_i = \frac{b_i - a_i}{\text{Max}(a_i, b_i)} \quad (6.5)$$

where  $a_i$  expresses the mean intra-cluster distance, and  $b_i$  the mean nearest-cluster distance. Hence,  $a_i$  is a measure of similarity of the clustered object to its assigned cluster, while  $b_i$  is a measure of similarity to the nearest other cluster that the object is not a part of. The Silhouette score ranges from -1 to 1, where a higher score indicates better clustering performance.

The Silhouette score was computed for a variety of different combinations of the two DBSCAN parameters. Besides, the percentage of trajectories assigned as noise was computed, and the total number of clusters was computed. The results, for epsilon values of 0.16, 0.20, and 0.24 respectively, are shown in

Figure 6.8. An epsilon of 0.16 shows the worst performance with a relatively low Silhouette score compared to the other results. Besides, many of the trajectories are assigned as noise as could be observed from the percentage of outliers that increases steadily to approximately 80% as MinPts increases.

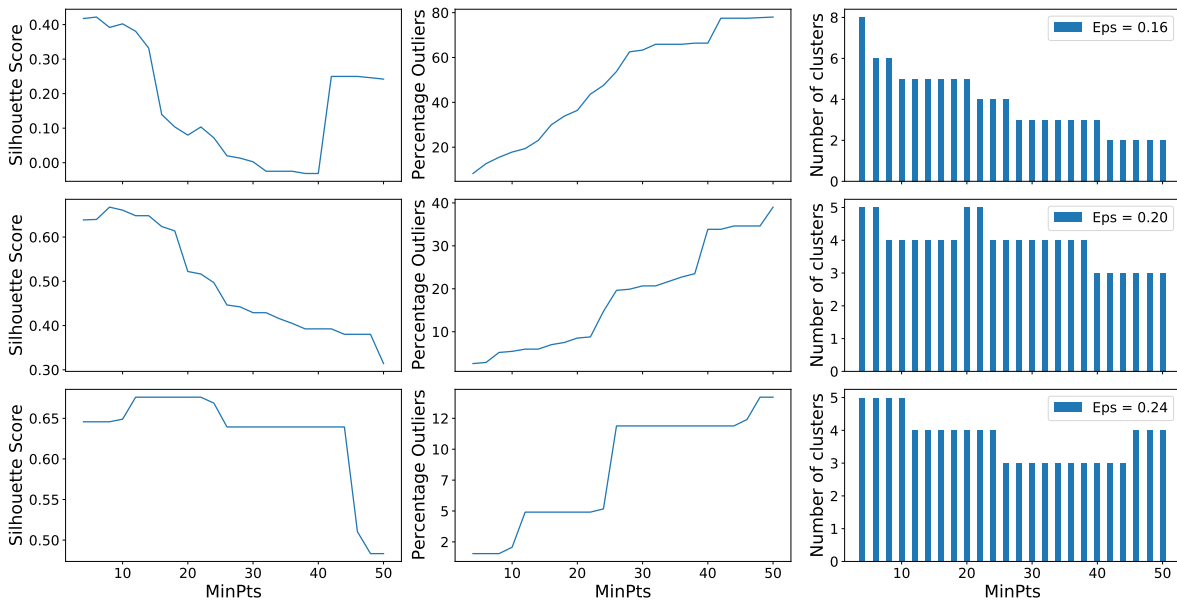


Figure 6.8: Evaluation of DBSCAN clustering performance for various parameter configurations

Based on the results described above, and a visual inspection of the clustered trajectories, the epsilon value was set to 0.24, while MinPts was set to 10. This indicates that each cluster includes at least 10 trajectories. Figure 6.9 shows the resulting clusters obtained from the DBSCAN application with the specified parameters. A total of five clusters were identified. This includes a cluster of trajectories that are assigned as noise, which are labelled to -1. It could be observed that the clusters clearly link the three different airports from the dataset. Besides, the clustering algorithm is able to distinguish trajectories that follow the same track in opposite directions.

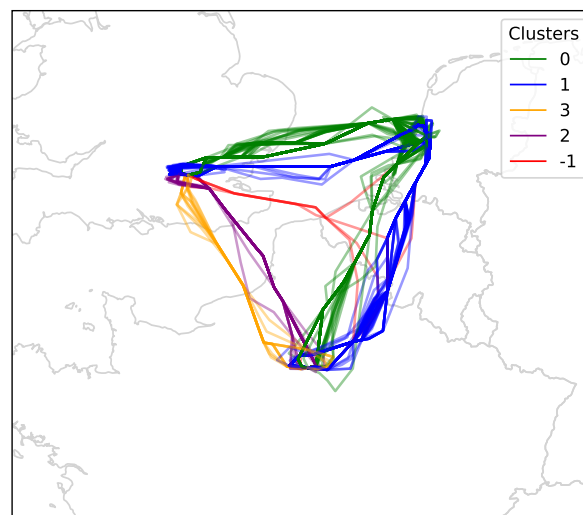


Figure 6.9: Visualisation of clustered trajectories obtained from DBSCAN application to flights operating from and to Amsterdam, London Heathrow, and Paris

### 6.5.2. Application of DBSCAN to final dataset

The previous section applied the DBSCAN clustering algorithm to a small subset of the data in order to evaluate the performance of the algorithm applied to the available data. The same procedure of parameter configuration is applied to the final dataset in order to cluster all trajectories. The model is trained on trajectories operated during the first week of June 2018, which includes 34201 flights. Once again, the optimum value for epsilon was found to be approximately 0.2. Figure 6.11 below shows a snippet of the clustering performance for various parameter configurations, where epsilon is set to 0.15, 0.25, and 0.35 respectively. Since the dataset comprises more flights, the MinPts should be set to a larger value in order to obtain relevant clusters with sufficient flights in it. When both epsilon and MinPts are assigned to relatively low values, the number of identified clusters increases up to around 25 clusters. The number of identified clusters decreases as the MinPts parameter is increased.

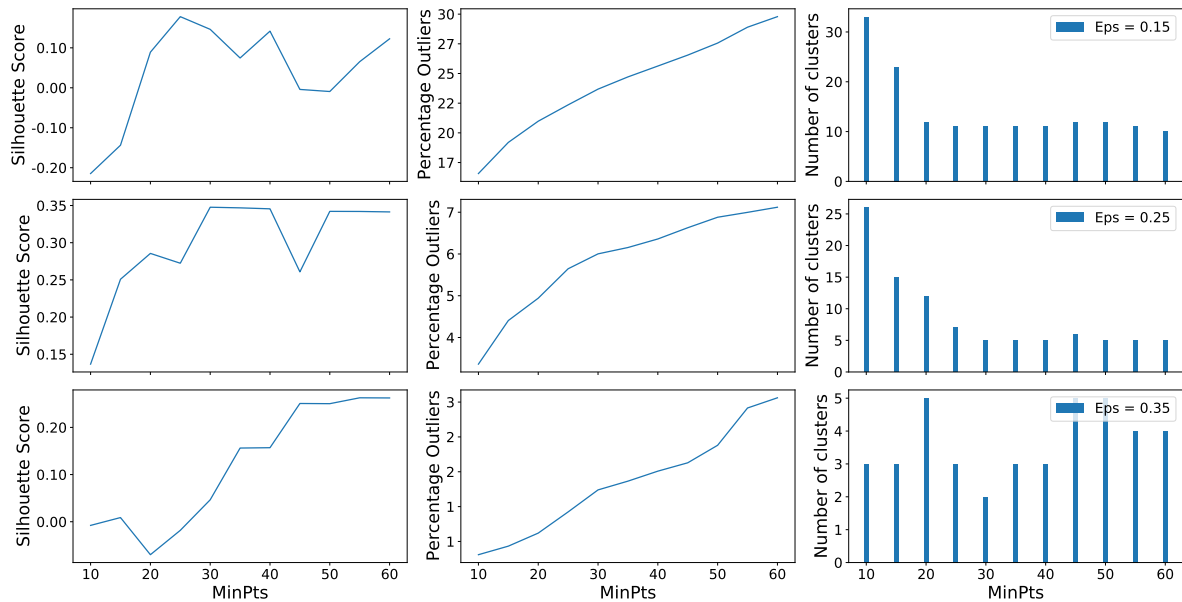


Figure 6.10: Evaluation of DBSCAN clustering performance for various parameter configurations on one week of flight data

Eventually, epsilon was set to 0.30 and MinPts was set to 40. The performance of the clustering algorithm was also tested for larger values of MinPts, but this would not improve the performance of the algorithm nor change the number of identified clusters. The selected configuration of parameters resulted in five different clusters, including the cluster of noisy trajectories. A visualisation of the clustered trajectories is shown in Figure 6.11 below. The clustering algorithm clearly distinguishes trajectories operating in four different directions. Trajectories clustered as noise are labelled to -1.

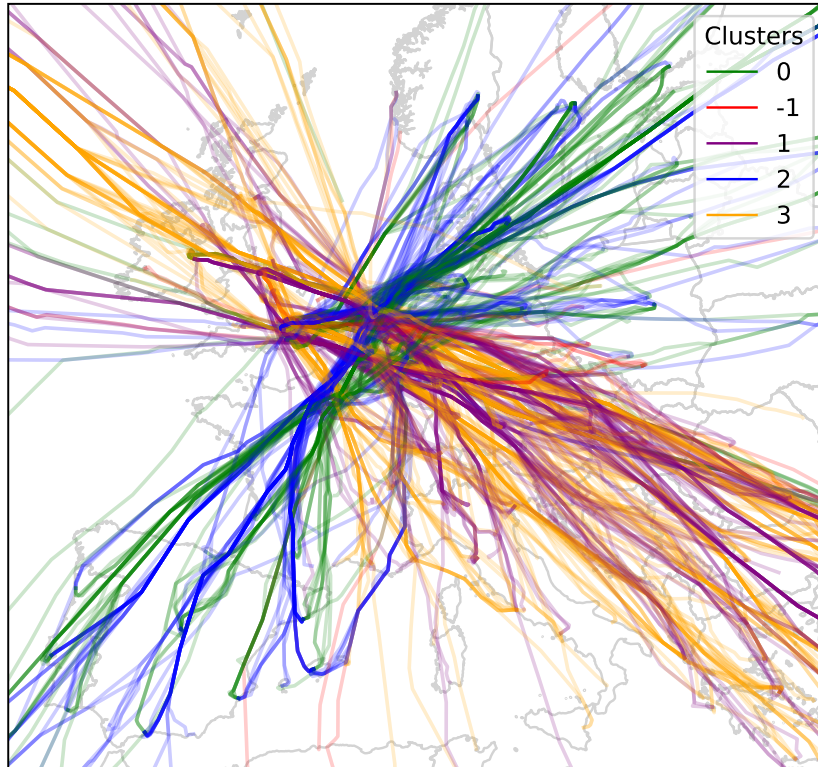


Figure 6.11: Visualisation of clustered trajectories obtained from DBSCAN application



# 7

## Model development and analysis

This chapter outlines the upcoming phases of the project. The second phase of the project concerns the development of the predictive models by using the final dataset constructed in the previous phase (Section 7.1). Different experiments will be conducted, where each experiment uses a different subset of the constructed dataset (Section 7.2). The trained models will be applied and the predictive capability will be evaluated in terms of the predictive accuracy and uncertainty. The analysis aims to identify the effects of including different sets of data on the predictive capability of the models. The results of both models will be compared (Section 7.3).

---

### 7.1. Development of predictive models

The final dataset is constructed and different subsets of trajectories are classified according to the applied clustering algorithm. The predictive models will be trained using these subsets of trajectories in order to efficiently construct a model for each cluster of trajectories. If the initial clustering results seem to be inefficient to train the models, subsequent clustering steps could be applied to further distinguish different trajectories. Subsequent clustering could be based upon the filtering of flights on their departure- or arrival airport. As mentioned, two different probabilistic prediction techniques will be applied: the model-based Sequential Monte Carlo (SMC) method and the data-driven Gaussian Process Regression (GPR). The purpose of the application of these models is to derive a probabilistic distribution of predicted trajectories. This probabilistic approach allows for the quantification of the uncertainty of the predicted trajectories.

Both models will be trained by using the constructed final dataset as described in Section 6.4. However, while the GPR model will include all features of the dataset, the SMC model will only incorporate a subset of ADS-B data that is used as input to the particle filter to update the weights of the particles. To evaluate the predictive models, part of the data should be used as training data while the other part should be used to test the trained model onto data that has not been used for the development of the models. A common way of testing predictive models is by splitting the entire dataset into a training set and a test set. The main disadvantage of this technique is that the trained model might be over-fitted to the training data. When the training dataset does not accurately represent the entire dataset, the model might perform poorly on other data from the testing dataset. To overcome this problem, cross-validation techniques could be applied. This method subdivides the dataset into  $k$  different folds. Then, the model is trained using  $k-1$  subsets, and the remaining set is used to test the model. This procedure is performed for each of the subsets. In this case, all data is used both for training and testing the predictive models.

Since it is expected that the uncertainty in the predictions would vary among different phases, the models will be trained on datasets that have been filtered on the corresponding flight phase. Overall, the cruise phase is expected to be the most predictable phase of the flight, as the aircraft commonly travels with a fairly constant speed without any variation in altitude. The descent and climb phases are less straightforward and the lack of detailed aircraft intent in terms of the climb- or descent profiles

are likely to increase the predictive errors during these phases. Initially, the models will be trained on trajectories of aircraft in the cruise phase. Subsequently, the models will be trained on the other phases as well.

## 7.2. Model experiments

As mentioned, the SMC model will use part of the ADS-B data as observations that are used as input to the particle filter. This model will act as the baseline model and the outcomes of the GPR model will be compared to the SMC model. A variety of experiments will be conducted in which different subsets of data are used to train and fit a GPR model to a cluster of trajectories. Table 7.1 provides an overview of four different experiments that use different subsets of data to train these models.

Table 7.1: Overview of experiments with varying sets of training data to develop GPR models

Experiment	Training data
1	ADS-B only
2	ADS-B and Flight Plans
3	ADS-B and ERA5
4	ADS-B and Flight Plans and ERA5

Depending on the available time and the progress of the research project, the experiments could be further specified on the parameter level. For example, the experiment with ADS-B data could be further specified by only selecting certain parameters from the ADS-B database in order to identify the effects of including particular parameters.

## 7.3. Analysis of results

In order to answer the main research question of this project, the predictive capability of both models should be assessed. The predictive capability is defined by two different performance metrics: the predictive accuracy and the predictive uncertainty. The accuracy is defined by measuring the spatial and temporal errors of the predictions. In order to measure the accuracy, the mean of the predictive distribution is considered as the most likely trajectory and this prediction is compared to the known ground truth obtained from the reconstructed trajectories from the ADS-B dataset. The focus of this project lies on the assessment of the predictive uncertainty. This uncertainty is specified by computing the standard deviation of the predictive distribution. Subsequently, this standard deviation could be used to derive a 95%-confidence interval of the predictions. The larger the standard deviation, the larger the spread of the predictions, which is an indication of increased predictive uncertainty.

Both the accuracy and the uncertainty are measured for varying look-ahead times in order to identify the effects of increasing the prediction horizon on the predictive capability. Furthermore, a sensitivity analysis will be performed to identify the effects on the predictive capability of including different subsets of data as input parameters to the models.





# Bibliography

- [1] J. Bronsvort, G. McDonald, J. Lopez-Leones, and H. G. Visser, "Improved trajectory prediction for air traffic management by simulation of guidance logic and inferred aircraft intent using existing data-link technology," AIAA Guidance, Navigation, and Control Conference 2012, no. August, pp. 1–3, 2012.
- [2] S. Mondoloni, S. Swierstra, and M. Paglione, "Assessing trajectory prediction performance - Metrics definition," AIAA/IEEE Digital Avionics Systems Conference - Proceedings, vol. 1, no. January, 2005.
- [3] A. O'Hagan, "Bayesian statistics: principles and benefits," Bayesian statistics and quality modelling in agro-food production chain (Wageningen UR Frontis Series), pp. 31–45, 2004.
- [4] International Civil Aviation Organization, Doc 4444 - Air Traffic Management - Procedures for Air Navigation Services. 16 ed., 2016.
- [5] European Organisation for the Safety of Air Navigation (EUROCONTROL), "Performance Review Report," tech. rep., Eurocontrol, Brussels, 2020.
- [6] T. Radišić, The Effect of Trajectory-Based Operations on Air Traffic Complexity. PhD thesis, University of Zagreb, 2014.
- [7] J. López-Leonés, M. A. Vilaplana, E. Gallo, F. A. Navarro, and C. Querejeta, "The aircraft intent description language: A key enabler for air-ground Synchronization in trajectory-based operations," AIAA/IEEE Digital Avionics Systems Conference - Proceedings, pp. 1–12, 2007.
- [8] S. Swierstra and S. M. Green, "Common Trajectory Prediction Capability for Decision Support Tools," pp. 1–10, 2003.
- [9] Engage KTN, "Thematic Challenge 2: Data-driven trajectory prediction," tech. rep., 2018.
- [10] DART, "Data-Driven Aircraft Trajectory Prediction Exploratory Research," tech. rep., 2017.
- [11] M. A. Konyak, "Improving Ground-Based Trajectory Prediction through Communication of Aircraft Intent," AIAA Guidance, Navigation and Control Conference and Exhibit, no. August, pp. 1–25, 2009.
- [12] M. A. Konyak, D. Warburton, J. Lopez-Leones, and P. C. Parks, "A demonstration of an aircraft intent interchange specification for facilitating trajectory-based operations in the national airspace system," AIAA Guidance, Navigation and Control Conference and Exhibit, no. August, pp. 1–17, 2008.
- [13] J. Bronsvort, G. McDonald, M. Paglione, C. Garcia-Avello, I. Bayraktutar, and C. M. Young, "Impact of missing longitudinal aircraft intent on descent trajectory prediction," AIAA/IEEE Digital Avionics Systems Conference - Proceedings, pp. 1–14, 2011.
- [14] J. Zhang, J. Liu, R. Hu, and H. Zhu, "Online four dimensional trajectory prediction method based on aircraft intent updating," Aerospace Science and Technology, vol. 77, pp. 774–787, 2018.
- [15] R. Alligier, "Predictive distribution of mass and speed profile to improve aircraft climb prediction," Journal of Air Transportation, vol. 28, no. 3, p. 114, 2020.
- [16] E. Gallo, J. López-Leonés, M. A. Vilaplana, F. A. Navarro, and A. Nuic, "Trajectory computation infrastructure based on BADA aircraft performance model," AIAA/IEEE Digital Avionics Systems Conference - Proceedings, pp. 1–13, 2007.

- [17] A. Nuic, D. Poles, and V. Mouillet, "BADA: An advanced aircraft performance model for present and future ATM systems," *International Journal of Adaptive Control and Signal Processing*, vol. 24, no. 10, pp. 850–866, 2010.
- [18] E. Gallo, F. A. Navarro, A. Nuic, and M. Iagaru, "Advanced aircraft performance modeling for ATM: BADA 4.0 results," *AIAA/IEEE Digital Avionics Systems Conference - Proceedings*, pp. 1–12, 2006.
- [19] I. Lympieropoulos and J. Lygeros, "Adaptive aircraft trajectory prediction using particle filters," *AIAA Guidance, Navigation and Control Conference and Exhibit*, no. August, pp. 1–16, 2008.
- [20] A. M. de Leege, M. M. van Paassen, and M. Mulder, "A machine learning approach to trajectory prediction," *AIAA Guidance, Navigation, and Control (GNC) Conference*, pp. 1–14, 2013.
- [21] R. Alligier, D. Gianazza, and N. Durand, "Learning the aircraft mass and thrust to improve the ground-based trajectory prediction of climbing flights," *Transportation Research Part C: Emerging Technologies*, vol. 36, pp. 45–60, 2013.
- [22] W. Kun and P. Wei, "A 4-D trajectory prediction model based on radar data," *Proceedings of the 27th Chinese Control Conference, CCC*, pp. 591–594, 2008.
- [23] I. Lympieropoulos and J. Lygeros, "Improved multi-aircraft ground trajectory prediction for air traffic control," *Journal of Guidance, Control, and Dynamics*, vol. 33, no. 2, pp. 347–362, 2010.
- [24] J. Zhang, W. Liu, and Y. Zhu, "Study of ADS-B data evaluation," *Chinese Journal of Aeronautics*, vol. 24, no. 4, pp. 461–466, 2011.
- [25] O. Rodionova, D. Delahaye, M. Sbihi, and M. Mongeau, "Trajectory prediction in North Atlantic oceanic airspace by wind networking," *AIAA/IEEE Digital Avionics Systems Conference - Proceedings*, pp. 31–7, 2014.
- [26] S. Ayhan and H. Samet, "Aircraft trajectory prediction made easy with predictive analytics," *Proceedings of the ACM SIGKDD International Conference on Knowledge Discovery and Data Mining*, vol. 13-17-Aug, pp. 21–30, 2016.
- [27] I. Lympieropoulos, J. Lygeros, and A. Lecchini, "Model based aircraft trajectory prediction during takeoff," *Collection of Technical Papers - AIAA Guidance, Navigation, and Control Conference 2006*, vol. 2, no. August, pp. 843–854, 2006.
- [28] National Oceanic and Atmospheric Administration, "The Global Forecast System (GFS) - Global Spectral Model (GSM)," 2019.
- [29] R. A. Coppenbarger, "En route climb trajectory prediction enhancement using airline flight-planning information," *1999 Guidance, Navigation, and Control Conference and Exhibit*, pp. 1077–1087, 1999.
- [30] S. Ayhan and H. Samet, "Dclerge: Divide-cluster-merge framework for clustering aircraft trajectories," *ACM International Conference Proceeding Series*, no. November, pp. 7–14, 2015.
- [31] X. Olive and L. Basora, "A python toolbox for processing air traffic data: A use case with trajectory clustering," *EPiC Series in Computing*, vol. 67, pp. 73–84, 2019.
- [32] J. Bian, D. Tian, Y. Tang, and D. Tao, "A survey on trajectory clustering analysis," 2018.
- [33] M. Gariel, A. N. Srivastava, and E. Feron, "Trajectory clustering and an application to airspace monitoring," *IEEE Transactions on Intelligent Transportation Systems*, vol. 12, no. 4, pp. 1511–1524, 2011.
- [34] J. Sun, J. Ellerbroek, and J. Hoekstra, "Flight extraction and phase identification for large automatic dependent surveillance-broadcast datasets," *Journal of Aerospace Information Systems*, vol. 14, no. 10, pp. 566–571, 2017.

- [35] A. M. Churchill and M. Bloem, "Clustering aircraft trajectories on the airport surface," 13th USA/Europe Air Traffic Management Research and Development Seminar 2019, 2019.
- [36] Y. Song, P. Cheng, and C. Mu, "An improved trajectory prediction algorithm based on trajectory data mining for air traffic management," 2012 IEEE International Conference on Information and Automation, ICIA 2012, no. June, pp. 981–986, 2012.
- [37] L. Basora, J. Morio, and C. Mailhot, "A trajectory clustering framework to analyse air traffic flows," SESAR Innovation Days, no. November, 2017.
- [38] A. Bombelli, A. S. Torné, E. Trumbauer, and K. D. Mease, "Improved Clustering for Route-Based Eulerian Air Traffic Modeling," *Journal of Guidance, Control, and Dynamics*, vol. 42, no. 5, pp. 1064–1077, 2019.
- [39] J. G. Lee, J. Han, and K. Y. Whang, "Trajectory clustering: A partition-and-group framework," *Proceedings of the ACM SIGMOD International Conference on Management of Data*, pp. 593–604, 2007.
- [40] Z. Zhao, W. Zeng, Z. Quan, M. Chen, and Z. Yang, "Aircraft trajectory prediction using deep long short-term memory networks," *CICTP 2019: Transportation in China - Connecting the World - Proceedings of the 19th COTA International Conference of Transportation Professionals*, no. January, pp. 124–135, 2019.
- [41] M. G. Hamed, D. Gianazza, M. Serrurier, and N. Durand, "Statistical prediction of aircraft trajectory: regression methods vs point-mass model," 10th USA/Europe ATM R&D Seminar, vol. 2013, no. June, p. pp, 2013.
- [42] K. Yang, M. Bi, Y. Liu, and Y. Zhang, "LSTM-based deep learning model for civil aircraft position and attitude prediction approach," *Chinese Control Conference, CCC*, vol. 2019-July, pp. 8689–8694, 2019.
- [43] Y. Pang, N. Xu, and Y. Liu, "Aircraft trajectory prediction using lstm neural network with embedded convolutional layer," *Proceedings of the Annual Conference of the Prognostics and Health Management Society, PHM*, vol. 11, no. 1, 2019.
- [44] Z. Wang, M. Liang, and D. Delahaye, "Short-term 4D trajectory prediction using machine learning methods," *SESAR Innovation Days*, no. November, 2017.
- [45] R. Alligier, D. Gianazza, and N. Durand, "Machine Learning and Mass Estimation Methods for Ground-Based Aircraft Climb Prediction," *IEEE Transactions on Intelligent Transportation Systems*, vol. 16, no. 6, pp. 3138–3149, 2015.
- [46] C. Gong and D. McNally, "A methodology for automated trajectory prediction analysis," *Collection of Technical Papers - AIAA Guidance, Navigation, and Control Conference*, vol. 1, no. August, pp. 432–445, 2004.
- [47] J. M. C. Rodríguez, L. G. Déniz, J. G. Herrero, J. B. Portas, and J. R. C. Corredera, "A model to 4D descent trajectory guidance," *AIAA/IEEE Digital Avionics Systems Conference - Proceedings*, no. November, 2007.
- [48] P. Thompson, C. G. Piecuh, M. A. Merrifield, J. P. McCreary, and E. Firing, "An overview of uncertainty quantification techniques with application to oceanic and oil-spill simulations," *Journal of Geophysical Research: Oceans*, vol. 121, no. 9, pp. 6762–6778, 2016.
- [49] M. McKay, *Evaluating Prediction Uncertainty*. PhD thesis, Los Alamos National Laboratory, 1995.
- [50] W. Walker, P. Harremoës, J. Rotmans, J. Sluijs, M. Van Der Asselt, P. Van Janssen, and M. Kraye Von Krauss, "A conceptual basis for uncertainty management," *Integrated Assessment*, vol. 4, no. 1, pp. 5–17, 2003.

- [51] E. Casado, C. Goodchild, and M. Vilaplana, "Identification and Initial Characterization of Sources of Uncertainty Affecting the Performance of Future Trajectory Management Automation Systems," *Proceedings of the 2nd International Conference on Application and Theory of Automation in Command and Control Systems*, no. May, pp. 170–175, 2012.
- [52] K. T. Mueller, J. A. Sorensen, and G. J. Couluris, "Strategic aircraft trajectory prediction uncertainty and statistical sector traffic load modeling," *AIAA Guidance, Navigation, and Control Conference and Exhibit*, no. August, pp. 1–11, 2002.
- [53] E. Casado, M. L. Civita, M. Vilaplana, and E. W. McGookin, "Quantification of aircraft trajectory prediction uncertainty using polynomial chaos expansions," *AIAA/IEEE Digital Avionics Systems Conference - Proceedings*, vol. 2017-Septe, no. 699274, 2017.
- [54] A. Rodríguez-Sanz, F. Gómez Comendador, R. M. Arnaldo Valdés, J. A. Pérez-Castán, P. González García, and M. N. G. Najar Godoy, "4D-trajectory time windows: definition and uncertainty management," *Aircraft Engineering and Aerospace Technology*, vol. 91, no. 5, pp. 761–782, 2019.
- [55] J. Rudnyk, J. Ellerbroek, and J. M. Hoekstra, "Trajectory prediction sensitivity analysis using monte carlo simulations based on inputs' distributions," *Journal of Air Transportation*, vol. 27, no. 4, pp. 181–198, 2019.
- [56] S. Sankararaman and M. Daigle, "Uncertainty quantification in trajectory prediction for aircraft operations," *AIAA Guidance, Navigation, and Control Conference*, 2017, pp. 1–11, 2017.
- [57] D. P. Loucks, E. van Beek, J. R. Stedinger, J. P. Dijkman, and M. T. Villars, "9 Model Sensitivity and Uncertainty Analysis," in *Water Resources Systems Planning and Management: An Introduction to Methods, Models and Applications*, pp. 254–290, UNESCO, 2005.
- [58] J. Rudnyk, J. Ellerbroek, and J. M. Hoekstra, "Trajectory prediction sensitivity analysis using monte carlo simulations," *2018 Aviation Technology, Integration, and Operations Conference*, pp. 1–20, 2018.
- [59] J. Morio, "Global and local sensitivity analysis methods for a physical system," *European Journal of Physics*, vol. 32, no. 6, pp. 1577–1583, 2011.
- [60] C. Marzban, "Variance-based sensitivity analysis: An illustration on the lorenz'63 model," *Monthly Weather Review*, vol. 141, no. 11, pp. 4069–4079, 2013.
- [61] J. A. Scales and R. Snieder, "To Bayes or not to Bayes?," *Geophysics*, vol. 62, no. 4, pp. 1045–1046, 1997.
- [62] H. Yang and S. J. Novick, "Basics of Bayesian Statistics," in *Bayesian Analysis with R for Drug Development*, pp. 17–40, Boca Raton : CRC Press, Taylor & Francis Group, 2019.: Chapman and Hall/CRC, 6 2019.
- [63] G. Consonni, D. Fouskakis, B. Liseo, and I. Ntzoufras, "Prior distributions for objective Bayesian analysis," *Bayesian Analysis*, vol. 13, no. 2, pp. 627–679, 2018.
- [64] E. Crisostomi, A. Lecchini-Visintini, and J. Maciejowski, "Combining monte carlo and worst-case methods for trajectory prediction in air traffic control: A case study," *6th EUROCONTROL Innovative Research Workshop and Exhibition: Disseminating ATM Innovative Research*, pp. 259–265, 2007.
- [65] S. Tyson, D. Donovan, B. Thompson, S. Lynch, and M. Tas, *Uncertainty Modelling with Polynomial Chaos Expansion Stage 1 Final Report*. No. November, 2015.
- [66] A. O'Hagan, "Polynomial Chaos: A Tutorial and Critique from a Statistician's Perspective," *Tonyohagan.Co.Uk*, pp. 1–16, 2011.
- [67] V. N. Vapnik, *Statistics for Engineering and Information Science*. 1999.

- [68] M. S. Arulampalam, S. Maskell, N. Gordon, and T. Clapp, "A tutorial on particle filters for on-line nonlinear/nongaussian bayesian tracking," *Bayesian Bounds for Parameter Estimation and Nonlinear Filtering/Tracking*, vol. 50, no. 2, pp. 723–737, 2007.
- [69] Q. Wang, J. Huang, and F. Lu, "An improved particle filtering algorithm for aircraft engine gas-path fault diagnosis," *Advances in Mechanical Engineering*, vol. 8, no. 7, pp. 1–13, 2016.
- [70] P. M. Djuric, J. H. Kotecha, J. Zhang, Y. Huang, T. Ghirmai, M. F. Bugallo, and J. Míguez, "Particle filtering," *IEEE Signal Processing Magazine*, vol. 20, no. 5, pp. 19–38, 2003.
- [71] T. Li, S. Sun, T. Sattar, and J. Corchado, "Fighting against Sample Degeneracy and Impoverishment in Particle Filters: Particularly on Intelligent Choices," *23.7-Expert Systems with Applications*, pp. 1–34, 2013.
- [72] J. Sun, H. A. Blom, J. Ellerbroek, and J. M. Hoekstra, "Particle filter for aircraft mass estimation and uncertainty modeling," *Transportation Research Part C: Emerging Technologies*, vol. 105, no. June, pp. 145–162, 2019.
- [73] R. Conde, A. Ollero, and J. Cobano, "Method based on a particle filter for UAV trajectory prediction under uncertainties," *40th International Symposium of Robotics*, pp. 245–250, 2009.
- [74] Y. S. Chati and H. Balakrishnan, "A Gaussian Process Regression approach to model aircraft engine fuel flow rate," *Proceedings - 2017 ACM/IEEE 8th International Conference on Cyber-Physical Systems, ICCPS 2017 (part of CPS Week)*, pp. 131–140, 2017.
- [75] T. Kurdyaveva and A. Miliadis-Argeitis, "Efficient global sensitivity analysis of biochemical networks using Gaussian process regression," *Proceedings of the IEEE Conference on Decision and Control*, vol. 2018-December, no. Cdc, pp. 2673–2678, 2019.
- [76] Y. S. Chati and H. Balakrishnan, "Statistical modeling of aircraft takeoff weight," *12th USA/Europe Air Traffic Management R and D Seminar*, no. Atm, 2017.
- [77] C. Rasmussen and C. K. I. Williams, *Gaussian Processes for Machine Learning*. Massachusetts Institute of Technology, 2006.
- [78] H. Rong, A. P. Teixeira, and C. Guedes Soares, "Ship trajectory uncertainty prediction based on a Gaussian Process model," *Ocean Engineering*, vol. 182, no. August 2018, pp. 499–511, 2019.
- [79] S. A. Goli, B. H. Far, and A. O. Fapojuwo, "Vehicle Trajectory Prediction with Gaussian Process Regression in Connected Vehicle Environment," *IEEE Intelligent Vehicles Symposium, Proceedings*, vol. 2018-June, no. Iv, pp. 550–555, 2018.
- [80] Q. Tran and J. Firl, "Modelling of traffic situations at urban intersections with probabilistic non-parametric regression," *IEEE Intelligent Vehicles Symposium, Proceedings*, no. Iv, pp. 334–339, 2013.
- [81] N. Rahmah and I. S. Sitanggang, "Determination of Optimal Epsilon (Eps) Value on DBSCAN Algorithm to Clustering Data on Peatland Hotspots in Sumatra," *IOP Conference Series: Earth and Environmental Science*, vol. 31, no. 1, 2016.